Ribonuclease A: Disulfide Bonds, Conformational Stability, and Cytotoxicity

by

Tony A. Klink

A dissertation submitted in partial fulfillment
of the requirements for the degree of

Doctor of Philosophy
(Biochemistry)

at the

UNIVERSITY OF WISCONSIN-MADISON
2000

A dissertation entitled

Ribonuclease A: Disulfide Bonds, Conformational Stability and Cytotoxicity

submitted to the Graduate School of the
University of Wisconsin-Madison
in partial fulfillment of the requirements for the
degree of Doctor of Philosophy

by

Tony Anthony Klink

Date of Final Oral Examination: August 4, 2000

Month & Year Degree to be awarded: **December** **May** **August** 2000

Approval Signatures of Dissertation Readers:

Signature, Dean of Graduate School

Readers' Page: This page is not to be hand-written except for the signatures

Abstract

Disulfide bonds between the side chains of cysteine residues are the only common cross-links in proteins. Bovine pancreatic ribonuclease A (RNase A) is a 124-residue enzyme that contains four interweaving disulfide bonds (Cys26-Cys84, Cys40-Cys95, Cys58-Cys110, and Cys65-Cys72) and catalyzes the cleavage of RNA. The contribution of each disulfide bond to the conformational stability and catalytic activity of RNase A was determined using variants in which each cystine was replaced independently with a pair of alanine residues. Of the four disulfide bonds, the Cys40-Cys95 and Cys65-Cys72 cross-links are the least important to conformational stability. Removing these disulfide bonds leads to RNase A variants that have T_m values below that of the wild-type enzyme but above physiological temperature.

Unlike wild-type RNase A, G88R RNase A is toxic to cancer cells. To investigate the relationship between conformational stability and cytotoxicity, the C40A/C95A and C65A/C72A variants were made in the G88R background. Also, a new disulfide bond was introduced into G88R RNase A and a variant missing the Cys65-Cys72 disulfide bond. The T_m values of the four disulfide variants of G88R RNase A vary by nearly 30 °C. The conformational stability correlates directly with cytotoxicity as well as with resistance to proteolysis. These data indicate that conformational stability is a key determinant of RNase A cytotoxicity and suggest that cytotoxicity relies on avoiding proteolysis. This finding suggests a means to produce new cancer chemotherapeutic agents based on mammalian ribonucleases.

To be cytotoxic, ribonucleases must enter the cytosol and degrade cellular RNA. The cytosolic ribonucleolytic activity of RNase A is limited, however, by the presence of excess

ribonuclease inhibitor (RI). Ribonuclease inhibitor (RI) is a 50-kDa cytosolic scavenger of pancreatic-type ribonucleases. RI homologs contain 30 or so reduced cysteine residues, bind ribonucleases with 1:1 stoichiometry, and competitively inhibit their ribonucleolytic activity. We describe an overexpression system of porcine RI (pRI) that produces a 60-fold higher yield than expression systems reported previously. Using the *trp* promoter and minimal media, pRI remains in the cytosol and is in the soluble fraction during cell lysis. Differential scanning calorimetry was employed to study the conformational stability of pRI, RNase A, and the pRI•RNase A complex. The conformational stability of the complex is enhanced relative to that of the individual components.

Acknowledgements

The members of the Raines lab have been supportive in my research endeavors. Ken Woycechowsky and Kim Talyor were collaborators for Chapter 2. Ken also served as an excellent resource and offered constructive criticism. Marcia Haigis and Chiwook Park were instrumental in proposing the idea of the research shown in Chapter 3. Marcia's suggestions have enabled me to become a more thorough scientist. Chiwook was an excellent resource, especially when using equations and performing curve fitting. Brad Kelemen shared his considerable expertise in enzymic research. Pete Leland was a great resource in formatting this thesis. I am grateful that he was available when I arrived at my formatting obstacles. I thank Betsy Kersteen, Richele Abel, Steve Fuchs, Kim Dickson, Rob Hondel, and Uli Arnold the newest members of the Biochemistry lab, for looking beyond my research frustrations. The members of the Raines chemistry lab have added a new and positive dimension to my graduate experience. I am indebted to Marcia, Ken and Pete for editing my manuscripts. Darrell Mc Caslin was an excellent technical resource and supported me, especially during the last weeks of my graduate research.

Other friends have aided me considerably. Archna Bhasin, Dennis Brennen, Rick Buchman, Father Martin Carr, Sumedha Ghate, Dan Henderson, Janie Infalt, Quirin Klink, Paul Oleksy, Rebecca Provencal, Shelly Schink, Scott Weiss, and Beth Werner have been supportive constantly. Thanks for contributing to my enjoyment of life.

Ron Raines was a joy to work with. His enthusiasm and adeptness for research was enlightening. I appreciated his scientific insights and his support for my humanitarian

interests. Those pursuits have altered my life. I owe him thanks for his lenience. Your kindness will not be forgotten.

Finally, I thank my family. My parents have raised many caring individuals who have asked other caring people to become a part of our family. I reap (and take full advantage of) the benefit of their efforts. The humor, love, and support are unbounded. I also thank them for keeping the frustrations of graduate research in perspective. My nieces and nephews (and great nephew) have been simply joyous.

Table of Contents

List of Figures

List of Tables

List of Abbreviations

5′-ADP	adenosine 5′-diphosphate
BPTI	bovine pancreatic trypsin inhibitor
CNBr	cyanogen bromide
DEPC	diethylpyrocarbonate
DSC	differential scanning calorimetry
DTT	dithiothreitol
EDTA	ethylenediaminetetraacetic acid
6-FAM	6-carboxyfluorescein
5′-GDP	guanosine 5′-diphosphate
IPTG	isopropyl-1-thio-β-D-galactopyranoside
ITC	isothermal titration calorimetry
LB	Luria broth
LRR	leucine-rich repeats
MES	2-[N-morpholino]ethanesulfonic acid
M_r	relative molecular mass
OD	optical density
ONC	onconase
PAGE	polyacrylamide gel electrophoresis
PBS	Dulbecco's phosphate-buffered saline
PDB	Protein Data Bank
PIPES	1,4-piperazine diethane sulfonic acid

PMSF	phenylmethanesulfonylfluoride
poly(C)	poly(cytidylic acid)
pRI	porcine ribonuclease inhibitor
RI	ribonuclease inhibitor
RNase A	bovine pancreatic ribonuclease A
RNase B	bovine pancreatic ribonuclease B
TB	terrific broth
SDS	sodium dodecyl sulfate
6-TAMRA	6-carboxytetramethylaminorhodamine
Tris	tris(hydroxymethyl)aminomethane
T_m	midpoint of the thermal denaturation curve
UV	ultraviolet
3′-UMP	uridine 3′-monophosphate

Chapter 1

Introduction

The breadth of research utilizing Ribonuclease A (RNase A) is unprecedented. Biochemists have investigated this small enzyme in a myriad of ways. Due to its high conformational stability and reversible unfolding, RNase A is able to withstand harsh treatment. Thermal and chemical unfolding of RNase A has yielded a better understanding of how proteins fold (Sela *et al.*, 1957). RNase A was the fourth protein to have its structure determined (Avey *et al.*, 1967; Kartha *et al.*, 1967; Wyckoff *et al.*, 1967; Wyckoff *et al.*, 1967) and has provided a more complete understanding of protein structure (Figure 1). RNase A has been inactivated through chemical modification (Wolf *et al.*, 1970), site-directed mutagenesis (Trautwein *et al.*, 1991; Thompson & Raines, 1994; Messmore *et al.*, 1995), and the design (Findlay *et al.*, 1961; Findlay *et al.*, 1962; Stowell *et al.*, 1995) and isolation (Blackburn *et al.*, 1977; Lee *et al.*, 1989; Kobe & Deisenhofer, 1995) of natural inhibitors. Proteolytic enzymes have been used to study its partial breakdown *in vitro* (Ooi *et al.*, 1963; Rupley & Scheraga, 1963; Arnold & Ulbrich-Hofmann, 1997) and complete metabolic turnover *in vivo* (Backer *et al.*, 1983; McElligott *et al.*, 1985; Chiang & Dice, 1988). Our understanding of enzymology, protein folding, and structure–function relationships is due, in large part, to research utilizing RNase A. Indeed, this research has been rewarded with four Nobel prizes. Stanford Moore and William H. Stein received the Nobel prize in chemistry "for their contribution to the understanding of the connection between chemical structure and catalytic activity of the active centre of the ribonuclease molecule". Chistrian B. Anfinsen received recognition "for his work on ribonuclease,

especially concerning the connection between the amino acid sequence and the biologically active conformation". R. Bruce Merrifield's research was recognized "for his development of methodology for chemical synthesis on a solid matrix".

The active-site residues of RNase A (His12, Lys41, His119) are absolutely conserved through the homologous ribonuclease family (Beintema, 1987). The mechanistic roles of these residues have been inferred through chemical modification (Wolf *et al.*, 1970) and, more recently, site-directed mutagenesis studies (Trautwein *et al.*, 1991; Thompson & Raines, 1994; Messmore *et al.*, 1995). RNase A catalyzes the cleavage of the P–$O^{5'}$ bond of RNA on the 3′ end of pyrimidine residues (Richards & Wyckoff, 1971). Catalysis occurs through a cleavage reaction via transphosphorylation that yields a 2′,3′-cyclic phosphodiester, followed by a hydrolysis reaction that forms a 3′-phosphomonoester (Brown & Todd, 1953; Thompson *et al.*, 1994) (Figure 2). Crystalline structures of RNase A with substrate analogs (Wodak *et al.*, 1977; Fisher *et al.*, 1998), and a transition-state analog (Borah *et al.*, 1985) support the participation of these residues in RNA cleavage.

Disulfide Bonds

As the only common covalent crosslink in proteins, the disulfide bond is an integral part of biochemistry. Disulfide bonds were defined in 1810 (Jocelyn, 1972). However, they were not detected in proteins for nearly 100 years (Jocelyn, 1972). In aerobic biological systems, the net two-electron oxidation of two thiols to a disulfide bond is ultimately linked to the reduction of oxygen (Huggins *et al.*, 1951; Gilbert, 1990).

$$2R\text{–}SH \rightleftarrows R\text{–}SS\text{–}R + 2e^- + 2H^+ \qquad (1.1)$$

Interestingly, cysteine residues involved in disulfide bonds are the second most highly conserved residue in proteins (Thornton, 1981), presumably due to their being required in protein structure and function. These covalent crosslinks occur most frequently in extracellular proteins, as an oxidizing environment is required for the formation of the disulfide bond. Indeed, disulfide bonds are unable to form in the reducing environment of the cytoplasm (Gilbert, 1990).

During the 1960s, much research focussed on investigating the importance of disulfide bond formation to the structure of RNase A. Its small size aided in determining the location of its four disulfide bonds (Spackman *et al.*, 1960) and its primary sequence (Hirs *et al.*, 1960). The highly conserved disulfide bonds in RNase A (Beintema, 1987) are important for its tertiary structure (White, 1961; Herskovits & Laskowski, 1968) (Figure 1). The illustrious work by Anfinsen showed that the tertiary structure of a protein is determined by the sum of the interactions in the amino acid sequence (Sela *et al.*, 1957; Anfinsen *et al.*, 1961; Anfinsen, 1973). Still, the disulfide bonds of RNase A were thought to be required for its native structure. Without intact disulfide bonds, the conformation of RNase A is that of a random coil (White, 1961; Herskovits & Laskowski, 1968). Nonetheless, Garel showed that completely reduced RNase A has 0.04% ribonucleolytic activity relative to the fully oxidized enzyme (Garel, 1978). The "random coil" is sometimes, abeit infrequently, in the native state. With the knowledge of the RNase A structure, scientists began using sulfhydryl chemistry to delve into equally difficult questions regarding protein folding and conformational stability.

Protein Folding

The interweaving disulfide bond network of RNase A (Cys26–Cys84, Cys40–Cys95, Cys58–Cys110, and Cys65–Cys72) is intimately associated with its folding (Wedemeyer *et al.*, 2000). The oxidative folding of reduced RNase A occurs in a two-step process. A rapid formation of disulfide bonds is followed by the slow reshuffling of incorrectly paired disulfides (Creighton, 1977). The addition of protein disulfide isomerase, an enzyme that shuffles incorrectly formed disulfides, increases the rate of the slow folding reaction (Weissman & Kim, 1993).

Because the structure of RNase A was already defined, the disulfide bonds could be studied with relative ease. Early on, oxidative folding studies utilizing alkylating agents [Creighton, 1979 #849; Creighton, 1980 #692; (Galat *et al.*, 1981)] indicated that the Cys65–Cys72 disulfide bond was involved in the early folding intermediates (Creighton, 1979). The Cys65–Cys72 disulfide bond was therefore postulated to be a nucleation site for RNase A folding (Milburn & Scheraga, 1988). The large proportion of the native crosslink Cys65–Cys72 in early folding intermediates was shown to be the result of both enthalpic and entropic interactions (Altmann & Scheraga, 1990; Talluri *et al.*, 1993).

The RNase A folding pathway is complicated by the high number of folding intermediates. Although, eight reduced cysteine residues present 105 possible disulfide bond combinations (Anfinsen & Scheraga, 1975), the folding pathway is non-random (Creighton, 1979; Ruoppolo *et al.*, 1996; Xu *et al.*, 1996). Chemical modification of the cysteine residues [Creighton, 1979 #849; (Galat *et al.*, 1981)] and site-directed mutagenesis (Xu & Scheraga,

1998; Iwaoka *et al.*, 1999) indicate there are only fifteen distinct disulfide bond intermediates in the RNase A folding pathway (Anfinsen & Scheraga, 1975). Still, the details of the folding pathway remain unclear. There is conflicting evidence as to the role of the Cys65–Cys72 disulfide bond as a nucleation site of RNase A folding (Altmann & Scheraga, 1990; Ruoppolo *et al.*, 1996). Certainly, the folding pathway for this small protein is complex.

Conformational Stability

The folded protein is only marginally more stable than the series of unfolded structures. For example, the folded conformation of most proteins is less than 10 kcal/mol more stable than the unfolded conformations (Creighton, 1990). Most native disulfide bonds increase the conformational stability of proteins. Thus, these crosslinks may shift the equilibrium of protein folding to the native state.

Disulfide bonds have become useful tools to dissect the conformational stability of proteins. Sulfydryl-modifying reagents have aided in elucidating the disulfide bond-mediated contribution to protein stability. These reagents exploit the nucleophilicity of the cysteine sulfurs and prevent disulfide bonds from forming (Pace *et al.*, 1988; Talluri *et al.*, 1994; Zhang *et al.*, 1997). Yet, disulfide bonds are located most often in the protein interior (Thornton, 1981). The addition of sterically destabilizing groups in the protein interior can cause a perturbation to the native conformation (Pace *et al.*, 1988; Lim & Sauer, 1989) that leads to an artificially low conformational stability.

Flory postulated that crosslinks limit the number of polymer conformations, thereby destabilizing an unfolded state relative to a native state (Flory, 1956). If this loss of entropy

in the unfolded state were the only disulfide bond-mediated contribution to conformational stability, then disulfide bond-mediated stability would be reflected in the number of amino acid residues within the ring containing the disulfide bond (Flory, 1956; Pace *et al.*, 1988). A disulfide bond within a large ring would decrease the stability of the unfolded state more than one within a small ring. Although disulfide bond-mediated conformational stability has been attributed to such entropic effects (Frisch *et al.*, 1996; van den Burg *et al.*, 1998), crosslinking a larger loop does not always confer greater stability (Clark & Fersht, 1993; Vogl *et al.*, 1995). Moreover, introducing a disulfide bond into a protein may decrease its conformational stability (Wells & Powers, 1986; Matsumura *et al.*, 1989; Betz *et al.*, 1996).

This model makes a fundamental assumption: removing or adding a disulfide bond does not significantly affect the native state. This assumption is not necessarily valid (Tidor & Karplus, 1993; Hinck *et al.*, 1996). Moreover, if removing a disulfide bond increases the flexibility of the native protein, then the entropic contribution to conformational stability would be increased and the enthalpic contribution would be decreased.

The entropy of the native state is increased significantly in disulfide bond variants of human lysozyme (Kuroki *et al.*, 1992), as expected from a detailed computational analysis (Tidor & Karplus, 1993). In addition, increased flexibility of the native state could disrupt stabilizing interactions and thereby decrease the enthalpic contribution to stability. For example, an increase in the disorder of the native state has been observed by NMR spectroscopy in the disulfide variants of RNase A (Laity *et al.*, 1997; Shimotakahara *et al.*, 1997), relative to the wild-type enzyme. The increased perturbation of the native state caused by the missing crosslinks would also affect stabilizing hydrogen bonds, electrostatic and van der Waals interactions. Indeed, a single hydrogen bond can offer nearly 5 kcal/mol to the

conformational stability of a protein (Jeffrey & Saenger, 1994). Therefore, models of disulfide bond contributions to conformational stability that do not include the effect on the native state are incomplete.

Cytotoxicity

Recently, interesting biological activities have injected new fervor into the study of ribonucleases. RNase A homologs are capable of eliciting antitumor (Youle & D'Alessio, 1997), immunosuppressive (Tamburrini *et al.*, 1990) and angiogenic (Riordan, 1997) responses. Ribonucleases kill the target cell through an as yet unknown pathway in which they bind cells, enter the cytoplasm, and degrade RNA (Youle *et al.*, 1993).

The ribonucleolytic activity of cytotoxic ribonucleases is essential for their cytotoxicity (Ardelt *et al.*, 1991). Although ribonucleolytic activity is essential to produce a cytotoxic consequence, it is not the only requirement for cytotoxicity. RNase A catalyzes the cleavage of RNA near the limit of diffusion (Kelemen & Raines, 1999), but RNase A is not cytotoxic. RNase A homologs are less efficient catalysts of RNA cleavage. For example, onconase (ONC) is capable of producing an antitumor response (Mikulski *et al.*, 1995), but is 500-fold less efficient at RNA cleavage than RNase A (Wu *et al.*, 1993).

The cell has evolved a defense mechanism against the destruction of extracellular ribonucleases. Ribonucleolytic activity is controlled *in vivo* by the ribonuclease inhibitor protein (RI). In the cell, unbound RI is present at a 6-fold molar excess relative to RNase A (Blackburn & Moore, 1982). RI is a 50-kDa horseshoe-shaped cytosolic protein that engulfs ribonucleases and competitively inhibits the ribonucleolytic activity (Lee *et al.*, 1989)

(Figure 3). RNase A is susceptible to inhibition by RI ($K_d = 4 \times 10^{-14}$ M) (Lee *et al.*, 1989), but ONC is able to evade inhibition ($K_i > 10^{-6}$ M) (Lee *et al.*, 1989; Boix *et al.*, 1996). Giving RNase A the ability to evade binding to RI is sufficient to produce a cytotoxic effect. The G88R and G88D RNase A variants have lower RI affinity and are cytotoxic to human leukemia cells (Leland *et al.*, 1998).

RNase A cytotoxicity is increased by 10^3-fold when the enzyme is microinjected directly into cells (Saxena *et al.*, 1991). This finding suggests that a major barrier to RNase A cytotoxicity is its ability to enter the cytoplasm. Still, it remains unclear how ribonucleases transverse the plasma membrane. It has been suggested that translocation is accomplished by absorptive endocytosis (Kim *et al.*, 1995).

The plasma membranes of some tumor cells have a higher net negative charge than do plasma membranes of normal cells (Robbins & Nicolson, 1975). Each of the ribonucleases that are selectively cytotoxic to malignant cells are more basic than is RNase A (Ardelt *et al.*, 1991; Mancheno *et al.*, 1994; Kim *et al.*, 1995). Consequently, RNase A may have a lower affinity for the anionic cell surface than do the cytotoxic ribonucleases. In addition, molecular modeling shows that there is a negative cluster on the RNase A surface away from its active site. This negative cluster (Glu49 and Asp53) is not apparent in cytotoxic ribonucleases. Yet, replacing Glu49 and Asp53 with a pair of lysine residues did not endow RNase A with cytotoxicity (T.A. Klink and R.T. Raines, unpublished results). Likewise, E49K/D53K/G88R RNase A and G88R RNase A have similar cytotoxicity. Therefore, the negative cluster of residues does not appear to affect RNase A cytotoxicity.

Metabolic Turnover

Proteolytic degradation studies on RNase A were originally performed *in vitro* (Ooi *et al.*, 1963; Rupley & Scheraga, 1963). Studies show that proteins are more susceptible to proteolytic degradation when unfolded (Pace & Barrett, 1984). Indeed, RNase A is degraded more readily by proteases in the presence of denaturants and elevated temperatures (Anfinsen and Scheraga, 1975). Consequently, one protein that is measurably more stable than another should be less susceptible to degradation.

A protein must resist the proteolytic enzymes long enough in order to function within the cell. This resistance may not be trivial. The rates of intracellular protein turnover vary by 10^3-fold (Isenman & Dice, 1989). RNase A is better able to thwart the proteolytic machinery than many proteins (Rechsteiner *et al.*, 1987; Rogers & Rechsteiner, 1988). The qualities that endow a protein with a slow metabolic turnover remain ambiguous. Protein size, isoelectric point, flexibility, hydrophobicity, and thermal stability are among those many qualities that have been implicated in the rate of metabolic turnover (Rechsteiner *et al.*, 1987; Rogers & Rechsteiner, 1988). Yet, drawing conclusions from these studies is problematic because the proteins studied were divergent in characteristics that have been implicated in metabolic turnover.

This Thesis

Using various techniques, I have advanced our understanding of the conformational stability and cytotoxicity of RNase A. Chapter 2 describes the contribution of each disulfide bond to the conformational stability and catalytic activity of RNase A. I found that the two

terminal disulfide bonds in the amino acid sequence (Cys26–Cys84 and Cys58–Cys110) enhance stability more than do the two embedded disulfide bonds (Cys40–Cys95 and Cys65–Cys72). Remarkably, these two embedded disulfide bonds, which are least important to conformational stability, are most important to catalytic activity.

Chapter 3 describes a method to use disulfide variants of RNase A to investigate the relationship between conformational stability and cytotoxicity. I found that removing the Cys40–Cys95 and Cys65–Cys72 disulfide bonds leads to RNase A variants that have T_m values (which is the temperature at the midpoint of the thermal denaturation curve) below that of the wild-type enzyme but above physiological temperature (37°C). G88R RNase A is cytotoxic (Leland *et al.*, 1998). The C40A/C95A and C65A/C72A variants were made in the G88R background to search for a correlation between conformational stability and cytotoxicity. In addition, a non-native disulfide bond (between residues 4 and 118) was introduced into G88R RNase A and a variant missing the Cys65–Cys72 disulfide bond. The data indicate that a relationship between conformational stability and RNase A cytotoxicity does indeed exist and suggest that cytotoxicity relies on avoiding proteolysis.

Chapter 4 describes the first expression system of soluble porcine ribonuclease inhibitor (RI). The application of protein engineering techniques to RI has been limited by the low yield obtained during the folding of insoluble RI. An expression system that produces soluble RI is ideal for large-scale production of this important protein. RI was produced in the soluble fraction of the cell lysate and was isolated at 15 mgs per L of culture. Using this expression system, a 60-fold increase in active pRI was recovered, relative to previously reported recombinant DNA systems. Differential scanning calorimetry was used to study the heat denaturation of pRI, RNase A, and pRI•RNase A complex. The

conformational stability of the complex is increased relative to that of the individual components.

Figure 1.1. Structural representation of ribonuclease A.

The ribbon diagram contains inscriptions referring to the location of the disulfide bonds (PDB entry 7RSA).

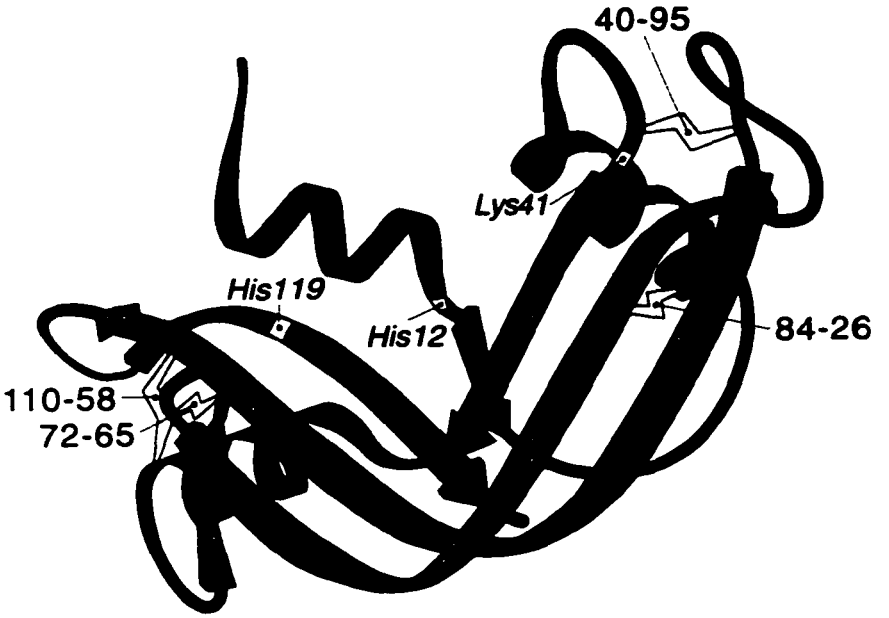
40-95
Lys41
His119
His12
84-26
110-58
72-65

Figure 1.2. Mechanism of the reactions catalyzed by ribonuclease A.

In the transphosphorylation step, His12 (**B**) deprotonates the attacking 2′-OH of ribose, and His119 (**A**) protonates the 5′-OH leaving group. The cleavage reaction yields a cyclic phosphodiester and a free 5′-OH. In the hydrolysis step, His119 assists the attack of a water molecule on the cyclic phosphodiester yielding a 3′-phosphomonoester and His12 assists in the departure of the 2′-oxygen leaving group.

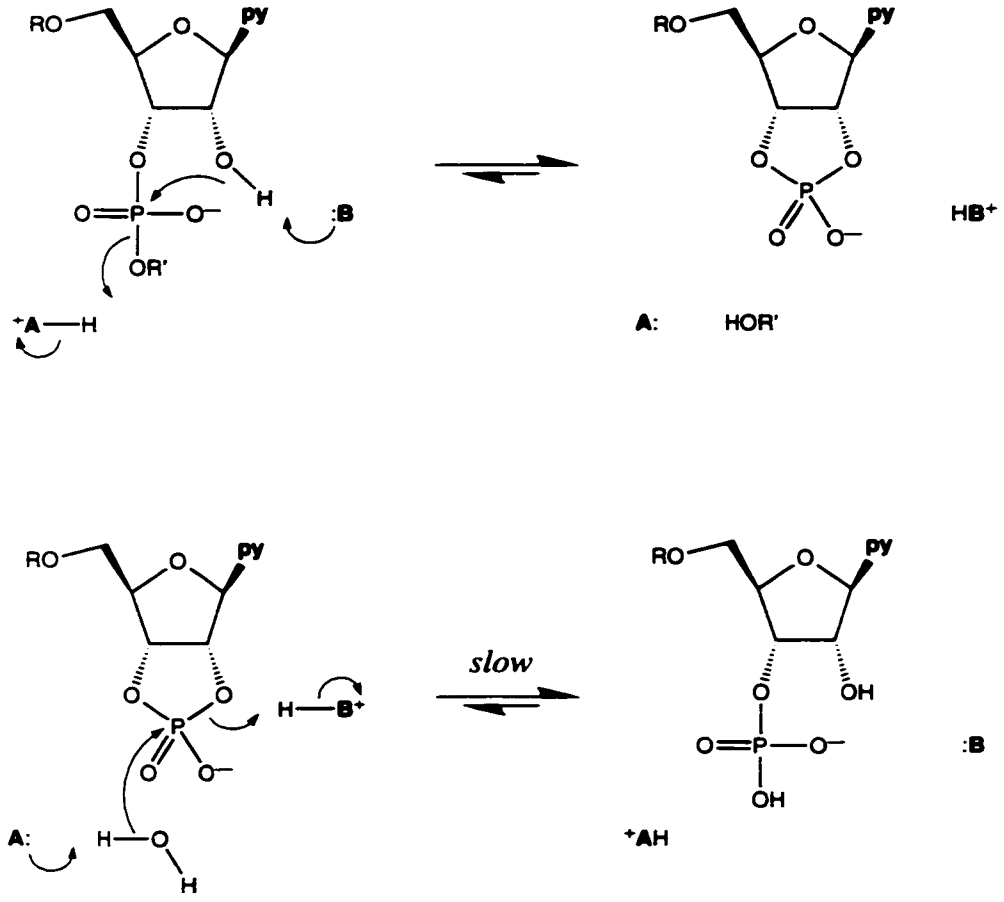
RO
py
O
O
O
P
O
H
:B
OR'
+A—H
A:
HOR'
HB+
RO
py
O
O
O
P
O
H—B+
A:
H—O
H
slow
RO
py
O
OH
O
P
O
OH
:B
+AH

Figure 1.3. Structural representation of the ribonuclease inhibitor:ribonuclease A complex.

Ribonuclease A is in blue, ribonuclease inhibitor is in red. Ribbon diagrams were created with programs MOLSCRIPT (Kraulis, 1991) and RASTER3D (Merritt & Murphy, 1994) by using coordinated derived from x-ray analysis (PDB entry 1DFJ)(Kobe & Deisenhofer, 1995)(Kobe & Deisenhofer, 1993).

Ribonuclease Inhibitor

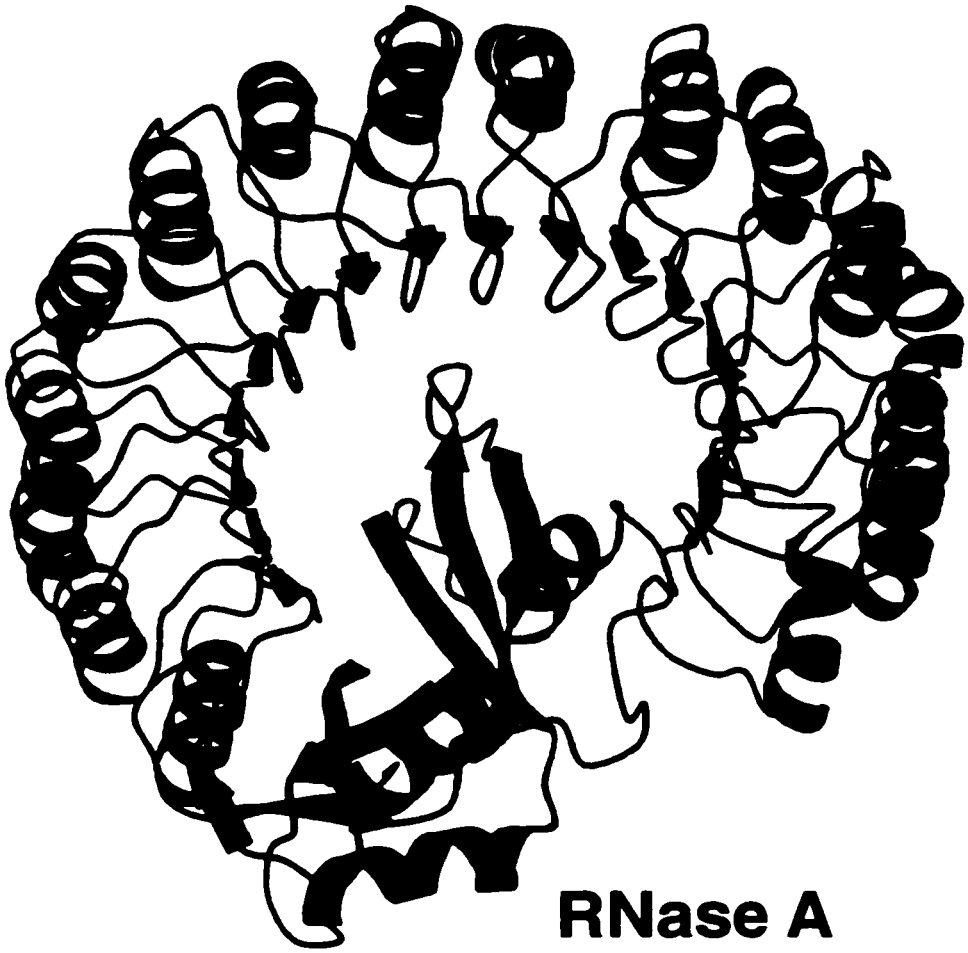

Chapter 2

Contribution of Disulfide Bonds to the Conformational Stability and Catalytic Activity of Ribonuclease A

This chapter was published as:

Klink, T.A., Woycechowsky, K.J., Taylor, K.M., and Raines, R.T. (2000) Contribution of disulfide bonds to the conformational stability and catalytic activity of ribonuclease A. *Eur. J. Biochem.* **267** 566-572.

Abbreviations. BPTI, bovine pancreatic trypsin inhibitor; DSC, differential scanning calorimetry; MES, 2-(*N*-morpholino)ethanesulfonic acid; PAGE, polyacrylamide gel electrophoresis; PDB, Protein Data Bank (http://www.rcsb.org/pdb/); poly(C), poly(cytidylic acid); RNase A, bovine pancreatic ribonuclease A; SDS, sodium dodecyl sulfate.

2.1 Abstract

Disulfide bonds between the side chains of cysteine residues are the only common crosslinks in proteins. Bovine pancreatic ribonuclease A (RNase A) is a 124-residue enzyme that contains four interweaving disulfide bonds (Cys26–Cys84, Cys40–Cys95, Cys58–Cys110, and Cys65–Cys72) and catalyzes the cleavage of RNA. The contribution of each disulfide bond to the conformational stability and catalytic activity of RNase A has been determined by using variants in which each cystine is replaced independently with a pair of alanine residues. Thermal unfolding experiments monitored by ultraviolet spectroscopy and differential scanning calorimetry reveal that wild-type RNase A and each disulfide variant unfold in a two-state process and that each disulfide bond contributes substantially to conformational stability. The two terminal disulfide bonds in the amino acid sequence (Cys26–Cys84 and Cys58–Cys110) enhance stability more than do the two embedded ones (Cys40–Cys95 and Cys65–Cys72). Removing either one of the terminal disulfide bonds liberates a similar number of residues and has a similar effect on conformational stability, decreasing the midpoint of the thermal transition by almost 40 °C. The disulfide variants catalyze the cleavage of poly(cytidylic acid) with values of k_{cat}/K_m that are 2- to 40-fold less than that of wild-type RNase A. The two embedded disulfide bonds, which are least important to conformational stability, are most important to catalytic activity. These embedded disulfide bonds likely contribute to the proper alignment of residues (such as Lys41 and Lys66) that are necessary for efficient catalysis of RNA cleavage.

2.2 Introduction

A polypeptide chain can adopt many conformations. Yet, the sequence of its amino acid residues directs folding to a particular native state (Anfinsen, 1973). The loss of conformational entropy associated with folding destabilizes the native conformation. This destabilization is overcome by the hydrophobic effect, hydrogen bonds, other noncovalent interactions, and (for many proteins) disulfide bonds (Dill, 1990).

Bovine pancreatic ribonuclease A (RNase A; EC 3.1.27.5 (D'Alessio & Riordan, 1997; Raines, 1998)) provides a superb template with which to dissect the contribution of disulfide bonds to conformational stability. RNase A consists of 124 amino acid residues and contains four intrachain disulfide bonds (Cys26–Cys84, Cys40–Cys95, Cys58–Cys110, and Cys65–Cys72; Fig. 2.1). The four disulfide bonds are conserved in all 40 of the known sequences of homologous mammalian pancreatic ribonucleases (Beintema *et al.*, 1988). Two disulfide bonds (Cys40–Cys95 and Cys65–Cys72) link together surface loops, and two link an α-helix to a β-sheet in the protein core (Cys26–Cys84 and Cys58–Cys110). Three disulfide bonds enclose a loop of similar size (Cys26–Cys84, Cys40–Cys95 and Cys58–Cys110; $\eta = 59$, 56, and 53, respectively), and the other disulfide bond (Cys65–Cys72; $\eta = 8$) encloses a smaller loop.

In previous work, the cystines of RNase A were replaced with pairs of serine residues (Laity *et al.*, 1993). Drawing conclusions from this study is problematic because replacing a cystine with a pair of serine residues can result in an overestimation of the importance of disulfide bonds (Chothia, 1976). Cystine residues are nonpolar and are usually buried in folded proteins (Thornton, 1981; Saunders *et al.*, 1993). Indeed, the disulfide bonds of native RNase A have little or no solvent-accessible surface area (Fig. 2.1). In contrast, a serine side chain is polar and likely to be highly destabilizing in the hydrophobic environment of a protein core.

Here, we have used site-directed mutagenesis to replace each cystine in RNase A with a pair of alanine residues. The four disulfide variants are active catalysts of RNA cleavage. We assessed the contribution of disulfide bonds to the conformational stability of each variant by monitoring thermal unfolding using ultraviolet spectroscopy and differential scanning calorimetry (DSC). We find that the disulfide bonds that restrict the *N*- and *C*-termini (Cys26–Cys84 and Cys58–Cys110) are the most important to conformational stability. In constrast, the disulfide bonds proximal to active site residues (Cys65–Cys72 and Cys40–Cys95) are most important to catalytic activity.

2.3 Experimental Procedures

Escherichia coli strains DH11S and DH5α were from Gibco BRL (Gaithersburg, MD). *E. coli* strain BL21(DE3) (F^- ompT $r_B^-m_B^-$) was from Novagen (Madison, WI). *E. coli* strain CJ236 and helper phage M13K07 were from Bio-Rad (Richmond, CA). All enzymes for the manipulation of recombinant DNA were from Promega (Madison, WI) or New England Biolabs (Beverly, MA). Purified oligonucleotides were obtained from Gibco BRL. DNA was sequenced with a Sequenase 2.0 kit from United States Biochemicals (Cleveland, OH) or with an ABI 373 Automated Sequencer using an ABI PRISM Dye Terminator Cycle Sequencing Ready Reaction Kit with AmpliTaq DNA Polymerase, FS (Foster City, CA) and an MJ Research PTC-100 Programmable Thermal Controller (Watertown, MA). FPLC Hiload 26/60 Superdex 75 gel filtration column and mono-S HR10/10 cation-exchange columns were from Pharmacia LKB (Piscataway, NJ). Poly(cytidylic acid) [poly(C)] was from Midland Certified Reagent (Midland, TX) and was precipitated from ethanol and washed with aqueous ethanol (70% v/v) before use. IPTG was from Gold Biotechnology (St. Louis, MO). Bacto yeast extract, Bacto tryptone, Bacto peptone, and Bacto agar, were from Difco (Detroit, MI). LB medium contained (in 1.00 L) Bacto tryptone (10 g), Bacto yeast extract (5 g), and sodium chloride (10 g). TB contained (in 1.00 L) Bacto tryptone (12 g),

Bacto yeast extract (24 g), glycerol (4 mL), KH_2PO_4 (2.31 g), and K_2HPO_4 (12.54 g). All media were prepared in distilled, deionized water and autoclaved. All other chemical reagents were of commercial reagent grade or better, and were used without further purification unless indicated otherwise. *E. coli* cell lysis was performed using a French pressure cell from SLM Aminco (Urbana, IL). Ultraviolet and visible absorbance measurements were made with a Cary 3 double beam spectrophotometer equipped with a Cary temperature controller from Varian (Sugar Land, TX). Calorimetry experiments were performed with an MCS differential scanning calorimeter (DSC) from MicroCal (Northampton, MA).

Preparation of Ribonuclease A Variants

Oligonucleotide-mediated site-directed mutagenesis was used to create four RNase A variants in which a cystine was replaced with a pair of alanine residues. Plasmid pBXR directs the expression of RNase A in *E. coli* (delCardayré *et al.*, 1995). Mutagenesis was performed on plasmid pBXR replicated in *E. coli* strain DH11S or CJ236 (Kunkel *et al.*, 1987). To produce the DNA encoding C26A/C84A RNase A, the TGT codon for Cys26 in the wild-type plasmid pBXR was replaced with GCG (reverse complement in bold) using the oligonucleotide: AGGTTCCGGCTTTTCATCATCTGGTTCGCGTAGTTGGAGC, and the TGC codon for Cys84 was replaced with GCC (reverse complement in bold) using the oligonucleotide: CTGCCGGTCTCCCGGGCGTCGGTGATGC. DNA encoding C40A/C95A RNase A was produced by replacing the TGC codon for Cys40 with GCG (reverse complement in bold) using the oligonucleotide: GTTCACTGGCTTCGCTCGATCTTTGGT, and the TGT codon for Cys95 was replaced with GCG (reverse complement in bold) using the oligonucleotide: GGTCTTGTAGGCCGCGTTGGGGTACTT. DNA encoding C58A/C110A RNase A was

produced by replacing the TGC codon for Cys58 with GCG (reverse complement in bold) using the oligonucleotide: TTCTGGGA**CGC**CACGGCCTGGACGTCAGCCAG, and the TGT codon for Cys110 was replaced with GCG (reverse complement in bold) using the oligonucleotide: GGCACGTATGGGTTTCCCTC**CGC**AGCCACAA. Replacing the TGC codons for Cys65 and Cys72 with GCG produced DNA encoding C65A/C72A RNase A (reverse complements in bold) using the oligonucleotide: CTCTGGTA**CGC**ATTGGTCTGCCCATTCTT**CGC**GGCAACAT. Mutagenesis reaction mixtures were transformed into competent DH5α cells, and the isolated plasmid DNA of transformants was analyzed by sequencing.

Wild-type RNase A and the disulfide variants were produced and purified by methods described previously (Kim & Raines, 1993; delCardayré *et al.*, 1995), with the following modifications. The inclusion body pellet was resuspended in solubilization buffer (12 mL), which was 20 mM Tris-HCl buffer (pH 8.0) containing guanidine-HCl (7 M), DTT (0.10 M), and EDTA (10 mM), and shaken at room temperature for 3 h. The reduced protein solution was diluted 10-fold with 20 mM acetic acid and centrifuged for 30 min at 15300*g*. The supernatant was dialyzed exhaustively against 20 mM acetic acid. The soluble fraction was added to folding buffer (1.00 L), which was 0.10 M Tris-acetic acid buffer (pH 8.5) containing NaCl (0.10 M), reduced glutathione (1.0 mM), and oxidized glutathione (0.2 mM), and was stirred gently at 4 °C for 48 h. The purity of the protein after gel filtration and cation-exchange chromatography was assessed by SDS-PAGE and by its A_{280}/A_{260} ratio. Removing a disulfide bond is expected to alter the extinction coefficient of RNase A by <1% (Gill & von Hippel, 1989; Pace *et al.*, 1995). Hence, concentrations of wild-type RNase A and the disulfide variants were determined by using $\varepsilon = 0.72$ mL $mg^{-1}cm^{-1}$ at 277.5 nm (Sela *et al.*, 1957).

Thermal Unfolding Monitored by Ultraviolet Spectroscopy

UV spectroscopy was used to determine the effect of replacing a cystine with a pair of alanine residues on the thermal stability of RNase A. As RNase A is unfolded, its six tyrosine residues become exposed to solvent and its molar absorptivity at 287 nm decreases significantly (Hermans & Scheraga, 1961). The thermal stabilities of RNase A and the disulfide variants were assessed by monitoring the change in absorbance at 287 nm with temperature (Pace *et al.*, 1989; Eberhardt *et al.*, 1996). Solutions of protein were dialyzed exhaustively at 4 °C in 30 mM sodium acetate buffer (pH 6.0) containing NaCl (0.10 M). The pH of the acetate buffer does not change significantly (less than 0.3 pH units) over the temperature used in the experiment. The perturbation of T_m within this pH range is minimal (Quirk *et al.*, 1998). Thermal unfolding curves were obtained as follows. A buffer vs buffer blank was performed in matched cuvettes at 287 nm at the initial temperature. The absorbance of protein (1.6 mL of a 0.10 – 0.15 mg/mL solution) vs a buffer blank at 287 nm was recorded at the initial temperature (5 °C) after an 8-min temperature equilibration. As the temperature was increased (from 5 °C to 80 °C in 1-°C increments), absorbance at 287 nm was recorded after an 8-min equilibration at each temperature. As the temperature was decreased from 80 °C to 5 °C in 1-°C increments, the absorbance at 287 nm was recorded after a 5-min equilibration at each temperature.

Thermal unfolding monitored by differential scanning calorimetry

DSC was used to verify the results obtained from UV spectroscopy by monitoring the heat absorbed during the unfolding of wild-type RNase A and the disulfide variants. To prepare samples for DSC, wild-type RNase A and the variants were dialyzed exhaustively against 30 mM sodium acetate buffer (pH 6.0) containing NaCl (0.10 M). Protein solutions and a sample of the final dialysis buffer were centrifuged at 15300*g* for 30 min to remove

particulates. The supernatants were degassed under vacuum, and their protein concentrations (0.64 – 2.54 mg/mL) were determined immediately prior to loading the DSC sample cell. Calorimetric measurements were made on samples under N_2(g) (30 psi) at a scan rate of 1.0 °C min^{-1}. The dialysis buffer was used to perform a buffer vs buffer baseline scan and as the blank in the protein vs buffer scan. A single transition was observed in each DSC thermogram, and each scan was terminated approximately 20 °C beyond the transition. The unfolding of wild-type RNase A and all four of the disulfide variants was >99% reversible, as demonstrated by reheating protein samples (data not shown). Data were collected with the program ORIGIN (MicroCal Software; Northampton, MA). Buffer vs buffer baseline data were subtracted from protein vs buffer data. Molar heat capacity was obtained by dividing this subtracted quantity by the number of moles of protein in the sample cell.

Steady-state kinetic analyses

The ability of RNase A and the disulfide variants to catalyze the cleavage of poly(C) was assessed using UV spectroscopy. Concentrations of mononucleotide units in poly(C) were determined by UV absorption in 10 mM Tris-HCl buffer (pH 7.8) containing EDTA (1.0 mM) by assuming that $\varepsilon = 6200\ M^{-1}cm^{-1}$ at 268 nm (Eberhardt *et al.*, 1996). The difference in molar absorptivity between a mononucleotide unit in the polynucleotide substrate and the mononucleotide 2′,3′-cyclic phosphate product was assumed to be $\Delta\varepsilon = 2{,}380\ M^{-1}cm^{-1}$ at 250 nm (delCardayré *et al.*, 1995). All assays were performed at 10 °C in 0.10 M MES-NaOH buffer (pH 6.0) containing NaCl (0.10 M), poly(C) (1.18 μM – 2.7 mM), and an appropriate amount of enzyme. Values of k_{cat}, K_m, and k_{cat}/K_m were determined from the initial velocity data with the program HYPERO (Cleland, 1979).

2.4 Results

Protein production and purification

An *Escherichia coli* (*E. coli*) T7 RNA polymerase system was used to direct the expression of wild-type RNase A and the disulfide variants (delCardayré *et al.*, 1995). The target proteins accumulated as inclusion bodies, and were folded and purified by using both gel filtration and cation exchange chromatography. After purification, each protein was determined to be >99% pure by SDS–PAGE. In addition, each protein had $A_{280}/A_{260} > 1.8$, indicating that the preparations were not contaminated significantly with nucleic acid (Layne, 1957). Approximately 40 mg of pure wild-type RNase A were obtained per L of culture. Following expression of appropriately mutated cDNA in *E. coli* strain BL21(DE3), similar yields were obtained of the C65A/C72A, C40A/C95A and C26A/C84A variants. The C58A/C110A variant was more difficult to fold correctly, yielding only 5 mg of pure protein per L of culture.

Thermal unfolding monitored by ultraviolet spectroscopy

A plot of A_{287} vs temperature was converted into one of f_u vs temperature, where f_u is the fraction of unfolded protein at a given temperature (Pace *et al.*, 1989). The reversible thermal unfolding curves of wild-type RNase A and the C65A/C72A, C40A/C95A, C26A/C84A, and C58A/C110A variants are shown in Fig. 2.2A. The thermal transition of each of the disulfide variants occurred at a lower temperature than did that of wild-type RNase A. The Cys65–Cys72 and Cys40–Cys95 disulfide bonds crosslink surface loops in RNase A. The absence of either disulfide bond destabilizes the protein significantly. In wild-type RNase A, the disulfide bonds between Cys26–Cys84 and Cys58–Cys110 link an α-helix to a β-sheet. The conformational stability of C26A/C84A RNase A or C58A/C110A RNase A is still

lower than that of the C65A/C72A or C40A/C95A variant. The absence of either cystine lowers stability such that the C26A/C84A and C58A/C110A variants are approximately half folded at room temperature.

The disulfide bond contribution to conformational stability was determined by fitting the f_u vs temperature data for wild-type RNase A and the disulfide variants using the program SIGMA PLOT 4.16 (Jandel Scientific; SanRafael, CA) to the equations (Pace *et al.*, 1989):

$$\Delta G(T) = \Delta H_m(1 - T/T_m) + \Delta C_p[T - T_m - T\ln(T/T_m)] \quad (2.1)$$

$$\Delta G(T) = -RT\ln K = -RT\ln[f_u/(1 - f_u)] \quad (2.2)$$

where the subscript "*m*" refers to values at the midpoint of the thermal unfolding curve and ΔC_p = 1.15 kcal/(mol·K) for wild-type RNase A (Pace *et al.*, 1999) and the disulfide variants. As listed in Table 2.1, the value of T_m^{UV} (where the superscript "*UV*" refers to parameters obtained by UV spectroscopy) for the wild-type protein is consistent with values published previously (Santoro *et al.*, 1992; Eberhardt *et al.*, 1996; Catanzano *et al.*, 1997). The values of T_m^{UV} for C65A/C72A RNase A and C40A/C95A RNase A are decreased by 19.4 °C and 21.2 °C, respectively. Absolute values of T_m^{UV} could not be compared to literature values because of differing solution conditions. Still, the value of ΔT_m^{UV} for C40A/C95A RNase A is similar to a value determined previously (Laity *et al.*, 1997). Also, replacing Cys65 and Cys72 with a pair of serine residues results in a value of ΔT_m^{UV} that is similar to that for C65A/C72A RNase A (Laity *et al.*, 1993). The values of T_m^{UV} for C26A/C84A RNase A and C58A/C110A RNase A are decreased by 34.4 °C and 37.7 °C, respectively. Replacing Cys26 and Cys84 or Cys58 and Cys110 with a pair of serine residues results in variants that are too unstable to allow for the determination of T_m^{UV} values (Laity *et al.*, 1993). The removal of

each crosslink caused a large perturbation to the protein and therefore the free energy of perturbation could not be determined for the disulfide variants (Becktel & Schellman, 1987).

Thermal unfolding monitored by differential scanning calorimetry

Solution conditions used during DSC experiments were identical to those used during UV spectroscopic studies. The reversible DSC profiles of the relative heat capacity are shown in Fig. 2.2B. These profiles were fitted to equations describing a two-state model for unfolding: $N \rightleftarrows U$ where N is the native state and U is the unfolded state. The change in heat capacity (ΔC_p) upon unfolding has traditionally been assumed to be constant with temperature. Privalov and coworkers have shown that ΔC_p may only be constant over a narrow temperature range and can vary greatly over a broad range of temperature (Wintrode *et al.*, 1994). Our experiments were performed over a broad range of temperature. To model the temperature-dependence in heat capacity, we employed the methods of Privalov and coworkers (Privalov *et al.*, 1989). Curve fitting was done by non-linear regression analysis using the program NLREG (P. H. Sherrod, unpublished results). As is apparent from Fig. 2.2B, the thermal unfolding of wild-type RNase A, C65A/C72A RNase A, and C40A/C95A RNase A fit well to the two-state model. The thermal transition of C26A/C84A RNase A and C58A/C110A RNase A begin below 15 °C and fit less well to the two-state model. Attempts to fit the data to a cold denaturation model were unsuccessful.

Compared to wild-type RNase A, the values of T_m^{DSC} (where the superscript "*DSC*" refers to parameters obtained by DSC) for the C65A/C72A, C40A/C95A, C26A/C84A, and C58A/C110A variants are decreased by 19.4, 22.8, 35.3, and 36.3 °C, respectively (Table 2.1). The values of ΔH_m^{DSC} for the variants are less than that for the wild-type protein. Moreover, as the T_m^{DSC} of a variant decreases, the value of ΔH_m^{DSC} decreases. The values of

ΔH_m^{DSC} for wild-type RNase A and the C65A/C72A, C40A/C95A, C26A/C84A and C58A/C110A variants are 113.7, 91.8, 77.3, 70.2, and 45.5 kcal/mol, respectively.

The values of van't Hoff enthalpy (ΔH_{vH}) for the unfolding of the wild-type and variant proteins were calculated from the shapes of the calorimetric scans with the equation (Privalov & Potekhin, 1986; Carra *et al.*, 1996):

$$\Delta H_{vH} = \frac{4RT_m^2}{\Delta H_{cal}}\left(\langle C_p \rangle_{max} - \frac{\Delta C_p}{2}\right) \tag{2.3}$$

where $\langle C_p \rangle_{max}$ is the heat capacity at the T_m^{DSC} and the calorimetric enthalpy (ΔH_{cal}) is equal to the area under the DSC curve (Fig. 2.2B). A van't Hoff enthalpy equal to the calorimetric enthalpy is evidence of two-state unfolding (Carra *et al.*, 1996). As listed in Table 2.1, the values of $\Delta H_{vH}/\Delta H_{cal}$ for wild-type RNase A and the C65A/C72A, C40A/C95A, C26A/C84A, and C58A/C110A variants are 1.00, 0.98, 0.97, 0.96, and 1.05, respectively.

Steady-state kinetic parameters

Wild-type RNase A enhances the rate of RNA cleavage by 10^{12}-fold compared to the uncatalyzed reaction (Thompson *et al.*, 1995). All four disulfide variants are also efficient catalysts of RNA cleavage. This efficiency is consistent with each disulfide variant being folded correctly and having a three-dimensional structure similar to that of wild-type RNase A. Wild-type RNase A and the disulfide variants all begin their thermal unfolding transitions above 13 °C (Fig. 2.2). Steady-state kinetic parameters for the cleavage of poly(C) by wild-type RNase A and the disulfide variants were therefore determined at 10 °C, where all proteins are >99% folded. The values of these parameters are listed in Table 2.2.

The replacement of a cystine with a pair of alanine residues decreases the value of k_{cat} (Table 2.2). C58A/C110A RNase A and C26A/C84A RNase A have a 1.3- to 1.4-fold lower

k_{cat} than does the wild-type enzyme. The value of k_{cat} is affected more significantly for C40A/C95A RNase A and C65A/C72A RNase A (4.3- to 4.4-fold). A moderate (1.8- to 8.9-fold) increase in the value of K_m is apparent for each disulfide variant relative to that of wild-type RNase A. Furthermore, the values of K_m for the C65A/C72A and C40A/C95A variants are increased to a greater extent than are those for the C58A/C110A and C26A/C84A variants. The values of k_{cat}/K_m for the RNase A disulfide variants are 2.3- to 40-fold lower than that of the wild-type enzyme (Table 2.2).

2.5 Discussion

The stability of RNase A is legendary. For example, the classical procedure for the purification of RNase A from a bovine pancreas relies on the enzyme maintaining its integrity and solubility under harsh conditions: first, 0.25 N sulfuric acid at 5 °C, and then, pH 3.0 at 95–100 °C (Kunitz & McDonald, 1953). These conditions disrupt noncovalent interactions but do not break the four disulfide bonds of RNase A, which are disposed in an interweaving but symmetrical network that crosslinks various elements of its secondary structure (Fig. 2.1).

Disulfide bond-mediated contributions to conformational stability

Disulfide bonds are the only common covalent crosslinks in polypeptide chains. Crosslinks limit the number of unfolded conformations of a polypeptide chain, thereby destabilizing the unfolded state relative to the native state (Flory, 1956). If this loss of entropy in the unfolded state were the only disulfide bond-mediated contribution to conformational stability, then disulfide bond-mediated stability would be reflected in the loop size—the number of amino acid residues (η) within the ring containing the disulfide bond (Flory, 1956). This model has also been applied to proteins with interweaving crosslinks,

including RNase A (Poland & Scheraga, 1965; Pace *et al.*, 1988). A disulfide bond within a large ring would decrease the stability of the unfolded state more than one within a small ring. Introduction of a new disulfide bond into a protein structure can either increase (Villafranca *et al.*, 1987; Matsumura *et al.*, 1989; Ko *et al.*, 1996; Yamaguchi *et al.*, 1996) or decrease (Wells & Powers, 1986; Matsumura *et al.*, 1989; Betz *et al.*, 1996) conformational stability.

To dissect the contributions of disulfide bonds to the conformational stability and catalytic activity of RNase A, we chose to replace each cystine with a pair of alanine residues, which is the most conservative natural replacement for a cystine. Each cystine side chain of RNase A has a solvent-accessible surface area of <0.07 nm^2 (Fig. 2.1), which is <15% of the maximum. Replacing a buried cystine in BPTI with an alanine residue and a serine residue or with two serine residues was found to be more destabilizing than replacing it with a pair of alanine residues (Lui *et al.*, 1997). Likewise, the results of molecular dynamics simulations suggest that replacing a cysteine residue in the core of BPTI with serine is more unfavorable than is replacing it with alanine (Darby *et al.*, 1991; Staley & Kim, 1992).

The thermal unfolding of wild-type RNase A and each of the four disulfide variants were monitored by UV spectroscopy and DSC. These two methods probe different aspects of protein unfolding. UV spectroscopy reports on the change in molar absorptivity as the protein unfolds. DSC reports directly on the heat absorbed during protein unfolding. The values of T_m obtained by these two distinct methods are in gratifying agreement (Table 2.1), and show that each disulfide bond of RNase A contributes significantly to its thermal stability.

The relative contribution of each disulfide bond to the conformational stability of RNase A depends on its location within the polypeptide chain relative to the other disulfide bonds. This disulfide bond connectivity is shown in Fig. 2.1. Disulfide bonds that tether otherwise free residues of a polypeptide chain are likely to decrease the conformational

entropy of the unfolded state (and thus enhance conformational stability) more than disulfide bonds that crosslink residues that are otherwise restrained (Thornton, 1981; Harrison & Sternberg, 1994). Of the four RNase A disulfide bonds, Cys26–Cys84 and Cys58–Cys110 contribute most significantly to conformational stability (Table 2.1). These disulfide bonds are the outermost crosslinks in the polypeptide chain. When the Cys26–Cys84 disulfide bond is removed, 14 *N*-terminal residues become less restricted. Likewise, when the Cys58–Cys110 disulfide bond is removed, 15 *C*-terminal residues are liberated.

The Cys40–Cys95 disulfide bond encloses a loop of similar size to that of the Cys26–Cys84 and Cys58–Cys110 disulfide bonds (Fig. 2.1). Yet, the Cys40–Cys95 disulfide bond contributes less to conformational stability (Table 2.1). Residues 40 – 95 are constrained by 3 overlapping disulfide bonds: Cys26–Cys84, Cys40–Cys95, and Cys58–Cys110. Even in the absence of the Cys40–Cys95 disulfide bond, residues 40 – 95 are restricted by the two more terminal crosslinks.

Of the four disulfide bonds in RNase A, the Cys65–Cys72 disulfide bond encloses the smallest loop and contributes least to conformational stability. Interestingly, the Cys65–Cys72 disulfide bond is the only disulfide bond that is not absolutely conserved throughout the ribonuclease A superfamily (Beintema *et al.*, 1988). For example, this disulfide bond is absent from the RNase A homologs in snapping turtle (Beintema & van der Laan, 1986) and iguana (Zhao *et al.*, 1994) as well as from the angiogenins (Strydom *et al.*, 1985; Bond *et al.*, 1993) and Onconase™ (Ardelt *et al.*, 1991). The ribonucleolytic activity of each of these enzymes is less than that of RNase A [Zhao, 1994 #684; Katoh, 1986 #193; Boix, 1996 #767; (Leland *et al.*, 1998; Kelemen *et al.*, 1999), as expected from our analysis of catalysis by the C65A/C72A variant (*vide infra*).

Disulfide bond-mediated contributions to catalytic activity

Disulfide bonds can be important for the function of a protein, as well as its conformational stability. Indeed, replacing a native disulfide bond with a pair of alanine residues can result in a variant protein that has greater conformational stability than does the wild-type protein (Zhu *et al.*, 1995). In other words, a native disulfide bond can actually destabilize the tertiary structure. Such disulfide bonds may be retained by natural selection to enable a particular function (Blake *et al.*, 1994; Wang *et al.*, 1997).

RNase A catalyzes the cleavage of the P-$O^{5'}$ bond of RNA on the 3′ side of pyrimidine residues to yield a 2′,3′-cyclic phosphodiester. His12 and His119 are the base and acid that mediate the transphosphorylation reaction (Findlay *et al.*, 1961). Lys41 assists in transition state stabilization (Messmore *et al.*, 1995). Replacing any of these three residues with alanine hinders catalysis by 10^4- to 10^5-fold (Raines, 1998). To achieve the maximal rate of substrate cleavage, each active-site residue must be aligned precisely.

The steady-state kinetic parameters for catalysis by the disulfide variants are similar to those of the wild-type enzyme. Yet for each variant enzyme, the value of K_m is increased and the value of k_{cat} is decreased (Table 2.2). Apparently, each disulfide bond serves to orient more precisely the active-site residues.

The disulfide bonds that are least important to conformational stability are most important to catalytic activity. The loss of a disulfide bond near the active site (Cys65–Cys72 and Cys40–Cys95; Fig. 2.1) affects catalysis more dramatically than does the loss of a more remote disulfide bond (Cys26–Cys84 and Cys58–Cys110). The Cys65–Cys72 and Cys40–Cys95 disulfide bonds contribute 40- and 31-fold, respectively, to k_{cat}/K_m, whereas the Cys26–Cys84 and Cys58–Cys110 disulfide bonds contribute only 6- and 2-fold, respectively (Table 2.2).

The Cys65–Cys72 and Cys40–Cys95 disulfide bonds are proximal to key enzymic residues. The half-cystine at residue 40 is adjacent to Lys41. Removing a hydrogen bond to the main-chain oxygen of Lys41 diminishes catalytic activity (Eberhardt *et al.*, 1996). In the C40A/C95A variant, large localized perturbations disrupt the orientation of Lys41 (Laity *et al.*, 1997). Likewise, without the Cys65–Cys72 disulfide bond, the 65–72 surface loop is more flexible (Shimotakahara *et al.*, 1997). The half-cystine at residue 65 is adjacent to Lys66. The main chain of Lys66 assists in aligning His119 (Schultz *et al.*, 1998). Moreover, a Coulombic interaction between the side chain of Lys66 and an RNA substrate is important for catalysis (Fisher *et al.*, 1998). Thus, the Cys65–Cys72 and Cys40–Cys95 disulfide bonds may have evolved, at least in part, to position precisely residues important for catalysis of RNA cleavage.

2.6 Acknowledgements

We thank Drs. Darrell R. McCaslin and L. Wayne Schultz for assistance. This work was supported by grants GM44783 (National Institutes of Health) and BES-9604563 (National Science Foundation). T.A.K. was supported by an Advanced Opportunity Fellowship. K.J.W. was supported by a WARF predoctoral fellowship and Chemistry – Biology Interface Training Grant GM08505 (NIH). K.M.T. was supported by a Howard Hughes Medical Institute predoctoral fellowship. Calorimetry data were obtained at the University of Wisconsin–Madison Biophysical Instrumentation Facility, which is supported by the University of Wisconsin–Madison and grant BIR-9512577 (NSF).

Table 2.1. Thermodynamic Parameters for the Unfolding of Wild-Type Ribonuclease A and the C65A/C72A, C40A/C95A, C26A/C84A, and C58A/C110A Variants

Values were obtained by ultraviolet spectroscopy* and differential scanning calorimetry†

Ribonuclease A	T_m^{UV} (°C) *	T_m^{DSC} (°C) †	ΔH_m^{DSC} (kcal/mol) †	$\Delta H_{vH}/\Delta H_{cal}$ †
wild-type	61.6 ± 0.3	62.1 ± 0.2	113.7 ± 2.8	1.00
C65A/C72A	42.3 ± 0.2	42.7 ± 0.1	91.8 ± 3.3	0.98
C40A/C95A	40.4 ± 0.2	39.3 ± 1.0	77.3 ± 2.1	0.97
C26A/C84A	27.2 ± 1.7	26.8 ± 0.9	70.2 ± 2.5	0.96
C58A/C110A	23.9 ± 0.2	26.1 ± 0.3	45.5 ± 0.7	1.05

*Values (± SE) from ultraviolet spectroscopy are for triplicate experiments in 0.030 M sodium acetate buffer (pH 6.0) containing NaCl (0.10 M). Values of SE are the standard errors from replicate experiments.

†Values (± SE) from differential scanning calorimetry are for duplicate experiments performed in 0.030 M sodium acetate buffer (pH 6.0) containing NaCl (0.10 M). Values of SE are the standard errors from replicate experiments. Determinate errors for T_m^{DSC} and ΔH_m^{DSC} are approximately 1% and 5%, respectively.

Table 2.2. Steady-State Kinetic Parameters for Catalysis by Wild-Type Ribonuclease A and the C65A/C72A, C40A/C95A, C26A/C84A, and C58A/C110A Variants

Values are for the cleavage of poly(cytidylic acid).

Ribonuclease A	k_{cat} (s^{-1})	K_m (mM)	k_{cat}/K_m (10^6 $M^{-1}s^{-1}$)
wild-type	190 ± 11	0.047 ± 0.011	4.0 ± 1.0
C65A/C72A	43 ± 5	0.42 ± 0.13	0.10 ± 0.03
C40A/C95A	44 ± 3	0.34 ± 0.07	0.13 ± 0.03
C26A/C84A	135 ± 20	0.19 ± 0.07	0.71 ± 0.28
C58A/C110A	147 ± 3	0.084 ± 0.007	1.76 ± 0.15

*Assays were performed at 10 °C in 0.10 M MES-NaOH buffer (pH 6.0) containing NaCl (0.10 M). Values (± SE) of K_m and k_{cat}/K_m are based on nucleotide units in poly(C).

Figure. 2.1. Structural representations of ribonuclease A.

(A) Ribbon diagram with inscriptions referring to the location of the disulfide bonds and active-site residues. The solvent-accessible surface area (0.52 nm^2 = 100%) of the cystine side chains in the crystalline protein (PDB entry 7RSA) are Cys26–Cys84, 0 nm^2; Cys58–Cys110, 0.02 nm^2; Cys40–Cys95, 0.06 nm^2; and Cys65–Cys72, 0.07 nm^2. (B) Scheme showing the connectivity of the disulfide bonds. The secondary structural context of the half-cystines is indicated by H, α-helix; L, surface loop; or S, β-sheet.

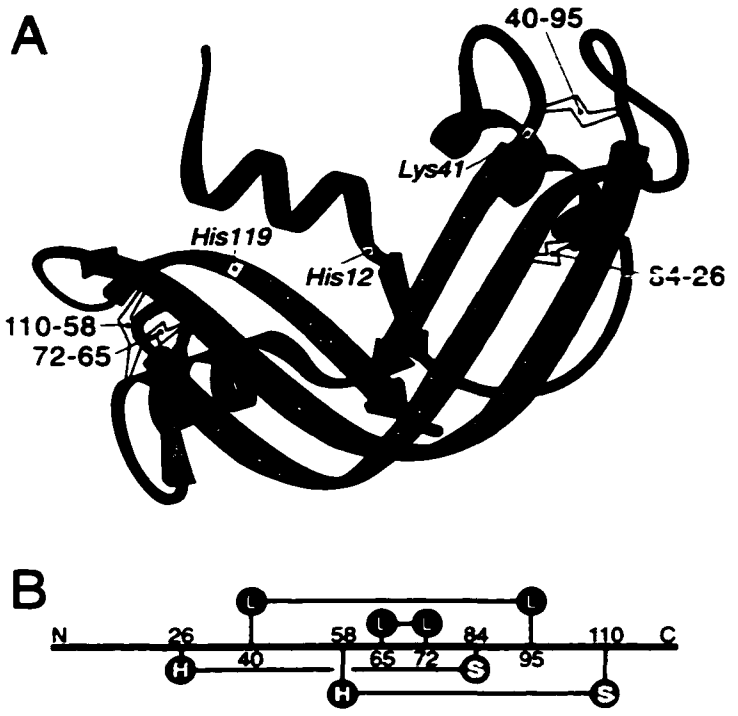
A
40-95
Lys41
His119
His12
84-26
110-58
72-65
B
N
26
58
84
110
C
40
65
72
95
L
H
S

Figure. 2.2. Unfolding of wild-type ribonuclease A and disulfide variants as monitored by (A) ultraviolet spectroscopy and (B) differential scanning calorimetry.

Data are for wild-type RNase A, and the C65A/C72A, C40A/C95A, C26A/C84A, and C58A/C110A variants in 0.030 M sodium acetate buffer (pH 6.0) containing NaCl (0.10 M). Inset in (A) shows raw data for the thermal denaturation and renaturation of C58A/C110A RNase A. Data in (B) have been shifted along the ordinate to equalize the value of C_p for each unfolded protein.

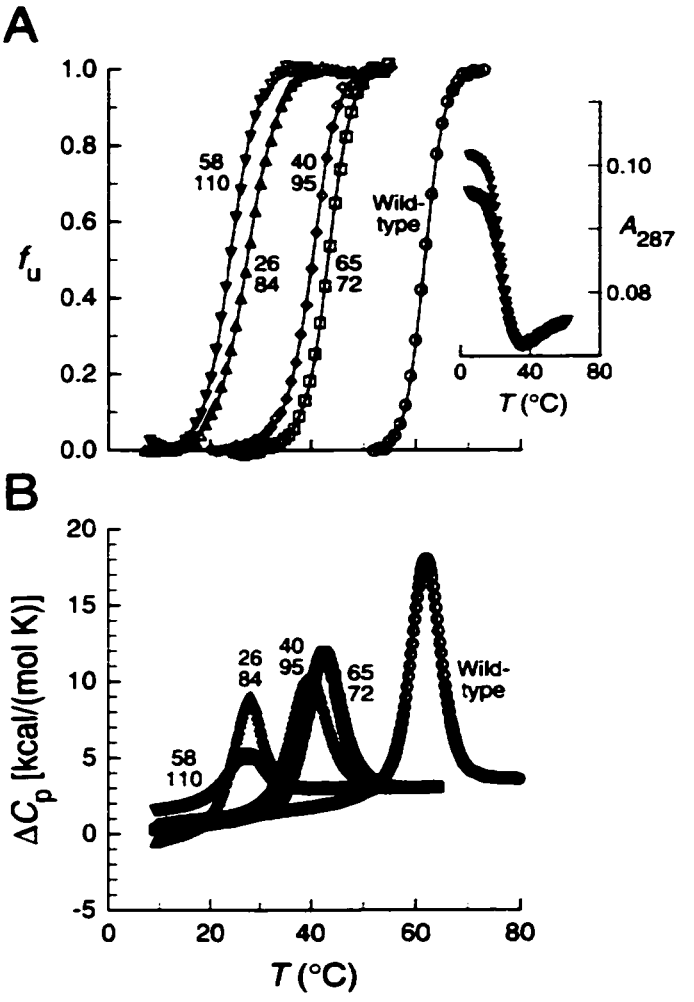
A
1.0
0.8
0.6
0.4
0.2
0.0
f_u
58
110
26
84
40
95
65
72
Wild-
type
0.10
0.08
A_{287}
0
40
80
T (°C)
B
20
15
10
5
0
-5
ΔC_p [kcal/(mol K)]
58
110
26
84
40
95
65
72
Wild-
type
0
20
40
60
80
T (°C)

Chapter 3

Conformational Stability is a Determinant of Ribonuclease A Cytotoxicity

Portions of this chapter were published as:

Klink, T.A. and Raines, R.T. (2000) Conformational stability is a determinant of ribonuclease A cytotoxicity *J. Biol. Chem.* **275** 17463-17467.

Abbreviations. DSC, differential scanning calorimetry; 6-FAM, 6-carboxyfluorescein; 6-TAMRA, 6-carboxytetramethylrhodamine; MES, 2-(N-morpholino)ethanesulfonic acid; PAGE, polyacrylamide gel electrophoresis; poly(C), poly(cytidylic acid); RI, ribonuclease inhibitor; RNase A, bovine pancreatic ribonuclease A; RNase B, bovine pancreatic ribonuclease B; SDS, sodium dodecyl sulfate; Tris, tris(hydroxymethyl)aminomethane.

3.1 Abstract

Onconase™, a homolog of ribonuclease A (RNase A) with high conformational stability, is cytotoxic and has efficacy as a cancer chemotherapeutic. Unlike wild-type RNase A, the G88R variant is toxic to cancer cells. Here, variants in which disulfide bonds were removed from or added to G88R RNase A were used to probe the relationship between conformational stability and cytotoxicity in a methodical manner. The conformational stability of the C40A/G88R/C95A and C65A/C72A/G88R variants is less than that of G88R RNase A. In contrast, a new disulfide bond that links the *N*- and *C*-termini (residues 4 and 118) increases the conformational stability of G88R RNase A and C65A/C72A/G88R RNase A. These changes have little effect on the ribonucleolytic activity of the enzyme or on its ability to evade the cytosolic ribonuclease inhibitor protein. The changes do, however, have a substantial effect on toxicity towards human erythroleukemia cells. Specifically, conformational stability correlates directly with cytotoxicity as well as with resistance to proteolysis. These data indicate that conformational stability is a key determinant of RNase A cytotoxicity, and suggest that cytotoxicity relies on avoiding proteolysis. This finding suggests a means to produce new cancer chemotherapeutics based on mammalian ribonucleases.

3.2 Introduction

The free energy difference between the native and unfolded states of a protein is small—typically 5 – 15 kcal/mol (Dill, 1990; Richards, 1997). In their native state, many proteins are less susceptible to proteolytic degradation than when unfolded (Pace & Barrett, 1984). In the unfolded state, the steric protection of peptide bonds provided by the compact native state is lost (Vindigni *et al.*, 1994). For example, bovine pancreatic ribonuclease A [RNase A;[1] EC 3.1.27.5 (Raines, 1998; Raines, 1999)] is degraded more readily by proteases in the presence of denaturants or elevated temperatures (Mihalyi & Harrington, 1959; Ooi *et al.*, 1963; Rupley & Scheraga, 1963; Anfinsen & Scheraga, 1975), and less readily when glycoyslated (Arnold & Ulbrich-Hofmann, 1997).

The rates of intracellular protein turnover vary by 10^3-fold (Isenman & Dice, 1989). Apparently, some proteins are better able to thwart the proteolytic machinery (Rechsteiner *et al.*, 1987; Rogers & Rechsteiner, 1988). These proteins remain intact and retain activity longer within the cell. A correlation between the conformational stability of a protein and its catabolism was reported over twenty years ago (McLendon, 1977). Since then, studies using unrelated proteins have either supported (McLendon & Radany, 1978) or contradicted (Rogers & Rechsteiner, 1988; Rote *et al.*, 1989) this correlation. Drawing conclusions from these studies is problematic because the proteins were divergent in characteristics that have been implicated in metabolic turnover. In contrast, variants of a single protein, the *N*-terminal domain of the repressor protein from bacteriophage λ, have been used to demonstrate a definite link between conformational stability and metabolic turnover (Parsell & Sauer, 1989). More recently, the conformational stability of bovine pancreatic trypsin inhibitor

variants was shown to correlate with the yield of intact protein produced in a heterologous system (Kowalski *et al.*, 1998).

RNase A homologs elicit diverse biological activities, including specific toxicity to cancer cells (Youle & D'Alessio, 1997; Rybak & Newton, 1999). Onconase™, which is a homolog of RNase A in the Northern leopard frog, is now in Phase III clinical trials for the treatment of malignant mesothelioma. It has been shown that the ribonucleolytic activity of ribonucleases is essential to their cytotoxicity (Ardelt *et al.*, 1991; Kim *et al.*, 1995). Nonetheless, ribonucleolytic activity is not the only requirement for a ribonuclease to be a cytotoxin. For example, relative to Onconase, RNase A is a 500-fold more effective catalyst of RNA cleavage (Wu et al, 1993), yet RNase A is not toxic to cancer cells. Still, we propose that the high ribonucleolytic activity of RNase A could engender a potent cytotoxin. Indeed, substitutions at Gly-88 enable RNase A to mimic the ability of Onconase to evade the endogenous ribonuclease inhibitor protein (RI) and become cytotoxic (Leland *et al.*, 1998). Still, no RNase A homolog is as cytotoxic as Onconase.

Onconase and RNase A differ substantially in another property—conformational stability. The value of T_m (which is the temperature at the midpoint of the thermal transition) for Onconase [T_m = 90 °C] is much greater than that of RNase A [T_m = 63 °C] (Leland *et al.*, 1998). Is conformational stability a determinant of ribonuclease cytotoxicity? Answering this question requires a means to increase or decrease conformational stability without altering other important properties of the enzyme. We suspected that adding or removing disulfide bonds would provide such a subtle means.

RNase A contains four disulfide bonds (Cys-26–Cys-84, Cys-40–Cys-95, Cys-58–Cys-110, and Cys-65–Cys-72; Fig. 3.1). Previously, we dissected the contribution of

each disulfide bond to conformational stability by replacing each cystine with a pair of alanine residues (Klink *et al.*, 2000). Of the four disulfide bonds, the Cys-40–Cys-95 and Cys-65–Cys-72 crosslinks are the least important to conformational stability (Laity *et al.*, 1993; Klink *et al.*, 2000). Removing these disulfide bonds leads to RNase A variants that have T_m values below that of the wild-type enzyme but above physiological temperature.

Here, we investigate the relationship between the conformational stability and cytotoxicity of RNase A. Specifically, we construct G88R RNase A variants that are missing the Cys-40–Cys-95 or Cys-65–Cys-72 disulfide bonds. We also introduce a new disulfide bond into G88R RNase A and a variant missing the Cys-65–Cys-72 disulfide bond. We find that the T_m values for G88R RNase A and its four disulfide variants vary by nearly 30 °C. We show that conformational stability is linked to protease susceptibility *in vitro*. Finally, we demonstrate that each variant is toxic to cancer cells and, most significantly, that cytotoxicity is correlated with conformational stability.

3.3 Experimental Procedures

Materials

Escherichia coli strain BL21(DE3) (F^- ompT $r_B^-m_B^-$) was from Novagen (Madison, WI). *E. coli* strain DH5α, RPMI medium, fetal bovine serum, Proteinase K, penicillin, and streptomycin were from Gibco BRL (Gaithersburg, MD). *E. coli* strain CJ236 and helper phage M13K07 were from Bio-Rad (Richmond, CA). A plasmid encoding G88R RNase A was a generous gift of P. A. Leland (Leland *et al.*, 1998). All enzymes for the manipulation of recombinant DNA were from Promega (Madison, WI) or New England Biolabs (Beverly, MA). RI was from Promega. [*methyl*-^{3}H]Thymidine (6.7 Ci/mmol) was from DuPont/NEN

(Boston, MA). K-562 human erythroleukemia cells were from the American Type Culture Collection (Manassas, VA).

Purified oligodeoxyribonucleotides and the fluorogenic substrate 6-FAM~(dA)rU$(dA)_2$~6-TAMRA were from Integrated DNA Technologies Inc (Coralville, IA). Poly(cytidylic acid) [poly(C)] was from Midland Certified Reagents (Midland, TX) and was precipitated from ethanol and washed with aqueous ethanol (70% v/v) before use. DNA was sequenced with an ABI 373XL automated sequencer using an Perkin Elmer Big Dye kit, FS (Foster City, CA) and an MJ Research PTC-100 Programmable Thermal Controller (Watertown, MA) at the University of Wisconsin Biotechnology Center (Madison, WI). IPTG was from Gold Biotechnology (St. Louis, MO). Bacto yeast extract, Bacto tryptone, Bacto peptone, and Bacto agar were from Difco (Detroit, MI). LB medium contained (in 1.00 L) Bacto tryptone (10 g), Bacto yeast extract (5 g), and sodium chloride (10 g). TB medium contained (in 1.00 L) Bacto tryptone (12 g), Bacto yeast extract (24 g), glycerol (4 mL), KH_2PO_4 (2.31 g), and K_2HPO_4 (12.54 g). PBS (pH 7.3) contained (in 1.00 L) KCl (0.20 g), KH_2PO_4 (0.20 g), NaCl (8.0 g), and Na_2HPO_4:$7H_2O$ (2.16 g). *E. coli* cell lysis was performed using a French pressure cell from SLM Aminco (Urbana, IL). FPLC Hiload 26/60 Superdex 75 gel filtration column and mono-S HR10/10 cation-exchange column were from Amersham Pharmacia Biotech (Piscataway, NJ). All media were prepared in distilled, deionized water and autoclaved. All other chemical reagents were of commercial reagent grade or better, and were used without further purification.

Instruments

Ultraviolet and visible absorbance measurements were made with a Cary 3 double beam spectrophotometer equipped with a Cary temperature controller from Varian (Sugar Land,

TX). Calorimetry experiments were performed with an MCS differential scanning calorimeter from MicroCal (Northampton, MA). Fluorescence measurements were performed on a QuantaMaster1 photon counting fluorometer from Photon Technology International (South Brunswick, NJ) equipped with sample stirring. The concentration of 6-FAM~(dA)rU(dA)$_2$~6-TAMRA was determined using ε = 102,400 M^{-1} cm^{-1} at 260 nm (Kelemen *et al.*, 1999).

Design of a New Disulfide Bond

The *C*-terminal residue of Onconase, which has greater conformational stability than does any other known homolog of RNase A, is a heterologous half-cystine. To attempt to enhance the conformational stability of RNase A, a new disulfide bond was designed to crosslink the *N*- and *C*-termini. Such a crosslink would greatly restrict the number of conformations of the polypeptide chain, thereby destabilizing the unfolded state relative to the native state (Flory, 1956). The program SYBYL (Tripos; St. Louis, MO) and atomic coordinates derived from crystalline RNase A [PDB entry 7RSA (Wlodawer *et al.*, 1988)] were used to determine the placement of the new disulfide bond. According to our molecular modeling, replacing Ala-4 and Val-118 with two half-cystine residues would crosslink the *N*- and *C*-termini without perturbing the three-dimensional structure of RNase A (Fig. 3.1). Replacing Arg-4 and Val-118 in the human homolog of RNase A with two half-cystine residues has been reported to make that enzyme more resistant to proteolysis by trypsin (Futami *et al.*, May 12–16, 1999).

Preparation of Ribonuclease A Variants

Oligonucleotide-mediated site-directed mutagenesis was used to create the RNase A variants. Plasmids encoding the G88R (Leland *et al.*, 1998), C40A/C95A, and C65A/C72A

(Klink *et al.*, 2000) variants were derived from plasmid pBXR, which directs the expression of RNase A in *E. coli* (delCardayré *et al.*, 1995). Mutagenesis was performed on plasmids encoding the G88R, C40A/C95A, and C65A/C72A variants replicated in *E. coli* strain CJ236 (Kunkel *et al.*, 1987). To produce plasmids encoding the C40A/G88R/C95A and C65A/C72A/G88R variants, the GGC codon for Gly-88 was replaced in DNA encoding the C40A/C95A and C65A/C72A variants using the oligodeoxyribonucleotide: TTGGAGCT**ACGCGTCTCACG** (reverse complement in bold). To produce plasmids encoding the A4C/G88R/V118C and A4C/C65A/C72A/G88R/V118C variants, the GCA codon for Ala-4 was replaced in DNA encoding the G88R and C65A/C72A/G88R variants using the oligodeoxyribonucleotide: **CTTGGCTGCACAAGTTTCCTTGC** (reverse complement in bold) and the GTC codon for Val-118 was replaced using the oligodeoxyribonucleotide: GCATCAAAGT**GACATGGCACATACGGGTTTCC** (reverse complement in bold).

Wild-type RNase A and its variants were produced and purified by methods described previously (Kim & Raines, 1993; delCardayré *et al.*, 1995) except for minor modifications in the conditions for oxidative folding (Leland *et al.*, 1998; Klink *et al.*, 2000). The purity of each protein was assessed by SDS–PAGE. Adding or removing a disulfide bond is expected to alter the extinction coefficient of RNase A by <1% (Gill & von Hippel, 1989; Pace *et al.*, 1995). Hence, the concentrations of wild-type RNase A and the disulfide variants were determined by using $\varepsilon = 0.72$ mL $mg^{-1}cm^{-1}$ at 277.5 nm (Sela *et al.*, 1957).

Assays of Conformational Stability

Differential scanning calorimetry (DSC) was used to determine the conformational stability of each RNase A variant. DSC experiments were performed as described (Klink *et al.*, 2000), with the following modifications. Protein solutions (0.99 – 5.6 mg/mL) were dialyzed exhaustively against PBS and then centrifuged at 15,300*g* for 30 min to remove particulate matter. Data were collected with the program ORIGIN (MicroCal Software; Northampton, Massachusetts). The unfolding of wild-type RNase A and each of the variants was >90% reversible, as demonstrated by reheating of the protein samples (data not shown).

Assays of Cytotoxicity

The cytotoxicity of the RNase A variants was assessed using the continuous human erythroleukemia cell line K-562 as described (Leland *et al.*, 1998). Briefly, K-562 cells were grown at 37 °C in RPMI medium supplemented with fetal bovine serum (10% v/v) with penicillin (100 units/mL) and streptomycin (100 μg/mL) in the presence of wild-type RNase A, a variant, or a PBS control for 44 h, followed by a 4 h pulse with [*methyl*-^{3}H]thymidine (0.20 μCi per well). Each experiment is the average of triplicate determinations for each ribonuclease concentration. The standard error of the values from each protein concentration is ≤20%. The IC_{50} value is the concentration of an RNase A variant that kills 50% of the K-562 cells.

Assays of Ribonucleolytic Activity

A fluorogenic substrate, 6-FAM~(dA)rU$(dA)_2$~6-TAMRA, was used to determine the values of k_{cat}/K_m for the RNase A variants (Kelemen *et al.*, 1999). A large increase in

fluorescence occurs upon cleavage of the P–$O^{5'}$ bond on the 3′ side of the single ribonucleotide residue embedded within this substrate (Kelemen *et al.*, 1999). Assays were performed with stirring in 2.0 mL of 0.10 M MES-NaOH buffer (pH 6.0) containing NaCl (0.10 M), 6-FAM~(dA)rU$(dA)_2$~6-TAMRA (60 nM), and enzyme (5 pM – 0.50 nM). Fluorescence was monitored at 515 nm with excitation at 495 nm. Values of k_{cat}/K_m were determined using eq 3.1 (Kelemen *et al.*, 1999):

$$I = I_0 + (I_f - I_0)(k_{cat} / K_m)[E]t \tag{3.1}$$

where I is the fluorescence intensity in photon counts per second, I_0 is the intensity of the substrate prior to addition of enzyme, and I_f is the final intensity when all the substrate is cleaved. Values of k_{cat}/K_m were determined by linear least squares regression analysis of initial velocity data, assuming that assays were performed at substrate concentrations below the K_m, which is near 22 μM (Kelemen *et al.*, 1999).

Assays of Inhibition by Ribonuclease Inhibitor

RI is a competitive inhibitor of RNase A that binds with a 1:1 stoichiometry (Blackburn *et al.*, 1977; Lee *et al.*, 1989; Hofsteenge, 1997). We had shown previously that as RI affinity decreases, RNase A cytotoxicity increases (Leland *et al.*, 1998). Commercial RI is stored in aqueous glycerol (50% v/v). To eliminate errors caused by pipetting viscous solutions, a buffer exchange to remove glycerol was performed and the RI activity in the resulting low-viscosity solutions was determined as described (Bretscher *et al.*, 2000) .

To determine values of K_i, we monitored the cleavage of 6-FAM~(dA)rU(dA)$_2$~6-TAMRA by the RNase A variants as a function of RI concentration. Assays were performed with stirring in 2.00 mL of 0.10 M MES-NaOH buffer (pH 6.0) containing NaCl (0.10 M), DTT (8.0 mM), 6-FAM~(dA)rU(dA)$_2$~6-TAMRA (60 nM), and enzyme (5 pM – 0.50 nM). Fluorescence was monitored at 515 nm with excitation at 495 nm. The value of k_{cat}/K_m was determined using eq 3.1. After 5 min, an aliquot (0.5 µl) of RI (11.5 nM) was added, and the rate of substrate turnover was determined again. Additional aliquots of RI were added at 5 min intervals until the fluorescence change decreased to less than 10% of its original value. Values of K_i were determined by nonlinear least-squares regression analysis of data fitted to eq 3.2 (Kelemen *et al.*, 1999):

$$\Delta I / \Delta t = (\Delta I / \Delta t)_0 \{K_i /(K_i + [I])\} \tag{3.2}$$

where $(\Delta I/\Delta t)_0$ is the turnover rate prior to addition of RI.

Assays of Proteolytic Susceptibility

Proteinase K is a nonspecific protease that catalyzes the hydrolysis of accessible peptide bonds in proteins. A discontinuous assay was employed to determine the susceptibility of each RNase A variant to Proteinase K. An RNase A variant (6.1 µM) was incubated in triplicate at 25 °C with Proteinase K (5 µg/mL) in 50 mM Tris-HCl buffer (pH 8.0) containing $CaCl_2$ (1.0 mM). Controls were incubated in buffer without Proteinase K. At known times, aliquots were removed and diluted with 0.10 M MES-NaOH buffer (pH 6.0) containing NaCl (0.10 M). The turnover of 6-FAM~(dA)rU(dA)$_2$~6-TAMRA (60 nM) was

monitored in 2.00 mL of 0.10 M MES-NaOH buffer (pH 6.0) containing NaCl (0.10 M) and enzyme (5 – 600 pM). Fluorescence was monitored at 515 nm with excitation at 495 nm. Values of k_{cat}/K_m were determined using eq 3.1. A plot of relative ribonucleolytic activity as a function of time was fitted to a first-order rate equation to determine the pseudo first-order rate constant (k) for inactivation by Proteinase K digestion. Values of $t_{1/2}^{\text{Proteinase K}}$ were determined from the rate constant using the equation: $t_{1/2}^{\text{Proteinase K}} = \ln 2/k$.

3.4 Results

Conformational Stability

The reversible thermal transitions of wild-type RNase A and the G88R, A4C/G88R/V118C, C40A/G88R/C95A, C65A/C72A/G88R, and A4C/C65A/C72A/G88R/V118C variants were fitted to equations describing a two-state model for unfolding: $N \underset{\leftarrow}{\overset{\rightarrow}{}} U$, where N is the native state and U is the unfolded state. Removing a native disulfide bond in RNase A decreases the stability significantly (Laity *et al.*, 1993; Klink *et al.*, 2000). The C65A/C72A/G88R and C40A/G88R/C95A variants are approximately 90% and 60% folded at 37 °C, respectively (data not shown). Compared to G88R RNase A, the T_m values for the C65A/C72A/G88R and C40A/G88R/C95A variants are decreased by 18.1 and 23.6 °C, respectively. In contrast to these variants, wild-type RNase A and the G88R, A4C/G88R/V118C, and A4C/C65A/C72A/G88R/V118C variants are >99% folded at 37 °C. The T_m values of wild-type RNase A and G88R RNase A are 63.2 and 64.0 °C, respectively (Table 3.1). Most interestingly, the new Cys-4–Cys-118 disulfide bond

in A4C/G88R/V118C RNase A increases the T_m by 4.8 °C relative to that of G88R RNase A. A similar increase in T_m occurs in the A4C/C65A/C72A/G88R/V118C variant relative to that of C65A/C72A/G88R RNase A.

Cytotoxicity

The cytotoxicity of wild-type RNase A and the G88R, A4C/G88R/V118C, C40A/G88R/C95A, C65A/C72A/G88R, and A4C/C65A/C72A/G88R/V118C variants was assessed by measuring the incorporation of [*methyl*-^{3}H]thymidine into cellular DNA after a 44-h incubation with K-562 cells. Wild-type RNase A is not cytotoxic to K-562 cells at the concentrations used in this assay (Table 3.1, Fig. 3.2). The IC_{50} value of 9 μM for G88R RNase A agrees closely with those reported previously (Leland *et al.*, 1998; Bretscher *et al.*, 2000). Most significantly, adding the disulfide bond between residues 4 and 118 decreases the IC_{50} value for A4C/G88R/V118C RNase A by 3-fold (IC_{50} = 3 μM). Although still cytotoxic, each of the remaining variants is less cytotoxic than is G88R RNase A. The IC_{50} values for the C40A/G88R/C95A, C65A/C72A/G88R, and A4C/C65A/C72A/G88R/V118C variants are 25, 26, and 17 μM, respectively.

Ribonucleolytic Activity

A highly sensitive fluorometric assay was used to assess ribonucleolytic activity. The values of k_{cat}/K_m for wild-type RNase A and variants are the average of three independent assays. Each variant is a potent catalyst of RNA cleavage. At 25 °C, the values of k_{cat}/K_m for the variants are 2.4- to 90-fold lower than that of the wild-type enzyme (Table 3.1).

Inhibition by Ribonuclease Inhibitor

Inhibition of the ribonuclease-catalyzed cleavage of 6-FAM~(dA)rU$(dA)_2$~6-TAMRA by the RNase A variants was assessed in a continuous assay. The effect of RI concentration on the ribonucleolytic activity of each variant is reported as K_i (Table 3.1, Fig. 3.3). The value of K_i = 0.24 nM for G88R RNase A agrees closely with those reported previously (Leland *et al.*, 1998; Bretscher *et al.*, 2000). Removing or adding a disulfide bond to G88R RNase A affects only slightly its affinity for RI. The K_i values for the A4C/G88R/V118C, C40A/G88R/C95A, C65A/C72A/G88R, and A4C/C65A/C72A/G88R/V118C variants are 0.65, 0.35, 0.78, and 3.9 nM, respectively.

Protease Susceptibility

The proteolytic susceptibility of each of the RNase A variants was assessed by monitoring ribonucleolytic activity after exposure to Proteinase K. The C40A/G88R/C95A and C65A/C72A/G88R variants are the most susceptible to Proteinase K digestion. Further, the addition of the Cys-4–Cys-110 disulfide bond decreased the Proteinase K susceptibility of A4C/G88R/V118C RNase A and A4C/C65A/C72A/G88R/V118C RNase A relative to the G88R and C65A/C72A/G88R variants. The values of $t_{1/2}^{\text{Proteinase K}}$ for the A4C/G88R/V118C, G88R, A4C/C65A/C72A/G88R/V118C, C65A/C72A/G88R, and C40A/G88R/C95A variants are 6.9, 5.3, 5.3, 4.1, and 2.4 h^{-1}, respectively (Table 3.1).

3.5 Discussion

Disulfide bonds contribute to protein stability principally by limiting the flexibility of the unfolded polypeptide chain and thereby destabilizing the unfolded state relative to the native state (Flory, 1956). The loss of entropy in the unfolded state is not, however, the only effect of disulfide bonds on conformational stability. A disulfide bond can enhance (Kuroki *et al.*, 1992; Hinck *et al.*, 1996; Laity *et al.*, 1997) or diminish (Wells & Powers, 1986; Matsumura *et al.*, 1989; Zhu *et al.*, 1995; Betz *et al.*, 1996) interactions in the folded state that contribute to conformational stability. Thus, predicting the precise contribution of a particular native or nonnative disulfide bond to conformational stability is difficult. Still, we find that replacing a cystine with a pair of alanine residues is a superb means of altering conformational stability without affecting severely the other attributes of a protein. Moreover, the judicious addition of a new cystine to a protein expands the range of accessible stabilities.

Conformational Stability

RNase A contains four disulfide bonds that are important to its conformational stability (Klink *et al.*, 2000). Substitutions at Gly-88 have little effect on conformational stability but endow RNase A with cytotoxic activity (Leland *et al.*, 1998). We constructed four disulfide variants of G88R RNase A that are mostly folded at physiological temperature, which is the temperature of the cytotoxicity assays. The T_m values of the C65A/C72A/G88R and C40A/G88R/C95A variants are 18.1 and 23.6 °C lower, respectively, than that of G88R RNase A (Table 3.1). These decreases in conformational stability are similar to those suffered by the analogous disulfide variants of wild-type RNase A (Klink *et al.*, 2000). The other two variants have a new disulfide bond. A4C/G88R/V118C RNase A is the only known

disulfide variant of RNase A with greater conformational stability than the wild-type enzyme. Moreover, conformational stability lost by removing the native Cys-65–Cys-72 disulfide bond is recovered by adding the nonnative Cys-4–Cys-118 disulfide bond. The T_m values of the A4C/G88R/V118C and A4C/C65A/C72A/G88R/V118C variants are 4.8 and 4.5 °C higher, respectively, than that of the G88R and C65A/C72A/G88R variants (Table 3.1). Thus, the T_m values of the RNase A variants studied herein range from 40.4 to 68.8 °C.

Within the G88R RNase A variants, cytotoxicity correlates well with conformational stability (Fig. 3.5). For example, A4C/G88R/V118C RNase A has the highest T_m value of the five enzymes and is the most potent cytotoxin. In contrast, the C40A/G88R/C95A and C65A/C72A/G88R variants have the lowest T_m values and the highest IC_{50} values. The G88R and A4C/C65A/C72A/G88R/V118C variants have intermediate T_m values and intermediate IC_{50} values. These data are consistent with a model in which conformational stability is a determinant of cytotoxicity.

This model ignores the low thermodynamic stability of disulfide bonds in the reducing environment of the cytosol (Hwang *et al.*, 1992). The four disulfide bonds in wild-type RNase A are virtually inaccessible to solvent (Klink *et al.*, 2000), and have considerable kinetic stability in a highly reducing environment (Li *et al.*, 1995). Indeed, the $t_{1/2}$ of RNase A in the cytosol is >44 h (McElligott *et al.*, 1985), which is the incubation time of our cytotoxicity assays. Hence, we suspect that the disulfide bonds of RNase A are not susceptible to reduction in the cytosol within the time course of our assays.

Ribonucleolytic Activity

Ribonucleases must retain ribonucleolytic activity to be toxic to cells (Kim *et al.*, 1995). We determined the values of k_{cat}/K_m for the cleavage of 6-FAM~(dA)rU$(dA)_2$~6-TAMRA to determine if differences in cytotoxicity were caused by differences in ribonucleolytic activity. Each of the disulfide variants is a somewhat less efficient catalyst of RNA cleavage than is G88R RNase A (Table 3.1). Ribonucleolytic activity does not, however, correlate with cytotoxicity. For example, G88R RNase A has a 3-fold larger k_{cat}/K_m value than does A4C/G88R/V118C RNase A, but is less cytotoxic. Further, the C65A/C72A/G88R and C40A/G88R/C95A variants are 9- and 19-fold more efficient catalysts of RNA cleavage but are less cytotoxic than is A4C/C65A/C72A/G88R/V118C RNase A.

Inhibition by Ribonuclease Inhibitor

Cytosolic ribonucleolytic activity is controlled by the presence of RI (Hofsteenge, 1997). RI is a 50-kDa scavenger of pancreatic-type ribonucleases and forms a tight noncovalent complex with wild-type RNase A [$K_d = 4 \times 10^{-14}$ M (Lee *et al.*, 1989)]. Hence, wild-type RNase A has low cytotoxicity. Still, large quantities of RNase A in the cytosol can overwhelm the sentry. For example, microinjection of RNase A greatly increases its cytotoxicity (Saxena *et al.*, 1991).

Ribonucleases that are capable of evading cytosolic RI are cytotoxic at much lower concentrations than is RNase A (Wu *et al.*, 1993; Kim *et al.*, 1995). Indeed, Onconase has $>10^8$-fold lower affinity for RI than does RNase A (Boix *et al.*, 1996). Variations at Gly-88, which is an important contact point within the RI•RNase A complex, allows RNase A to

evade RI binding more effectively and increases its cytotoxicity (Kobe & Deisenhofer, 1995; Leland *et al.*, 1998).

Each of the G88R disulfide variants has slightly less affinity for RI than does G88R RNase A (Table 3.1). The K_i values of the disulfide variants are between 1.5- and 16-fold lower than that of G88R RNase A. Nonetheless, the affinity of RI for the G88R disulfide variants does not correlate with their cytotoxicity (Table 3.1). For example, A4C/C65A/C72A/G88R/V118C RNase A has a 16-fold lower affinity for RI than does G88R RNase A, but is less cytotoxic.

Proteinase K Susceptibility

Proteolytic susceptibility is greater in misfolded or unfolded proteins, relative to folded proteins (Anfinsen & Scheraga, 1975; Pace & Barrett, 1984). Steric hindrance of the peptide bonds in a folded protein blocks possible protease cleavage sites. Indeed, simple glycosylation can slow proteolysis (Arnold & Ulbrich-Hofmann, 1997). A protein with low conformational stability will exist in an unfolded state to a greater extent than a protein with high conformational stability, increasing proteolytic susceptibility (Parsell & Sauer, 1989).

Is the conformational stability of a ribonuclease linked to its cytotoxicity via its proteolytic susceptibility? C40A/G88R/C95A RNase A and C65A/C72A/G88R RNase A have the lowest conformational stability and the highest IC_{50} values, and are also the most susceptible to inactivation by Proteinase K digestion (Table 3.1). In contrast, A4C/G88R/V118C RNase A has the highest T_m value, is the most cytotoxic, and is the least susceptible to inactivation by Proteinase K digestion. The addition of the Cys-4–Cys-118 disulfide bond increases the T_m value and decreases both the IC_{50} value and the $t_{1/2}^{\text{Proteinase K}}$

value of two different enzymes. Thus, high conformational stability is linked to both high cytotoxicity and low proteolytic susceptibility.

Implications for the Mechanism of Cytotoxicity

The cytotoxicity of ribonucleases is manifested in the cytosol. To gain access to the cytosol, an extracellular ribonuclease must cross a cellular membrane. Protein traffic through membranes is thought to require unfolding prior to translocation (Rapoport *et al.*, 1996; Matouschek *et al.*, 1997). For example, the translocation of barnase variants across the mitochondrial membrane decreases with increasing disulfide crosslinks and conformational stability (49). Our data are in apparent conflict with this model, as the disulfide variants with greater conformational stability are more cytotoxic (Table 3.1). An explanation of this discrepancy is that the translocation of RNase A and its variants could be relatively rapid and another step, such as cytosolic proteolysis, could limit cytotoxicity. Indeed, protease inhibitors are known to increase the cytotoxicity of other protein cytotoxins (Fiani *et al.*, 1993). Similarly, the addition of proteolytic degradation signals can decrease protein cytotoxicity (Falnes & Olsnes, 1998). Finally, it is noteworthy that protein toxins such as diphtheria toxin, enterotoxin, and abrin II have T_m values near that of RNase A (Ramsay & Freire, 1990; van den Akker *et al.*, 1997; Krupkakar *et al.*, 1999). Increasing the conformational stability of these protein toxins could increase their cytotoxicity, as we have shown with G88R RNase A.

Relevance to Cancer Chemotherapy

Onconase, which is from an amphibian, is on the verge of approval as a human cancer chemotherapeutic. We find that enhanced conformational stability can increase the toxicity of

a mammalian homolog of Onconase towards cancer cells. This finding suggests a means to produce new cancer chemotherapeutics based on mammalian ribonucleases.

3.6 Acknowledgments

We thank M. C. Haigis, C. Park, L. W. Schultz, U. Arnold, D. R. McCaslin, K. J. Woycechowsky, and P. A. Leland for advice. Calorimetry data were obtained at the University of Wisconsin–Madison Biophysical Instrumentation Facility, which is supported by the University of Wisconsin–Madison and grant BIR-9512577 (NSF).

Table 3.1 Conformational Stability, Cytotoxicity, Ribonucleolytic Activity, Inhibition by Ribonuclease Inhibitor, and Protease Susceptibility of Wild-type Ribonuclease A and Disulfide Variants

Ribonuclease A	T_m [a]	IC_{50} [b]	k_{cat}/K_m [c]	K_i [d]	$t_{1/2}$ Proteinase K [e]
	°C	μM	10^5 $M^{-1}s^{-1}$	nM	h^{-1}
A4C/G88R/V118C	68.8 ± 0.1	3	49 ± 6	0.65 ± 0.11	6.9
G88R	64.0 ± 0.1	9	150 ± 30	0.24 ± 0.05	5.3
Wild-type	63.2 ± 0.1	>100	360 ± 40[f]	ND	ND
A4C/C65A/C72A/G88R/V118C	50.4 ± 0.1	17	4.0 ± 0.7	3.9 ± 0.3	5.3
C65A/C72A/G88R	45.9 ± 0.1	26	36 ± 2	0.78 ± 0.16	4.1
C40A/G88R/C95A	40.4 ± 0.2	25	76 ± 1	0.35 ± 0.05	2.4

[a]Values (± SE) from differential scanning calorimetry are for triplicate experiments performed in PBS. Determinate errors for T_m values are approximately 1%.

[b] Proliferation was measured by incorporation of ^{3}H-thymidine into cellular DNA after incubation with a ribonuclease at 37 °C for 44 h. Values are from triplicate measurements for each ribonuclease concentration from each of three independent experiments.

[c]Values (± SE) for cleavage of 6-FAM~(dA)rU(dA)$_2$~6-TAMRA are for triplicate experiments at 25 °C in 0.10 M MES-NaOH buffer (pH 6.0) containing NaCl (0.10 M).

[d]Values (± SE) for RI affinity are for triplicate experiments at 25 °C in 0.10 M MES-NaOH buffer (pH 6.0) containing NaCl (0.10 M) and DTT (8.0 mM).

[e]Values for inactivation by Proteinase K are from triplicate experiments at 25 °C in 50 mM Tris-HCl buffer (pH 8.0) containing $CaCl_2$ (1.0 mM).

[f]Value from ref (22).

Figure. 3.1. Structural representations of ribonuclease A.

(A) Ribbon diagram with inscriptions referring to the location of native (Cys-26–Cys-84, Cys-40–Cys-95, Cys-58–Cys-110, and Cys-65–Cys-72) and nonnative (Cys-4–Cys-118) disulfide bonds (PDB entry 7RSA). (B) Scheme showing the connectivity of the five native and nonnative disulfide bonds. The secondary structural context of the half-cystines is indicated by H, α-helix; L, surface loop; or S, β-sheet.

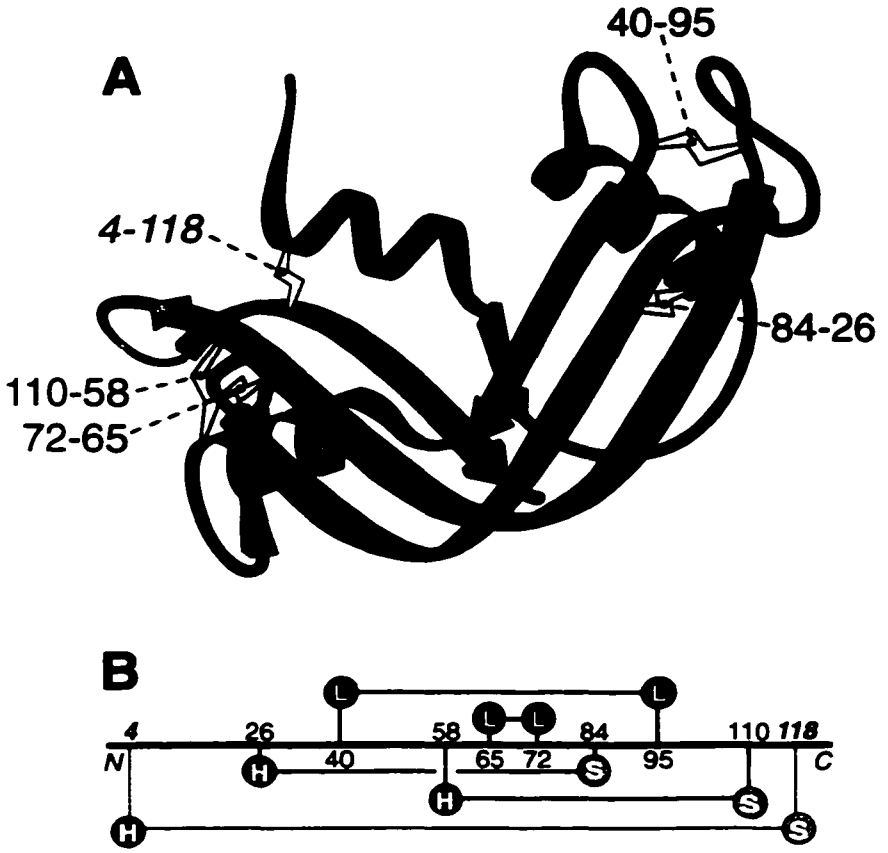
A
40-95
4-118
84-26
110-58
72-65
B
4
26
58
84
110
118
N
40
65
72
95
C
L
H
S

Figure. 3.2. Effect of ribonuclease A on the proliferation in culture of K-562 cells.

Data are for A4C/G88R/V118C (black), G88R (blue), A4C/C65A/C72A/G88R/V118C (orange), C40A/G88R/C95A (red), C65A/C72A/G88R (green), and wild-type RNase A (cyan). Proliferation was measured by incorporation of 3H-thymidine into cellular DNA after incubation of wild-type or variant ribonuclease A at 37 °C for 44-h. Values are from triplicate measurements from each of three independent experiments. The standard error of each value is 20% or less.

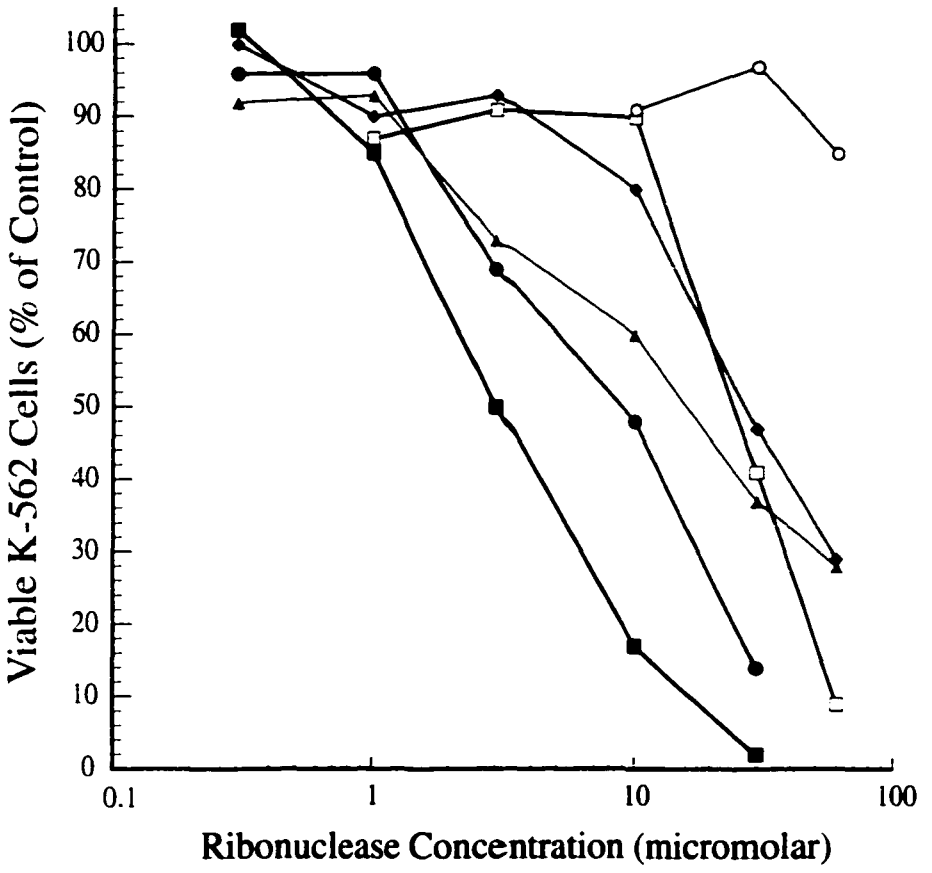
Viable K-562 Cells (% of Control)
100
90
80
70
60
50
40
30
20
10
0
0.1
1
10
100
Ribonuclease Concentration (micromolar)

Figure. 3.3. Dependence of the relative ribonucleolytic activity of ribonuclease A variants on the ribonuclease inhibitor concentration.

Data are for G88R (blue), C40A/G88R/C95A (red), A4C/G88R/V118C (black), C65A/C72A/G88R (green), and A4C/C65A/C72A/G88R/V118C (orange) RNase A. Values represent an average of triplicate experiments. Reactions were in 0.10 MES-NaOH (pH 6.0) containing NaCl (0.10 M) and DTT (8.0 mM). Data were analyzed using eq 3.2.

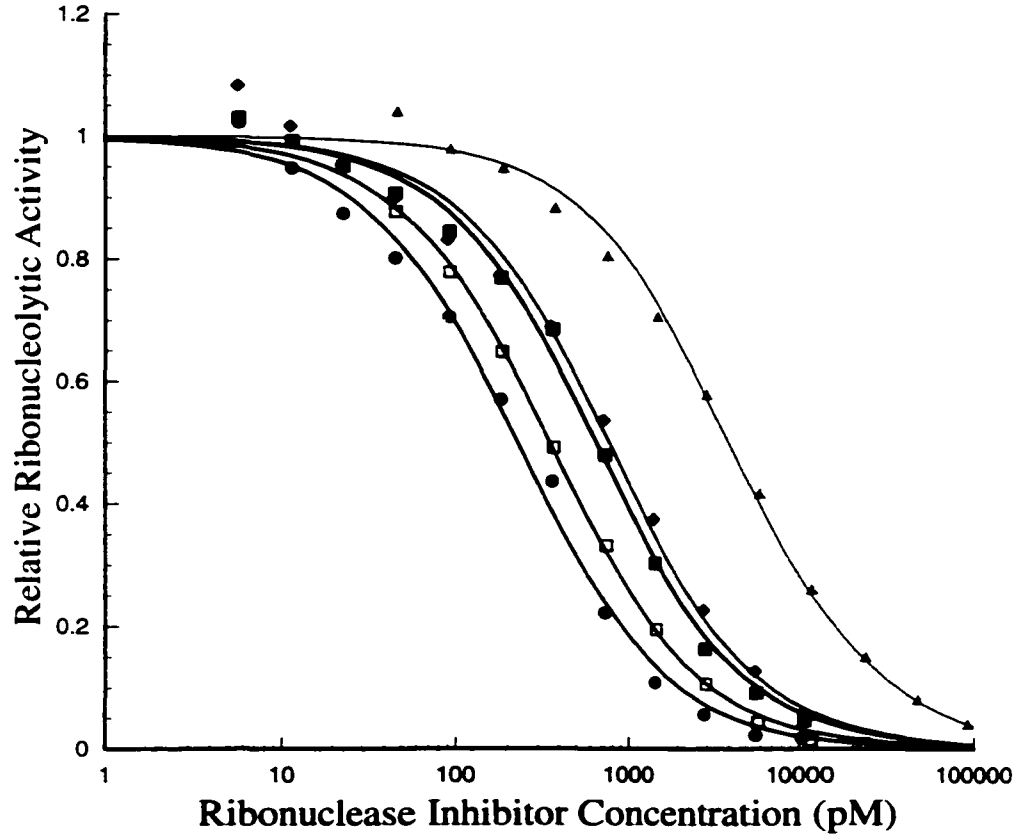
1.2
1
0.8
0.6
0.4
0.2
0
Relative Ribonucleolytic Activity
1
10
100
1000
10000
100000
Ribonuclease Inhibitor Concentration (pM)

Figure. 3.4. T_m values versus IC_{50} values for variants of ribonuclease A.

Data are from Table 3.1.

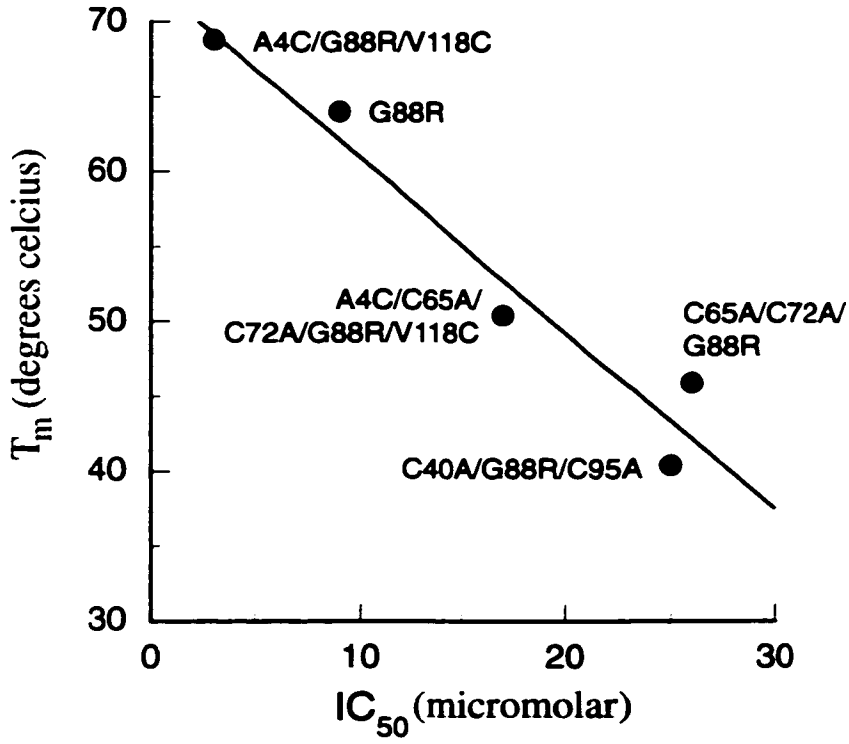
70
60
50
40
30
0
10
20
30
T_m (degrees celcius)
IC_{50} (micromolar)
A4C/G88R/V118C
G88R
A4C/C65A/
C72A/G88R/V118C
C65A/C72A/
G88R
C40A/G88R/C95A

Chapter 4

High-Level Soluble Production and Characterization of Porcine Ribonuclease Inhibitor

This work was performed in collaboration with Dr. Jan Hofsteenge (Friedrich Miescher-Institut, Basel, Switzerland).

Abbreviations: CNBr, cyanogen bromide; DSC, differential scanning calorimetry; DTT, dithiothreitol; 6-FAM, 6-carboxyfluorescein; 6-TAMRA, 6-carboxytetramethylrhodamine; LRR, leucine rich repeats; MES, 2-(*N*-morpholino)ethanesulfonic acid; PAGE, polyacrylamide gel electrophoresis; PIPES, 1,4-piperazine diethane sulfonic acid; PMSF, phenylmethylsulfonyl fluoride; pRI, porcine ribonuclease inhibitor; RI, ribonuclease inhibitor; RNase A, bovine pancreatic ribonuclease A; SDS, sodium dodecyl sulfate; Tris, tris(hydroxymethyl)aminomethane.

4.1 Abstract

Ribonucleases can be cytotoxic if they retain their ribonucleolytic activity in the cytosol. The cytosolic ribonucleolytic activity of bovine pancreatic ribonuclease A (RNase A) is limited by the presence of excess ribonuclease inhibitor (RI). RI is a 50-kDa cytosolic scavenger of pancreatic-type ribonucleases that competitively inhibits their ribonucleolytic activity. Previously, RI was overproduced as inclusion bodies. However, *in vitro* folding is inefficient. Here, porcine RI (pRI) was overproduced in *Escherichia coli* using the *trp* promoter and minimal media. This expression system maintains pRI in the soluble fraction of the cytosol. We achieved a yield of 15 mgs per L culture. Using this expression system, a 60-fold increase in active pRI was recovered, relative to previously reported recombinant DNA systems. Differential scanning calorimetry was used to study the heat denaturation of pRI, RNase A, and pRI•RNase A complex. The conformational stability of the complex is increased relative to that of the individual components.

4.2 Introduction

Ribonuclease inhibitor (RI) is a 50-kDa cytosolic scavenger of pancreatic-type ribonucleases. RI binds pancreatic type ribonucleases with 1:1 stoichiometry and competitively inhibits their ribonucleolytic activity (Blackburn *et al.*, 1977; Lee *et al.*, 1989; Hofsteenge, 1997). RI is expressed ubiquitously in mammalian cells and has been purified from many species and tissue types (Lee & Vallee, 1993). Its inhibition of ribonucleolytic activity and its cellular location has lead to the suggestions that RI protects cellular RNA from secretory ribonucleases or is involved in RNA metabolism (Hofsteenge, 1997). Nonetheless, RI has been isolated from mature red blood cells, which conduct little protein synthesis (Moenner *et al.*, 1998).

The amino acid residues of RI homologs from pig, cow, sheep, mouse, rat, and human are highly conserved (>70%) (Lee & Vallee, 1993). Each RI homolog consists of 15 leucine-rich repeats (LRR), which are commonly found in proteins that are involved in protein–protein interactions (Kobe & Deisenhofer, 1995). Another unusual aspect of the RI sequence is the presence of a large number (30 in porcine RI) of highly conserved cysteine residues (Blazquez *et al.*, 1996). The reduced form of the cysteine residues is essential for binding to ribonucleases. Consequently, oxidation of these residues is detrimental to inhibition of ribonucleolytic activity (Blazquez *et al.*, 1996). This feature allows RI to function only in a reducing environment, such as the cytosol.

Ribonucleases can be cytotoxic by entering the cytosol and degrading cellular RNA. Although RNase A has high ribonucleolytic activity (Kelemen *et al.*, 1999) and is capable of entering the cytosol (Wu, 1995), its ribonucleolytic activity there is limited by the presence

of excess RI (Blackburn & Moore, 1982; Hofsteenge, 1997). The noncovalent interactions of the RI•RNase A complex are uncompromising [$K_d = 6.7 \times 10^{-14}$ M(Vicentini *et al.*, 1990)]. However, other ribonucleases are able to evade inhibition by RI (Wu *et al.*, 1993; Kim *et al.*, 1995). Indeed, Onconase™, a homolog of ribonuclease A (RNase A) is cytotoxic and has $>10^8$-fold lower affinity for RI than does RNase A (Boix *et al.*, 1996).

The crystalline structure of the RI•RNase A complex has helped to explain the high affinity. RI is a horseshoe shaped protein that engulfs ribonucleases (Fig. 4.1) (Kobe & Deisenhofer, 1996). The binding of RI, which is acidic (p*I* = 4.7 (Kobe & Deisenhofer, 1996)), to ribonucleases, which are basic (p*I* > 9.0 (Ui, 1971; Ardelt *et al.*, 1991; Kim *et al.*, 1995)) likely has a Coulombic component (Kobe & Deisenhofer, 1996). Angiogenin, an RNase A homolog, also binds tightly to RI ($K_i = 7.1 \times 10^{-16}$ M) (Lee *et al.*, 1989). Yet, different intermolecular contacts are made by RI in binding RNase A and angiogenin (Chen & Shapiro, 1997). The conformational changes in RI upon ribonuclease binding allow RI to accommodate different ribonucleases (Kobe & Deisenhofer, 1996).

The interactions of RI and ribonucleases could enhance the understanding of tight protein–protein interactions. Unfortunately, biophysical studies are made problematic by the difficulty of isolating RI from natural tissues (Moenner *et al.*, 1998). Likewise, inclusion bodies are produced when RI is overexpressed in *Escherichia coli*. The requirement of the reduced cysteine residues of active RI complicate *in vitro* oxidative folding. Indeed, *in vitro* folding is inefficient, with a final yield of only 0.25 mg per liter of culture (Lee & Vallee, 1989).

Here, we report expression of porcine RI (pRI). Our system utilizes the *trp* promoter and minimal media. With this system, RI remains in the cytosol and is maintained in the

soluble fraction during cell lysis. The yield of RI from this expression and purification system is 60-fold higher than any reported previously. This high yield enabled us to perform biophysical experiments on pRI as well as the RI•RNase A complex.

4.3 Materials

Escherichia coli (*E. coli*) strain DH5α was from Gibco BRL (Gaithersburg, MD). *E. coli* strain BL21(DE3) was from Novagen (Madison, WI). *E. coli* strain TOPP3 BL21(DE3) was a generous gift from R. Lowery (PanVera, Madison, WI). RNase A used in the calorimetric assays was a generous gift from P.A. Leland. RNasin™ and all enzymes for the manipulation of DNA were from Promega (Madison, WI). SDS–PAGE molecular weight standards were from Bio-Rad Laboratories (Hercules, CA). Lyophilized wild-type RNase A, phenylmethylsulfonyl fluoride (PMSF), and 2-(*N*-morpholino)ethanesulfonic acid (MES) were from Sigma Chemical (St. Louis, MO). The fluorogenic substrate 6-FAM~(dA)rU$(dA)_2$~6-TAMRA was from Integrated DNA Technologies Inc. (Coralville, IA). 1,4-Piperazine diethane sulfonic acid (PIPES) was from FisherBiotech, (Fair Lawn, NJ). Cyanogen bromide- (CNBr-) activated Sepharose fast flow lab pack and the HiTrap Q column were from Amersham Pharmacia Biotech (Piscataway, NJ). M9 minimal salts (5x), Bacto yeast extract, and Bacto peptone were from Difco Laboratories (Detroit, MI).

LB medium contained (in 1.00 L) Bacto tryptone (10 g), Bacto yeast extract (5 g), and NaCl (10 g). PIPES M9 minimal medium contained (in 1.00 L) 7.1 mM PIPES buffer (pH 8.0), M9 minimal salts (1x), K_2HPO_4 (36.8 mM), NH_4Cl (3.0 mM), K_2SO_4 (2.4 mM), $CaCl_2$ (0.07 mM), $MgCl_2$ (1.0 mM) glycerol (0.64% v/v), and Tween 20 (0.05% v/v). All media were prepared in distilled, deionized water and autoclaved. All other chemicals were

of commercial grade or better, and were used without further purification unless indicated otherwise.

Analytical Instruments

Ultraviolet and visible absorbance measurements were made with a Cary 3 double beam spectrophotometer equipped with a Cary temperature controller from Varian (Sugar Land, TX). Calorimetry experiments were performed with an MCS differential scanning calorimeter from MicroCal (Northampton, MA). Fluorescence measurements were performed on a QuantaMaster1 photon counting fluorometer from Photon Technology International (South Brunswick, NJ) equipped with sample stirring. The concentration of 6-FAM~(dA)rU$(dA)_2$~6-TAMRA was determined using ε = 102,400 M^{-1} cm^{-1} at 260 nm (Kelemen *et al.*, 1999).

4.4 Methods

pRI Expression and Purification

The production of pRI began by transformation of pTrpmRI6.1 plasmid into TOPP3 BL21(DE3) cells that are plated on LB agar plates containing ampicillin (100 μg/mL) and kanamycin (40 μg/mL). A fresh colony was picked within 24 h of transformation, and a starter culture was grown to mid log phase (A_{600} = 0.5 OD) in LB medium containing ampicillin (200 μg/mL) and kanamycin (40 μg/mL). The starter culture was centrifuged at 5000x*g* for 10 min, and the pellet was resuspended in LB medium (25 mL). This suspension was used to innoculate LB medium (6.0 L), containing ampicillin (200 μg/mL) and kanamycin (40 μg/mL). The inoculated culture was shaken (200 rpm.) at 37 °C until it

reached late-log phase (A_{600} = 1.8 OD). Cells were collected by centrifugation and resuspended in PIPES M9 minimal media (2.0 L) containing ampicillin (200 μg/mL) and kanamycin (40 μg/mL) and shaken (200 rpm.) for 10 h at 37 °C. Cells were harvested by centrifugation at 5000x*g* for 10 min and frozen in a dry ice/ethanol bath before storage at –80 °C.

E. coli cell lysis was performed using a Sonifier 450 from Branson Ultrasonics (Danbury, CT). To lyse the cells, the cell pellet was thawed by resuspending in 200 mL of cell lysis buffer, which was 20 mM Tris-HCl buffer (pH 7.8) containing NaCl (0.10 M), EDTA (10 mM), DTT (10 mM), and PMSF (0.04 mM). Cells were lysed on ice by sonicating using a duty cycle of 50% and an output control setting of 6. The cell suspension was allowed to cool to 10 °C between each of the three 5-min cycles. To prepare an affinity column, RNase A was coupled to CNBr-activated Sepharose using the manufacturer's procedures. The lysate was centrifuged at 15300x*g* for 60 min, and the supernatant was loaded onto an RNase A-Sepharose column (7.0 cm x 1.6 cm^2) that had been equilibrated with equilibration buffer, which was 50 mM potassium phosphate buffer (pH 6.4) containing DTT (10 mM) and EDTA (1 mM). The RNase A-Sepharose column was washed with equilibration buffer (0.30 L) followed by 0.30 L of 50 mM potassium phosphate buffer (pH 6.4) containing NaCl (1.0 M), DTT (10 mM) and EDTA (1 mM). pRI was eluted using 0.10 M sodium acetate buffer (pH 5.0) containing NaCl (3 M), DTT (10 mM), and EDTA (1 mM). Fractions were collected and analyzed by SDS–PAGE.

The fractions that contained pRI were combined and dialyzed against 20 mM Tris-HCl buffer (pH 7.5) containing DTT (10 mM) and EDTA (1 mM). The dialysate was concentrated using an Amicon stirred cell and any precipitant was removed by centrifugation

for 30 min at 15300x*g*. The supernatant was loaded onto a HiTrap Q anion-exchange column (3.0 cm x 0.75 cm^2) equilibrated with HiTrap Q equilibration buffer, which was 20 mM Tris-HCl buffer (pH 7.5) containing DTT (10 mM) and EDTA (1 mM). The loaded column was washed with HiTrap Q equilibration buffer (40 mL), and eluted with a linear gradient of NaCl (0–0.50 M). pRI eluted as a single species at 0.30 M NaCl, and was collected and characterized. The purity of pRI was assessed by SDS–PAGE to be >99%. The concentration of purified pRI was determined by using $\varepsilon = 0.88$ mL $mg^{-1}cm^{-1}$ at 280 nm (Ferreras *et al.*, 1995).

The concentration of active pRI can be determined by titration with RNase A. Accordingly, the ribonucleolytic activity of RNase A was measured in the presence of impure protein during each step of the pRI purification. A solution from each purification step was added to 0.10 M MES-NaOH buffer (pH 6.0) containing RNase A (12.6 pM), NaCl (0.10 M), and DTT (5 mM) for 5 min at 25 °C. The ribonucleolytic activity of an aliquot of this solution was determined by its addition to 0.10 MES-NaOH buffer (pH 6.0) containing NaCl (0.10 M), DTT (5 mM), and 6-FAM~(dA)rU$(dA)_2$~6-TAMRA (0.60 μM). The units of active pRI during each purification step was determined using the definition that one unit of RI is the amount of inhibitor required to inhibit the activity of 5 ng of RNase A by 50% (Blackburn *et al.*, 1977).

Assays of Conformational Stability

Differential scanning calorimetry (DSC) was used to determine the conformational stability of RNase A, pRI, and the RI•RNase A complex. The RI•RNase A complex was prepared by adding 1 molar equivalent of RI to 1.5 molar equivalents of RNase A, followed

by gel filtration chromatography. The RI•RNase A complex and RNase A alone were separated well (data not shown). The concentration of RNase A was determined using ε = 0.72 mL $mg^{-1}cm^{-1}$ at 277.5 nm (Sela *et al.*, 1957). The concentration of the RI•RNase A complex was determined using ε = 0.86 mL $mg^{-1}cm^{-1}$ at 280 nm (Ferreras *et al.*, 1995).

DSC experiments were performed as described (Klink *et al.*, 2000) with the following modifications. Protein solutions (0.44–1.24 mg/ml) were dialyzed exhaustively against 0.1 M MES-NaOH buffer (pH 6.0) containing NaCl (0.10 M) and DTT (5 mM) and then centrifuged at 15,300*g* for 30 min to remove particulate matter. Data were collected with the program ORIGIN (MicroCal Software; Northampton, Massachusetts).

4.5 Results and discussion

pRI Production and Purification

The active form of pRI contains 30 reduced cysteine residues (Blazquez *et al.*, 1996). Therefore, the plasmid pTrpmRI6.1 was designed to direct the expressed protein to remain in the reducing environment of the cytoplasm. DNA encoding the pRI gene was cloned into plasmid pHR 148 (Schein *et al.*, 1992). An *Eco*RI restriction site was incorporated into the 3′ end and a *Bam*HI restriction site was incorporated into the 5′ end of the pRI gene by the polymerase chain reaction (PCR) (Vicentini *et al.*, 1994) The resulting plasmid, pTrpmRI6.1, carries a cDNA encoding pRI with expression controlled by the *trp* promoter.

The recombinant plasmid was transformed into the expression host, strain TOPP3 BL21(DE3). To optimize pRI expression conditions, cell cultures were grown to different cell densities. The optimal cell density for expression of soluble pRI occurred during late log phase (A_{600} between 1.5-2.0). The cells were collected by centrifugation, and expression was

induced by suspending the cells in PIPES M9 minimal media (2 L). pRI was produced in the soluble fraction. Induction at 37 °C for 6–12 h yielded 15 mg of purified pRI per L of the LB culture medium.

A summary of the pRI purification procedure is shown in Table 4.1 and Fig. 4.2. Cells were harvested by centrifugation and lysed by sonication. The resulting lysate was centrifuged, and the soluble fraction was loaded onto an RNase A-Sepharose column. The affinity of the RI•RNase A complex is in the femtamolar range (Lee *et al.*, 1989). This tight interaction was exploited to remove *E. coli* proteins that bind to the RNase A-Sepharose resin by washing with equilibration buffer that contained NaCl (1 M) (Blackburn *et al.*, 1977). When pRI eluted from the RNase A-Sepharose column (at 3 M NaCl), it was essentially pure. The RNase A-Sepharose pool produced a single band during SDS–PAGE (Fig. 4.2). The fractions that contained pRI were collected, dialyzed and loaded onto an anion-exchange column. The flow through contained material that exhibited an absorbance at 280 nm, but did not contain protein as judged by SDS–PAGE (data not shown). The anion-exchange column was eluted using a linear gradient, and pRI eluted as a single species at 0.30 M NaCl. The purity of pRI was judged to be >99% (Fig. 4.2).

Using the *trp* promotor allowed us to produce pRI that was maintained in the cytosol and was soluble during cell lysis. We achieved a yield of 1 mg per gram of cell paste. This amount corresponds to 15 mgs per L culture. Previously, RI expressed in *E. coli* produced yields that were 60-fold lower than those achieved here (Lee & Vallee, 1989; Kim *et al.*, 1999). The significant amount of pRI enables investigation of its interaction with ribonucleases.

Assays of Conformational Stability

The conformational stability of pRI or its homologs had not been determined previously. The high yield from the soluble expression of pRI allowed us to determine the value T_m for pRI. The unfolding of pRI, RNase A, and the pRI•RNase A complex were irreversible (data not shown). Fig 4.3A shows the calorimetric scan of pRI in 0.10 M MES-NaOH buffer (pH 6.0) containing NaCl (0.10 M) and DTT (5 mM). The pRI calorimetric curve contains one peak with a T_m value of 53.7 °C.

RNase A in many buffer systems shows a reversible two-state unfolding (Klink & Raines, 2000; Klink *et al.*, 2000). The unfolding of RNase A in the presence of 5 mM DTT was, however, irreversible (data not shown). In addition, the T_m value of RNase A in the presence of 5 mM DTT lowers slightly the T_m value of RNase A, relative to buffers without DTT (Klink & Raines, 2000; Klink *et al.*, 2000). The T_m value of RNase A is 58.6 °C (Fig 4.3 B). RNase A contains four buried disulfide bonds. As the disulfide bonds become exposed to solvent containing DTT, the disulfide bonds suffer reduction. Accordingly, the presence of reducing agent could lower the conformational stability, relative to buffer without reducing agent.

The calorimetric curve of the pRI•RNase A consists of two overlapping peaks with maxima at 61.3 °C and 65.4 °C (Fig. 4.3 C). The minor peak may correspond to the unfolding of the unbound portion of RNase A. However, each transition of the RI•RNase A complex is higher than the T_m values of its individual components. The major peak is 6.8 and 11.7 °C greater than the T_m value of RNase A and pRI, respectively.

Conclusion

The low quantity of purified RI from previous expression systems prevented biophysical examination of its complex with ribonucleases. We achieved a 60-fold greater yield than obtained from previously reported systems. This high yield allowed us to perform calorimetric experiments on pRI as well as the RI•RNase A complex. Future studies will investigate further the biophysical basis for the interaction between pRI and ribonucleases.

4.6 Acknowledgments

We thank Dr. D. R. McCaslin for advice. Calorimetry data were obtained at the University of Wisconsin–Madison Biophysical Instrumentation Facility, which is supported by the University of Wisconsin–Madison and grant BIR-9512577 (NSF).

Table 4.1 Purification of Recombinant Porcine Ribonuclease Inhibitor

Purification step	Activity[a] ($x10^5$ units)	Total Protein (mg)	Specific Activity (units/mg)	Purification Factor	Recovery (%)
Crude lysate supernatant	8.5	870	977	1.0	100
RNase A-Sepharose chromatography	5.8	74	7800	8.0	68
HiTrap Q chromatography	4.4	47	9400	9.5	52

[a]One unit of ribonuclease inhibitor is the amount required to inhibit the activity of 5 ng of ribonuclease A by 50% (Blackburn *et al.*, 1977).

Figure. 4.1. Structure of the complex between porcine ribonuclease inhibitor (red) and ribonuclease A (blue).

Ribbon diagrams were created with programs MOLSCRIPT (Kraulis, 1991) and RASTER3D (Merritt & Murphy, 1994) by using coordinated derived from x-ray analysis (PDB entry 1DFJ) (Kobe & Deisenhofer, 1995)(Kobe & Deisenhofer, 1993).

Ribonuclease Inhibitor

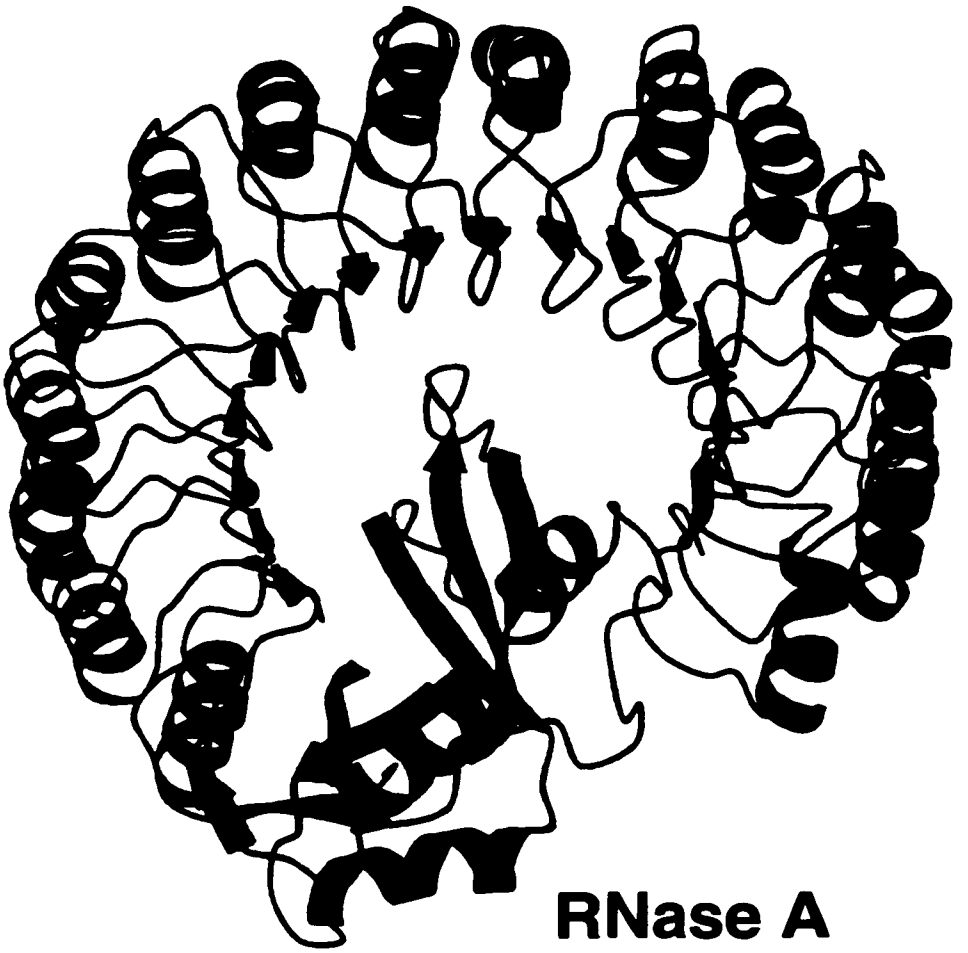

Figure. 4.2. Expression and purification of recombinant porcine ribonuclease inhibitor from *E. coli* strain TOPP3 BL21(DE3) harboring plasmid pTrpmRI6.1.

Expression of soluble pRI was performed at 37 °C for 10 h. Samples were analyzed by 10% SDS-PAGE. Lane 1, M_r standards; lane 2, RNasin standard; lane 3 soluble cell lysate before induction; lane 4, soluble cell lysate after inducing for 10 h; lane 5, pooled fractions from RNase A-Sepharose chromatography; lane 6, pooled fractions from HiTrap Q anion-exchange chromatography; lane 7, RNasin standard; lane 8, M_r standards. The major molecular mass proteins are phosphorylase B (107 kDa), bovine serum albumin (76.0 kDa), carbonic anhydrase (36.8 kDa), and soybean trypsin inhibitor (27.2 kDa)

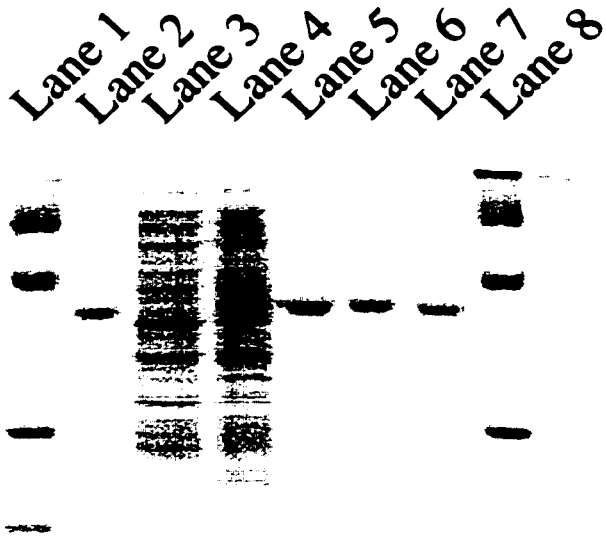
Lane 1
Lane 2
Lane 3
Lane 4
Lane 5
Lane 6
Lane 7
Lane 8

Figure. 4.3. **Differential scanning calorimetry thermal denaturation profiles of (A) porcine ribonuclease inhibitor, (B) ribonuclease A, and (C) porcine ribonuclease inhibitor complexed to ribonuclease A.**

Experiments were performed in 0.10 M MES-NaOH buffer (pH 6.0) containing NaCl (0.10 M) and DTT (5 mM). Curves in each were obtained after baseline subtraction. Data from the thermal transitions are in red. Deconvolution analysis of the calorimetric curve showed that the transition of the pRI•RNase A complex is presented as two overlapping transitions, seen here in green and blue.

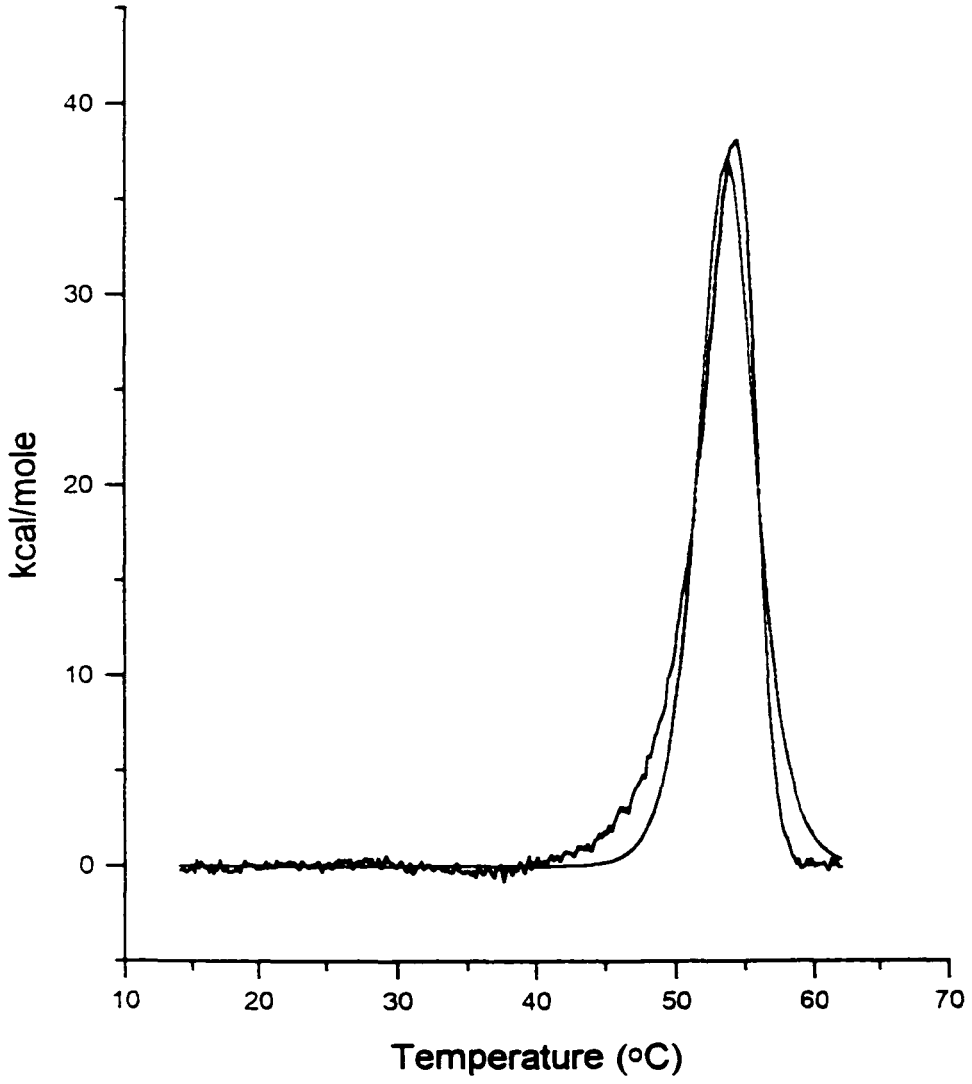
40
30
20
10
0
kcal/mole
10
20
30
40
50
60
70
Temperature (°C)

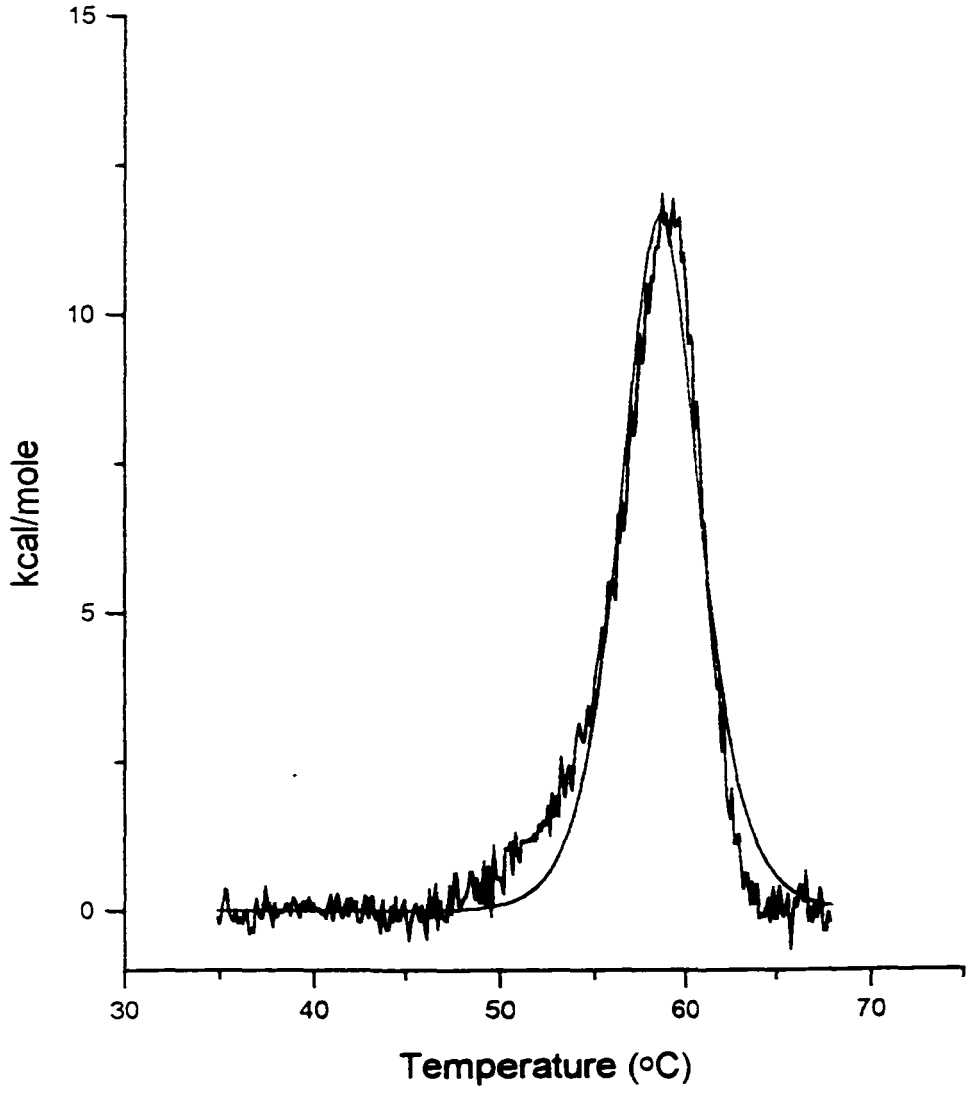
15
10
5
0
kcal/mole
30
40
50
60
70
Temperature (°C)

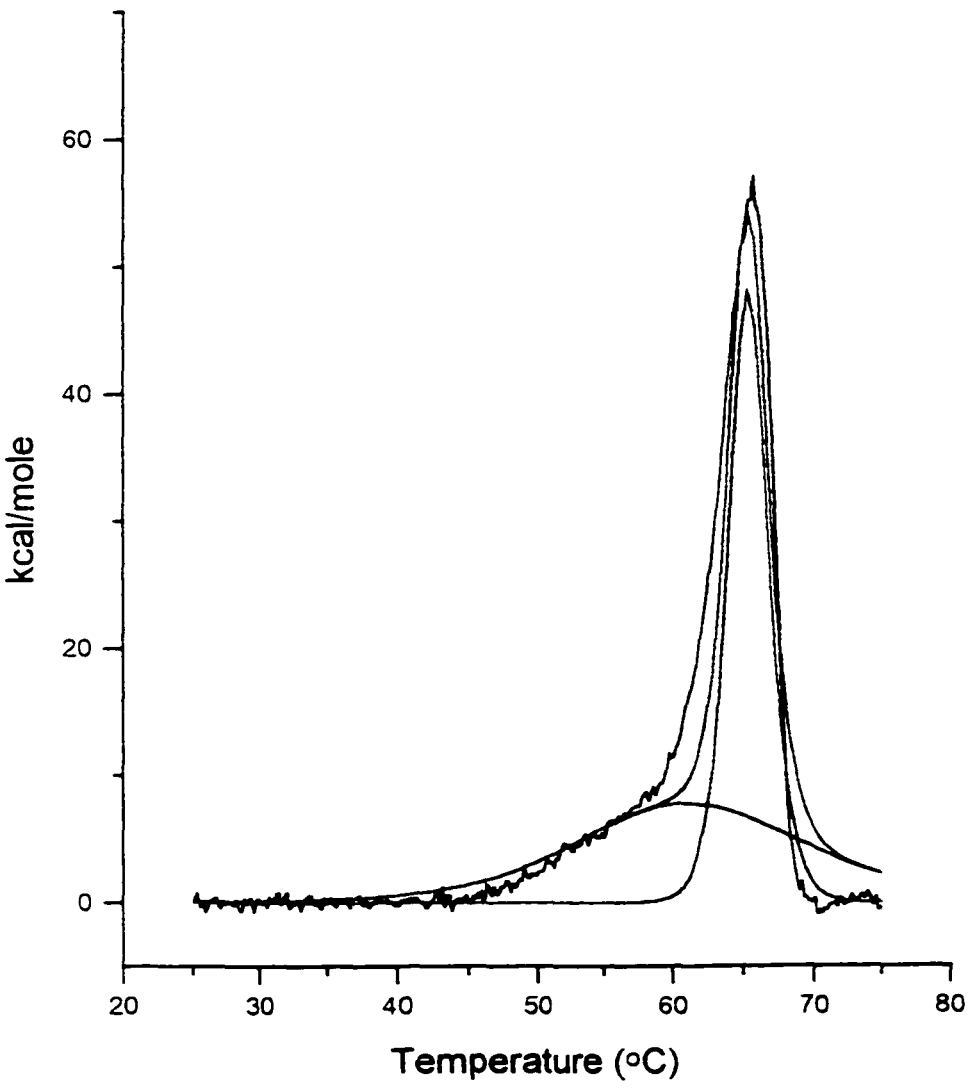
60
40
20
0
kcal/mole
20
30
40
50
60
70
80
Temperature (°C)

Appendix

Detecting Wild-type Ribonuclease A Contamination in Low Functioning Variant Enzyme Preparations

A.1 Introduction

Enzymes are capable of facilitating chemical reactions; however, the precise orientation of catalytic residues offered by the enzyme scaffold is not reproduced effortlessly. Enzyme mimics (Anslyn & Breslow, 1989) and catalytic antibodies achieve rate accelerations of several orders of magnitude over the uncatalyzed rate (Radzicka & Wolfenden, 1995). Still, researchers are unable to attain enzymic efficiency. Site-directed mutagenesis has been used extensively to reveal the mechanistic roles of residues involved in catalysis. Examining the scaffold could further improve understanding of the active-site residue geometry. The values of k_{cat} and k_{cat}/K_m for active-site variants can be decreased greatly (Kuliopulos *et al.*, 1990; Corey & Craik, 1992). RNase A has not been immune to these assaults. Indeed, the removal of the active-site residues of RNase A (His12, Lys41, and His119) decreases the k_{cat} and k_{cat}/K_m by greater than 4 orders of magnitude (Thompson & Raines, 1994; Messmore *et al.*, 1995).

The fluorogenic RNA substrate, 6-FAM~(dA)rU$(dA)_2$~6-TAMRA, provides a sensitive means to determine the low ribonucleolytic activity of variant ribonucleases. This Appendix describes the use of 6-FAM~(dA)rU$(dA)_2$~6-TAMRA to determine the K_i values for competitive inhibitors of ribonucleolytic activity. In addition, we show that a contaminating ribonucleolytic activity can be detected by determining K_i values. Specifically, if an active-site variant is contaminated with enough wild-type RNase A, then the K_i value of a competitive inhibitor is identical to that of wild-type RNase A. If the preparation is not contaminated, then the K_i value is different from that of wild-type RNase A.

A.2 Materials and Methods

Fluorogenic substrate 6-FAM~(dA)rU(dA)$_2$~6-TAMRA was from Integrated DNA Technologies Inc. (Coralville, IA). Lyophilized wild-type RNase A, uridine 3′-monophosphate (3′-UMP), adenosine 5′-diphosphate (5′-ADP), 2-(*N*-morpholino)ethanesulfonic acid (MES), and guanosine 5′-diphosphate (GDP) immobilized on 4% beaded agarose were from Sigma Chemical (St. Louis, MO). All enzymes for the manipulation of recombinant DNA were from Promega (Madison, WI) or New England Biolabs (Beverly, MA). The HiTrap SP column was from Amersham Pharmacia Biotech (Piscataway, NJ). All other reagents were of commercial grade or better. The concentration of wild-type and H12A/H119A RNase A were determined by using $\varepsilon = 0.72$ mL mg^{-1} cm^{-1} at 277.5 nm (Sela *et al.*, 1957). The concentration of 3′-UMP and 5′-ADP were determined by using $\varepsilon = 10{,}000$ M^{-1} cm^{-1} at 260 nm and $\varepsilon = 15{,}400$ M^{-1} cm^{-1} at 259 nm, respectively (Beaven *et al.*, 1955). The concentration of 6-FAM~(dA)rU(dA)$_2$~6-TAMRA was determined by using $\varepsilon = 102{,}400$ M^{-1} cm^{-1} at 260 nm (Kelemen *et al.*, 1999).

Analytical Instruments

Ultraviolet and visible absorbance measurements were made with a Cary 3 double-beam spectrophotometer equipped with a Cary temperature controller. Fluorescence measurements were made on a QuantaMaster1 photon counting fluorometer from Photon Technology International (South Brunswick, NJ) equipped with sample stirring. Calorimetry experiments were performed with an MCS isothermal titration calorimeter from MicroCal (Northampton, MA).

Preparation of H12A/H119A RNase A

Plasmids encoding H12A RNase A and H119A RNase A were a generous gift of J. E. Thompson (Thompson & Raines, 1994). These plasmids are derivatives of plasmid pBXR, which upon addition of IPTG directs the expression of RNase A in *Escherichia coli* (delCardayré *et al.*, 1995). To produce a plasmid encoding the H12A/H119A RNase A, plasmid DNA encoding the H12A variant was digested with *Apa*I and *Cla*I. Plasmid DNA encoding H12A and H119A contains only one cleavage site for each *Apa*I and *Cla*I. Consequently, two fragments of plasmid DNA were formed. One fragment contains codons 1-38 of RNase A and the second fragment contains codons 39-124. The digested fragments were subject to agarose gel electrophoresis, and the appropriate fragment gel purified. Plasmid DNA encoding H119A RNase A was treated in an identical manner. Subsequently, the DNA fragment encoding the first 38 codons of RNase A, including the H12A substitution, was ligated to the DNA fragment encoding codons 39-124 of RNase A, which includes the H119A substitution (Figure A.1)

Wild-type and H12A/H119A RNase A Purification

Wild-type RNase A from Sigma Chemical, required further purification. Gel filtration chromatography followed by cation-exchange chromatography, was performed as described (delCardayré *et al.*, 1995). H12A/H119A RNase A was produced and purified by methods described previously (delCardayré *et al.*, 1995), with the following modifications. Because of the presence of contaminating ribonucleolytic activity, H12A/H119A RNase A was purified by cation-exchange chromatography followed by GDP-linked agarose chromatography, as described below.

Extensive procedures were used to purify H12A/H119A RNase A from any contaminating ribonucleolytic activity. Specifically, all purification procedures were performed in a remote laboratory in a biological hood designated strictly for H12A/H119A RNase A. Also, a dedicated peristaltic pump, tubing, HiTrap SP column, pipetteman, and plasticware were used. All materials were wiped with a 10% v/v bleach solution prior to entering the biological hood.

H12A/H119A RNase A solutions were diluted into HiTrap SP equilibration buffer, which was 0.05 M sodium acetate buffer (pH 5.0) and loaded onto the HiTrap SP cation-exchange column (5 mL) that was equilibrated with the same buffer (40 mL). The loaded HiTrap SP column was washed with equilibration buffer (40 mL), and eluted with 0.05 M sodium acetate buffer (pH 5.0) containing NaCl (0.15 M). The removal of the two histidine residues decreased the binding affinity for the cation-exchange column, relative to wild-type RNase A. Wild-type RNase A eluted from the HiTrap SP resin in 0.05 M sodium acetate buffer (pH 5.0) containing NaCl (0.22 M). H12A/H119A RNase A fractions were pooled, diluted in 0.05 M sodium acetate buffer (pH 5.0), and applied to a GDP column.

The GDP resin was used for affinity chromatography step, as ribonucleases that have an intact active site will bind the phosphoryl groups in the active site (P1 subsite) and the guanosine base in the B2 subsite. Wild-type RNase A binds in 0.05 M sodium acetate buffer (pH 5.0), but H12A/H119A RNase A does not bind the GDP resin under these conditions. The H12A/H119A RNase A that flowed through the GDP resin was collected and analyzed. Utilizing these procedures decreased contamination from wild-type ribonucleolytic activity by >100-fold.

Assays of Ribonucleolytic Activity

The fluorogenic substrate, 6-FAM~(dA)rU(dA)$_2$~6-TAMRA, was used to determine the value of k_{cat}/K_m for wild-type RNase A. Assays were performed with stirring in 2.0 mL of 0.10 M MES-NaOH buffer (pH 6.0) containing NaCl (0.10 M), 6-FAM~(dA)rU(dA)$_2$~6-TAMRA (60 nM), and enzyme (5 pM – 0.50 nM). Fluorescence was monitored at 515 nm with excitation at 495 nm. A large increase in fluorescence occurs upon cleavage of the P–O$^{5'}$ bond on the 3′ side of the single ribonucleotide residue embedded within this substrate (Kelemen *et al.*, 1999). Values of k_{cat}/K_m were determined using eq A.1 (Kelemen *et al.*, 1999):

$$I = I_0 + (I_f - I_0)(k_{cat} / K_m)[E]t \qquad (A.1)$$

where I is the fluorescence intensity in photon counts per second, I_0 is the intensity of the substrate prior to addition of enzyme, I_f is the final intensity when all the substrate is cleaved. Values of k_{cat}/K_m were determined by linear least squares regression analysis of initial velocity data, assuming that assays were performed at substrate concentrations below the K_m, which is near 22 μM (Kelemen *et al.*, 1999).

Assays of Inhibition by 3′-UMP and 5′-ADP

To determine values of K_I, the cleavage of 6-FAM~(dA)rU(dA)$_2$~6-TAMRA by wild-type RNase A was monitored as a function of inhibitor concentration. Assays were performed with stirring in 2.00 mL of 0.10 M MES-NaOH buffer (pH 6.0) containing NaCl (0.10 M), 6-FAM~(dA)rU(dA)$_2$~6-TAMRA (60 nM), and wild-type RNase A (5 pM –

0.50 nM) or H12A/H119A RNase A (0.17 – 7.4 μM). The value of k_{cat}/K_m was determined using eq A.1. After 5 min, an aliquot (0.5 μl) of 3′-UMP (4.9 mM) or 5′-ADP (2.3 mM) was added to the reaction mixture. In all assays, the inhibitor concentrations in the reaction spanned the range from less than $K_i/10$ to greater than $10K_i$. Additional aliquots of inhibitor were added at 5 min intervals until the fluorescence change decreased to less than 10% of its original value. The value of k_{cat}/K_m was determined after each addition of inhibitor. Values of K_i were determined by nonlinear least-squares regression analysis of data fitted to eq A.2 (Kelemen *et al.*, 1999):

$$\Delta I / \Delta t = (\Delta I / \Delta t)_0 \{K_i /(K_i + [I])\} \qquad \text{(A.2)}$$

where $(\Delta I/\Delta t)_0$ is the turnover rate prior to addition of inhibitor. After completion of the assay, excess ribonuclease was added to cleave all substrate to ensure that the entire inhibition assay occurred during steady-state conditions (<10% cleaved substrate).

Isothermal Titration Calorimetry

The binding affinity of 3′-UMP for H12A/H119A RNase A was determined by ITC as described previously (Fisher *et al.*, 1998). Briefly, buffer (0.1 M MES-NaOH (pH 6.0) containing NaCl (0.1 M) or 0.1 M MES-NaOH (pH 6.0) containing NaCl (10 mM)) and protein samples were degassed prior to use. Following thermal equilibration of the system, there was a 600 s delay before beginning the 30 injections of 3′-UMP (5 μl of a 28.5 mM solution). The injections were performed at 240 s intervals, with heats of binding being measured after each injection.

A.3 Results

Ribonucleolytic Activity

A highly sensitive fluorometric assay was used to assess ribonucleolytic activity of wild-type RNase A and its variant. The k_{cat}/K_m value for the cleavage of 6-FAM~(dA)rU(dA)$_2$~6-TAMRA by wild-type RNase A was 3.0 x 10^7 M^{-1} s^{-1}. The k_{cat}/K_m value for H12A/H119A RNase A was <1.4 M^{-1} s^{-1}.

Inhibition by 3′-UMP and 5′-ADP

Inhibition of the ribonuclease-catalyzed cleavage of 6-FAM~(dA)rU(dA)$_2$~6-TAMRA by wild-type or H12A/H119A RNase A was assessed in a continuous assay. The effect of 3′-UMP and 5′-ADP concentration on relative activity $[(\Delta I/\Delta t)/(\Delta I/\Delta t)_0]$ is shown in Figure A.2. The effect of 5′-ADP concentration on absolute activity $[(\Delta I/\Delta t)]$ is shown in the inset of Figure A.2. The K_i values for inhibition of wild-type RNase A by 3′-UMP and 5′-ADP were 60 μM and 8.4 μM, respectively. The K_i value for the inhibition of H12A/H119A RNase A by 3′-UMP was 91 μM.

Isothermal Titration Calorimetry

ITC was used to probe the interaction between H12A/H119A RNase A and 3′-UMP. The buffer conditions were identical to those used to determine the value of the inhibition constant for the interaction between H12A/H119A RNase A and 3′-UMP. The affinity of 3′-UMP for H12A/H119A RNase A is weak. The value of K_d could not be determined for the experiment in high salt conditions (0.1 M MES-NaOH (pH 6.0) containing NaCl (0.1 M)).

However, the K_d value in low salt conditions (0.1 M MES-NaOH (pH 6.0) containing NaCl (10 mM)) is 1.3 mM. Thus, replacing the active-site histidine residues with a pair of alanine residues essentially obliterates binding of the 3′-UMP ligand to the active site of RNase A.

A.4 Discussion

H12A/H119A RNase A is an inefficient catalyst of RNA cleavage: the k_{cat}/K_m value for cleavage 6-FAM~(dA)rU(dA)$_2$~6-TAMRA by H12A/H119A RNase A is >10^7-fold lower than that of the wild-type enzyme.

The high sensitivity of the fluorogenic substrate 6-FAM~(dA)rU(dA)$_2$~6-TAMRA permits the rapid determination of inhibition constants for competitive inhibitors of ribonucleases. The K_i value of 60 μM for the inhibition of wild-type RNase A by 3′-UMP is in close agreement with the binding constant (K_d = 54 μM) determined previously (Fisher *et al.*, 1998). Furthermore, the K_i value of 8.4 μM for the inhibition of wild-type enzyme by 5′-ADP is comparable to the value of K_d (1.2 μM) reported previously (Russo *et al.*, 1997), even though solution conditions (in particular, salt concentrations) were not identical.

Traditionally, a protein is considered to be pure if it constitutes >99% of the protein on SDS-polyacrylamide gel. Nevertheless, analysis by SDS-polyacrylamide gel may not be sufficient if a contaminating enzyme is a significantly better catalyst than is the target enzyme. Also, a wild-type enzyme can co-migrate with a variant during SDS-polyacrylamide gel electrophoresis.

Surprisingly, we show that the K_i value (91 μM) for the inhibition of our preparation of H12A/H119A RNase A by 3′-UMP is near that of the wild-type enzyme. This result lead us

to suspect that the ribonucleolytic activity of the H12A/H119A variant was due (at least partially) to a contaminant. For example, wild-type RNase A could be introduced artificially during an H12A/H119A RNase A purification. Wild-type RNase A is $>10^7$-fold more efficient at RNA cleavage than is H12A/H119A RNase A. Thus, if there were a 0.0001% contamination of wild-type RNase A in an H12A/H119A RNase A preparation, then greater than 90% of the ribonucleolytic activity would be from the wild-type enzyme. Moreover, the value of K_i measured for the variant enzyme would be similar to that for the wild-type enzyme.

To determine if the K_i value for the inhibition of the ribonucleolytic activity of H12A/H119A RNase A by 3′-UMP corresponds to the K_d value of the H12A/H119A RNase A•3′-UMP complex, we performed ITC experiments using H12A/H119A RNase A and 3′-UMP. In the cystalline structure of the RNase A•3′-UMP, His12 and His119 form hydrogen bonds with the oxygens of the bound phosphoryl group (Fisher *et al.*, 1998). Replacement of either residue with an alanine residue should have a significant effect on 3′-UMP binding. Indeed, the values of K_d for the 3′-UMP complexes with H12A and H119A RNase A are increased by 10- and 7-fold, respectively, relative to wild-type RNase A (C. Park and R.T. Raines, unpublished results).

Replacing both active-site histidine residues with a pair of alanine residues should decrease ligand binding further. The ITC results confirm this prediction: an equilibrium dissociation could not be determined for the H12A/H119A RNase A•3′-UMP complex using conditions identical to the conditions used to determine the K_i value. However, the binding stoichiometry of 5 in low salt suggests that the 5 protein molecules of 3′-UMP ligands bind

each protein molecule nonspecifically. Thus, replacing the active-site histidine residues with a pair of alanine residues essentially obliterates ligand binding to the active site of RNase A. This result contradicts the results from the inhibition studies but supports our conclusion that the ribonucleolytic activity observed for our preparation of H12A/H119A RNase A is at least partially due to an underlying ribonuclease contaminant.

RNase A is the most highly studied and most efficient ribonuclease in its superfamily. Creating active-site variant enzymes has been utilized to more completely understand the high catalytic efficiency of RNase A. The activity of these variant enzymes can be masked by a contaminating ribonuclease. We show that a contaminating ribonuclease can be detected by comparing values of K_d with values of K_i. Here, we were unable to remove the underlying ribonucleolytic activity in the H12A/H119A RNase A preparation. Still, the extensive purification procedures and testing have been adopted by others and helped to ensure that the activity from other low-activity ribonucleases ($<10^4$-fold lower than wild-type RNase A) were legitimate (Kelemen *et al.*, 1999; Bretscher *et al.*, 2000).

Figure A.1. **Procedure used in subcloning of H12A/H119A ribonuclease A.** Plasmid DNA encoding H12A and H119A RNase A were cleaved with restriction endonucleases *Apa*I and *Cla*I. Subsequently, the DNA fragment encoding the first 38 codons of RNase A, including the H12A substitution, was ligated to the DNA fragment encoding codons 39 through 124 of RNase A which includes the H119A substitution to create a plasmid that encodes H12A/H119A RNase A.

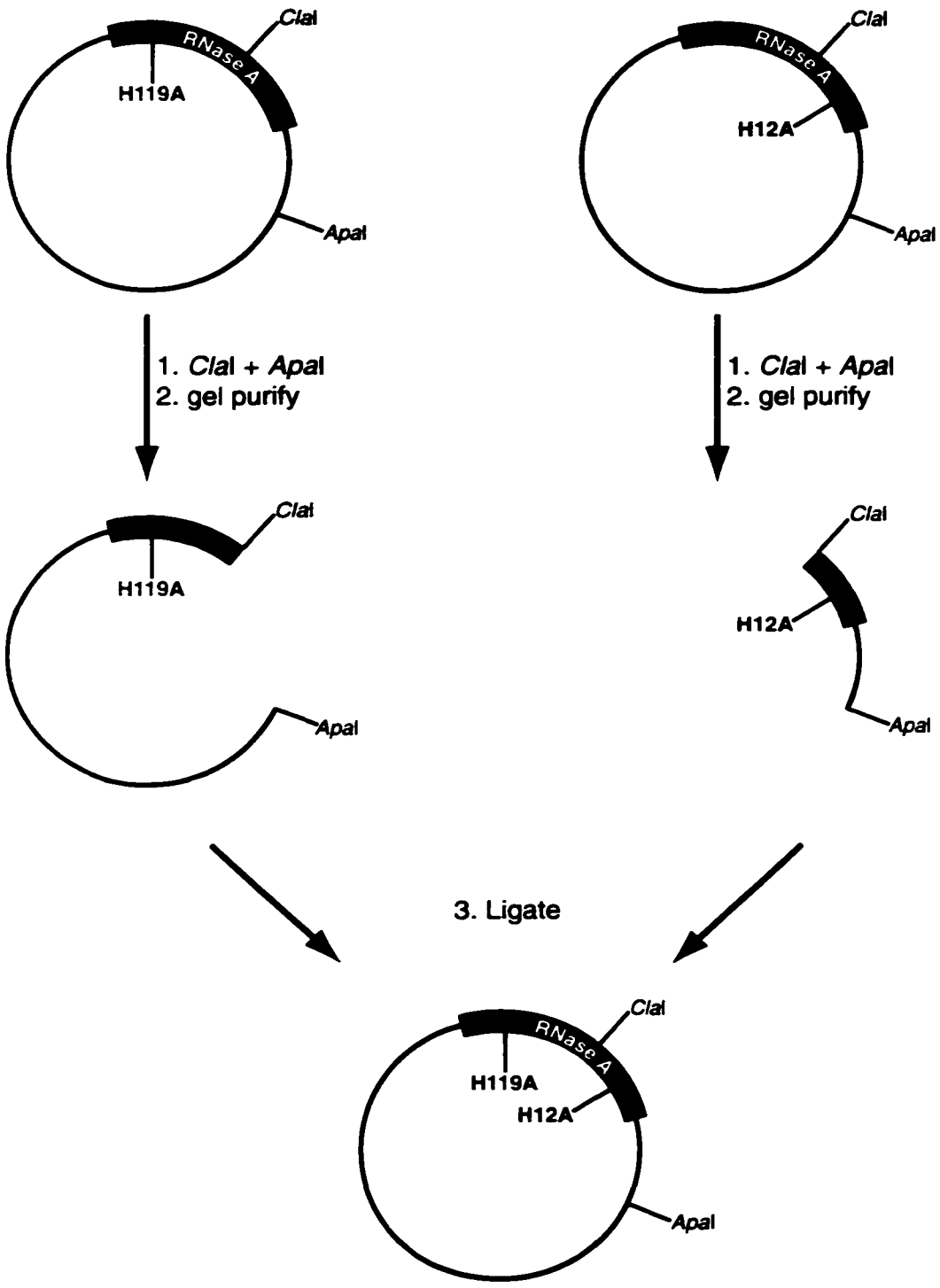
ClaI
RNase A
H119A
ApaI
1. ClaI + ApaI
2. gel purify
ClaI
H119A
ApaI
ClaI
RNase A
H12A
ApaI
1. ClaI + ApaI
2. gel purify
ClaI
H12A
ApaI
3. Ligate
ClaI
RNase A
H119A
H12A
ApaI

Figure A.2. **Dependence of the relative ribonucleolytic activity of ribonuclease A on the concentration of 3′-UMP or 5′-ADP.**

Triangle, circle and square symbols represent data collected in independent reactions. Open symbols represent data from 3′-UMP inhibition experiments. Closed symbols represent data from 5′-ADP inhibition experiments. (Inset) Dependence of absolute RNase A activity [$(\Delta I/\Delta t)$] on the concentration of 5′-ADP. Reactions were carried out in 0.10 M MES-NaOH buffer, pH 6.0, containing 0.10 NaCl. Data were analyzed using equation A.2.

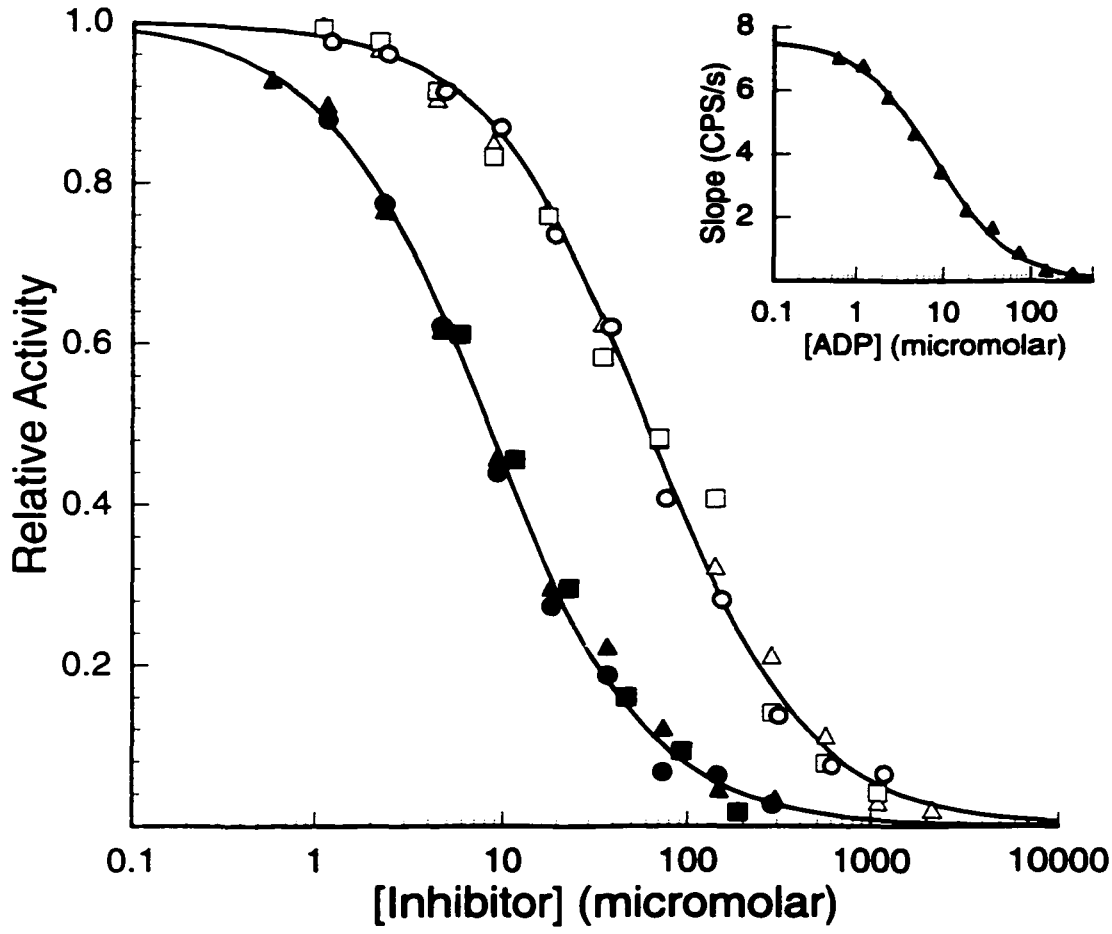
1.0
0.8
0.6
0.4
0.2
Relative Activity
0.1
1
10
100
1000
10000
[Inhibitor] (micromolar)
8
6
4
2
Slope (CPS/s)
0.1
1
10
100
[ADP] (micromolar)

Chapter 5

References

Altmann, K.-H. & Scheraga, H. A. (1990). Local structure in ribonuclease A. Effect of amino acid substitutions on the preferential formation of the native disulfide loop in synthetic peptides corresponding to residues Cys58-Cys72 of bovine pancreatic ribonuclease A. *J. Am. Chem. Soc.* **112**, 4926-4931.

Anfinsen, C. B. (1973). Principles that govern the folding of protein chains. *Science* **181**, 223-230.

Anfinsen, C. B., Haber, E., Sela, M. & White, F. H. J. (1961). The kinetics of formation of native ribonuclease during oxidation of the reduced polypeptide chain. *Proc. Nat. Acad. Sci. USA* **47**, 1309-1314.

Anfinsen, C. B. & Scheraga, H. A. (1975). Experimental and theoretical aspects of protein folding. In *Adv. Protein Chem.* (C. B. Anfinsen, J. T. Edsall & F. M. Richards, Ed.), pp. 205-300, Academic Press, New York.

Anslyn, E. & Breslow, R. (1989). Geometric evidence on the ribonuclease model mechanism. *Am. Chem. Soc.* **111**, 5972-5973.

Ardelt, W., Mikulski, S. M. & Shogen, K. (1991). Amino acid sequence of an anti-tumor protein from *Rana pipiens* oocytes and early embryos. *J. Biol. Chem.* **266**, 245-251.

Arnold, U. & Ulbrich-Hofmann, R. (1997). Kinetic and themodynamic thermal stabilities of ribonuclease A and ribonuclease B. *Biochemistry* **36**, 2166-2172.

Avey, H. P., Boles, M. O., Carlisle, C. H., Evans, S. A., Morris, S. J., Palmer, R. A., Woolhouse, B. A. & Shall, S. (1967). Structure of ribonuclease. *Nature* **213**, 557-562.

Backer, J. M., Bourret, L. & Dice, J. F. (1983). Regulation of catabolism of microinjected ribonuclease A requires the amino-terminal 20 amino acids. *Proc. Natl. Acad. Sci. USA* **80**, 2166-2170.

Beaven, G. H., Holiday, E. R. & Johnson, E. A. (1955). Optical properties of nucleic acids and their components. In *The Nucleic Acids, Chemistry and Biology* (E. Chargraff & J. N. Davidson, Ed.), pp. 493-553, Academic Press, New York.

Becktel, W. J. & Schellman, J. A. (1987). Protein stability curves. *Biopolymers* **26**, 1859-1877.

Beintema, J. (1987). Structure, properties and molecular evolution of pancreatic-type ribonucleases. *Life Chem. Rep.* **4**, 333-389.

Beintema, J. J., Schüller, C., Irie, M. & Carsana, A. (1988). Molecular evolution of the ribonuclease superfamily. *Prog. Biophys. Molec. Biol.* **51**, 165-192.

Beintema, J. J. & van der Laan, J. M. (1986). Comparison of turtle pancreatic ribonuclease with those of mammalian ribonucleases. *FEBS Lett.* **194**, 338-342.

Betz, S. F., Marmorion, J. L., Saunders, A. J., Doyle, D. F., Young, G. B. & Pielak, G. J. (1996). Unusual effects of an engineered disulfide on global and local protein stability. *Biochemistry* **35**, 7422-7428.

Blackburn, P. & Moore, S. (1982). Pancreatic ribonuclease. *The Enzymes* **15**, 317-433.

Blackburn, P., Wilson, G. & Moore, S. (1977). Ribonuclease inhibitor from human placenta. *J. Biol. Chem.* **252**, 5904-5910.

Blake, C. C., Ghosh, M., Harlos, K., Avezoux, A. & Anthony, C. (1994). The active site of methanol dehydrogenase contains a disulphide bridge between adjacent cysteine residues. *Nat. Struc. Biol.* **1**, 102-105.

Blazquez, M., Fominaya, J. M. & Hofsteenge, J. (1996). Oxidation of sulfhydryl groups of ribonuclease inhibitor in epithelial cells is sufficient for its intracellular degradation. *J. Biol. Chem.* **271**, 18638-18642.

Boix, E., Wu, Y.-N., Vasandani, V. M., Saxena, S. K., Ardelt, W., Ladner, J. & Youle, R. J. (1996). Role of the N terminus in RNase A homologues: Differences in catalytic activity, ribonuclease inhibitor interaction and cytotoxicity. *J. Mol. Biol.* **257**, 992-1007.

Bond, M. D., Strydom, D. J. & Vallee, B. L. (1993). Characterization and sequencing of rabbit, pig and mouse angiogenins: discernment of functionally important residues and regions. *Biochim. Biophys. Acta* **1162**, 177-186.

Borah, B., Chen, C., Egan, W., Miller, M., Wlodawer, A. & Cohen, J. S. (1985). Nuclear magnetic resonance and neutron diffraction studies of the complex of ribonuclease A with uridine vanadate, a transition-state analogue. *Biochemistry* **24**, 2058-2067.

Bretscher, L. E., Abel, R. L. & Raines, R. T. (2000). A ribonuclease A variant with low catalytic activity but potent cytoxicity. *J. Biol. Chem.* **275**, 9893-9896.

Brown, D. M. & Todd, A. R. (1953). Nucleotide, part XXI: the action of ribonuclease on simple esters of the monoribonucleotides. *J. Chem. Soc. (London)*, 44-52.

Carra, J. H., Murphy, E. C. & Privalov, P. L. (1996). Thermodynamic effects of mutations on the denturation of T4 Lysozyme. *Biophys. J.* **71**, 1994-2001.

Catanzano, F., Graziano, G., Cafaro, V., D'Alessio, G., Donato, A. D. & Barone, G. (1997). From ribonuclease A toward bovine seminal ribonuclease: A step by step thermodynamic analysis. *Biochemistry* **36**, 14403-14408.

Chen, C.-Z. & Shapiro, R. (1997). Site-specific mutagenesis reveals differences in the structural bases for tight binding of RNase inhibitor to angiogenin and RNase A. *Proc. Natl. Acad. Sci. USA* **94**, 1761-1766.

Chiang, H.-L. & Dice, J. F. (1988). Peptide sequences that target proteins for enhanced degradation during serum withdrawal. *J. Biol. Chem.* **263**, 6797-6805.

Chothia, C. (1976). The nature of the accessible and buried surfaces in proteins. *J. Mol. Biol.* **105**, 1-14.

Clark, J. & Fersht, A. R. (1993). Engineered disulfide bonds as probes of the folding pathway of barnase: Increasing the stability of proteins against the rate of denaturation. *Biochemistry* **32**, 4322-4329.

Cleland, W. W. (1979). Statistical analysis of enzyme kinetic data. *Methods Enzymol.* **63**, 103-138.

Corey, D. R. & Craik, C. S. (1992). An investigation into the minimum requirements for peptide hydrolysis by mutation of the catalytic triad of trypsin. *J. Am. Chem. Soc.* **114**, 1784-1790.

Creighton, T. E. (1977). Kinetics of refolding of reduced ribonuclease. *J. Mol. Biol.* **113**, 329-341.

Creighton, T. E. (1979). Intermediates in the refolding of reduced ribonuclease A. *J. Mol. Biol.* **129**, 411-431.

Creighton, T. E. (1990). Protein folding. *Biochem. J.* **270**, 1-16.

D'Alessio, G. & Riordan, J. F. (1997). *Ribonucleases: Structures and Functions*, Academic Press, New York.

Darby, N. J., van Mierlo, C. P. & Creighton, T. E. (1991). The [5-55] single-disulphide intermediate in folding of bovine pancreatic trypsin inhibitor. *FEBS Lett.* **279**, 61-64.

delCardayré, S. B., Ribó, M., Yokel, E. M., Quirk, D. J., Rutter, W. J. & Raines, R. T. (1995). Engineering ribonuclease A: Production, purification, and characterization of wild-type enzyme and mutants at Gln11. *Protein Eng.* **8**, 261-273.

Dill, K. A. (1990). Dominant forces in protein folding. *Biochemistry* **29**, 7133-7155.

Eberhardt, E. S., Wittmayer, P. K., Templer, B. M. & Raines, R. T. (1996). Contribution of a tyrosine side chain to ribonuclease A catalysis and stability. *Protein Sci.* **5**, 1697-1703.

Falnes, P. O. & Olsnes, S. (1998). Modulation of the intracellular stability and toxicity of diphtheria toxin through degradation by the N-end rule pathway. *EMBO J.* **17**, 615-625.

Ferreras, M., Gavilanes, J. G., Lopez-Otin, C. & Garcia-Serura, J. M. (1995). Thiol-disulfide exchange of ribonuclease inhibitor bound to ribonuclease A. *J. Biol. Chem.* **270**, 28570-28578.

Fiani, M. L., Blum, J. S. & Stahl, P. D. (1993). Endosomal proteolysis precedes ricin A-chain toxicity in macrophages. *Arch. Biochem. Biophys.* **307**, 225-230.

Findlay, D., Herries, D. G., Mathias, A. P., Rabin, B. R. & Ross, C. A. (1961). The active site and mechanism of action of bovine pancreatic ribonuclease. *Nature* **190**, 781-784.

Findlay, D., Mathias, A. P. & Rabin, B. R. (1962). The active site and mechanism of action of bovine pancreatic ribonuclease. *Biochem. J.* **85**, .

Fisher, B. M., Ha, J.-H. & Raines, R. T. (1998). Coulombic forces in protein–RNA interactions: Binding and cleavage by ribonuclease A and variants at Lys7, Arg10, and Lys66. *Biochemistry* **37**, 12121-12132.

Fisher, B. M., Schultz, L. W. & Raines, R. T. (1998). Coulombic effects of remote subsites on the active site of ribonuclease A. *Biochemistry* **37**, 17386-17401.

Flory, P. J. (1956). Theory of elastic mechanisms in fibrous proteins. *J. Am. Chem. Soc.* **78**, 5222-5235.

Frisch, C., Kolmar, H., Schmidt, A., Kleemann, G., Reinhardt, A., Pohl, E., Uson I Schneider, T. R. & Fritz, H. J. (1996). Contribution of the intramolecular disulfide bridge to the folding stability of REIv, the variable domain of a human immunoglobulin kappa light chain. *Folding & Design* **1**, 431-440.

Futami, J., Seno, M. & Yamada, H., Stabilization of human ribonuclease 1, R. Youles, Eds., Proceedings of the Fifth International Meeting on Ribonucleases Warrenton, VA, May 12–16, 1999), pp. 66.

Galat, A., Creighton, T. E., Lord, R. C. & Blout, E. R. (1981). Circular dichroism, raman spectroscopy, and gel filtration of trapped folding intermediates of ribonuclease. *Biochemistry* **20**, 594-601.

Garel, J.-R. (1978). Early steps in the refolding reaction of reduced ribonuclease A. *J. Mol. Biol.* **118**, 331-345.

Gilbert, H. F. (1990). Molecular and cellular aspects of thiol-disulfide exchange. In *Advances in Enzymology* (A. Meister, Ed.), pp. Interscience, New York.

Gill, S. C. & von Hippel, P. H. (1989). Calculation of protein extinction coefficients from amino acid sequence data. *Anal. Biochem.* **182**, 319-326.

Harrison, P. M. & Sternberg, M. J. E. (1994). Analysis and classification of disulphide connectivity in proteins-The entropic effect of cross-linkage. *J. Mol. Biol.* **244**, 448-463.

Hermans, J. J. & Scheraga, H. A. (1961). Structural studies of ribonuclease. V. Reversible change of configuration. *J. Am. Chem. Soc.* **83**, 3283-3292.

Herskovits, T. T. & Laskowski, M. J. (1968). Location of chromophoric residues in proteins by solvent perturbation. *J. Biol. Chem.* **243**, 2123-2129.

Hinck, A. P., Truckses, D. M. & Markley, J. L. (1996). Engineered disulfide bonds in staphylococcal nuclease: Effects on the stability and conformation of the folded protein. *Biochemistry* **35**, 10328-10338.

Hirs, C. H. W., Moore, S. & Stein, W. H. (1960). The sequence of the amino acid residues in performic acid-oxidized ribonuclease. *J. Biol. Chem.* **235**, 633-647.

Hofsteenge, J. (1997). Ribonuclease inhibitor. In *Ribonucleases: Structures and Functions* (G. D'Alessio & J. F. Riordan, Ed.), pp. 621-658, Academic Press, New York.

Huggins, C., Tapley, D. F. & Jensen, E. V. (1951). Sulphydryl-disulphide relationships in the induction of gels in proteins by urea. *Nature* **167**, 592-593.

Hwang, C., Sinskey, A. J. & Lodish, H. F. (1992). Oxidized redox state of glutathione in the endoplasmic reticulum. *Science* **257**, 1496-1502.

Isenman, L. D. & Dice, J. F. (1989). Secretion of intact proteins and peptide fragments by lysosomal pathways of protein degradation. *J. Biol. Chem.* **264**, 21591-21596.

Iwaoka, M., Wedemeyer, W. J. & Scheraga, H. A. (1999). Conformational unfolding studies of three-disulfide mutants of bovine pancreative ribonuclease A and the coupling of proline isomerization to disulfide redox reactions. *Biochemistry* **38**, 2805-2815.

Jeffrey, G. A. & Saenger, W. (1994). *Hydrogen Bonding in Biological Structures*, Jocelyn, P. C. (1972). *Biochemistry of the SH group*, Academic Press, New York.

Kartha, G., Bello, J. & Harker, D. (1967). Tertiary structure of ribonuclease. *Nature* **213**, 862-865.

Kelemen, B. R., Klink, T. A., Behlke, M. A., Eubanks, S. R., Leland, P. A. & Raines, R. T. (1999). Hypersensitive substrate for ribonucleases. *Nucleic Acids Res.* **27**, 3696-3701.

Kelemen, B. R. & Raines, R. T. (1999). Extending the limits of enzymatic catalysis: Diffusion of ribonuclease A in one dimension. *Biochemistry* **38**, 5302-5307.

Kim, B.-M., Schultz, L. W. & Raines, R. T. (1999). Variants of ribonuclease inhibitor that resist oxidation. *Protein Science* **8**, 430-434.

Kim, J.-S. & Raines, R. T. (1993). Bovine seminal ribonuclease produced from a synthetic gene. *J. Biol. Chem.* **268**, 17392-17396.

Kim, J.-S., Soucek, J., Matousek, J. & Raines, R. T. (1995). Catalytic activity of bovine seminal ribonuclease is essential for its immunosuppressive and other biological activities. *Biochem. J.* **308**, 547-550.

Kim, J.-S., Soucek, J., Matousek, J. & Raines, R. T. (1995). Mechanism of ribonuclease cytotoxicity. *J. Biol. Chem.* **270**, 31097-31102.

Kim, J.-S., Soucek, J., Matousek, J. & Raines, R. T. (1995). Structural basis for the biological activities of bovine seminal ribonuclease. *J. Biol. Chem.* **270**, 10525-10530.

Klink, T. A. & Raines, R. T. (2000). Conformational stability is a determinant of ribonuclease A cytotoxicity. *J. Biol. Chem.* **275**, 1763-17467.

Klink, T. A., Woycechowsky, K. J., Taylor, K. M. & Raines, R. T. (2000). Contribution of disulfide bonds to the conformational stability and catalytic activity of ribonuclease A. *Eur. J. Biochem.* **267**, 566-572.

Ko, J. H., Jang, W. H., Kim, E. K., Lee, H. B., Park, K. D., Chung, J. H. & Yoo, O. J. (1996). Enhancement of thermostability and catalytic efficiency of AprP, and alkaline protease from *Pseudomonas sp.*, by introduction of a disulfide bond. *Biochem. Biophys. Res. Commun.* **221**, 631-635.

Kobe, B. & Deisenhofer, J. (1993). Crystal structure of porcine ribonuclease inhibitor, a protein with leucine-rich repeats. *Nature* **366**, 751-756.

Kobe, B. & Deisenhofer, J. (1995). A structural basis of the interactions between leucine-rich repeats and protein ligands. *Nature* **374**, 183-186.

Kobe, B. & Deisenhofer, J. (1996). Mechanism of ribonuclease inhibition by ribonuclease inhibitor protein based on the crystal structure of its complex with ribonuclease A. *J. Mol. Biol.* **264**, 1028-1043.

Kowalski, J. M., Parekh, R. N. & Wittrup, K. D. (1998). Secretion efficiency in *Saccharomyces cerevisiae* of bovine pancreatic trypsin inhibitor mutants lacking disulfide bonds is correlated with thermodynamic stability. *Biochemistry* **37**, 1264-1273.

Kraulis, P. J. (1991). **MOLSCRIPT: a program to produce both detailed and schematic plots** of protein structures. *J. Appl. Crystallogr.* **24**, 946-950.

Krupkakar, J., Swaminathan, C. P., Das, P. K., Suokia, A. & Podder, S. K. (1999). Calorimetric studies on the stability of the ribosome-inactivating protein abrin II: effects of pH and ligand binding. *Biochem. J.* **338**, 273-279.

Kuliopulos, A., Talalay, P. & Mildvan, A. S. (1990). Combined effects of two mutations of catalytic residues on the ketosteroid isomerase reaction. *Biochemistry* **29**, 10271-10280.

Kunitz, M. & McDonald, M. R. (1953). Ribonuclease. *Biochem. Prep.* **3**, 9-19.

Kunkel, T. A., Roberts, J. D. & Zakour, R. A. (1987). Rapid and efficient site-specific mutagenesis without phenotypic selection. *Methods Enzymol.* **154**, 367-382.

Kuroki, R., Inaka, K., Taniyama, Y., Kidokoro, S.-I., Matsushima, M., Kikuchi, M. & Yutani, K. (1992). Enthalpic destabilization of a mutant human lysozyme lacking a disulfide bridge between cysteine-77 and cysteine-95. *Biochemistry* **31**, 8323-8328.

Laity, J. H., Lester, C. C., Shimotakahara, S., Zimmerman, D. E., Montelione, G. T. & Scheraga, H. A. (1997). Structural characterization of an analog of the major rate-determining disulfide folding intermediate of bovine pancreatic ribonuclease A. *Biochemistry* **36**, 12683-12699.

Laity, J. H., Shimotakahara, S. & Scheraga, H. A. (1993). Expression of wild-type and mutant bovine pancreatic ribonuclease A in *Escherichia coli*. *Proc. Natl. Acad. Sci. USA* **90**, 615-619.

Layne, E. (1957). Spectrophotometric and turbidimetric methods for measuring proteins. *Methods Enzymol.* **3**, 447-454.

Lee, F. S., Shapiro, R. & Vallee, B. L. (1989). Tight-binding inhibition of angiogenin and ribonuclease A by placental ribonuclease inhibitor. *Biochemistry* **28**, 225-230.

Lee, F. S. & Vallee, B. L. (1989). Expression of human placental ribonuclease inhibitor in *Escherichia coli*. *Biochem. Biophys. Res. Comm.* **160**, 115-120.

Lee, F. S. & Vallee, B. L. (1993). Structure and action of mammalian ribonuclease (angiogenin) inhibitor. *Progress Nucl. Acid Res. Molec. Biol.* **44**, 1-30.

Leland, P. A., Schultz, L. W., Kim, B.-M. & Raines, R. T. (1998). Ribonuclease A variants with potent cytotoxic activity. *Proc. Natl. Acad. Sci. USA* **95**, 10407-10412.

Li, Y.-J., Rothwarf, D. M. & Scheraga, H. A. (1995). *Nature Struct. Biol.* **2**, 489-494.

Lim, W. A. & Sauer, R. T. (1989). Alternative packing arrangements in the hydrophobic core of λ repressor. *Nature* **339**, 31-36.

Lui, Y., Breslauer, K. & Anderson, S. (1997). "Designing out" disulfide bonds: Thermodynamic properties of 30–51 cystine substitution mutants of bovine trypsin inhibitor. *Biochemistry* **36**, 5323-5335.

Mancheno, J. M., Gasset, M., Onaderra, M., Gavilanes, J. G. & D'Alessio, G. (1994). Bovine seminal ribonuclease destabilizes negatively charged membranes. *Biochem. Biophys. Res.* **199**, 119-124.

Matouschek, A., Azem, A., Ratliff, K., Glick, B. S., Schmid, K. & Schatz, G. (1997). Active unfolding of precursor proteins during mitochondrial protein import. *EMBO J.* **16**, 6727-6736.

Matsumura, M., Becktel, W. J., Levitt, M. & Matthews, B. W. (1989). Stabilization of phage T4 lysozyme by engineered disulfide bonds. *Proc. Natl. Acad. Sci. USA* **86**, 6562-6566.

Matsumura, M., Signor, G. & Matthews, B. W. (1989). Substantial increase of protein stability by multiple disulphide bonds. *Nature* **342**, 291-293.

McElligott, M. A., Miao, P. & Dice, J. F. (1985). Lysosomal degradation of ribonuclease A and ribonuclease S-protein microinjected into the cytosol of human fibroblasts. *J. Biol. Chem.* **260**, 11986-11993.

McLendon, G. (1977). A correlation between myoglobin thermodynamic stabilities and species metabolic rates. *Biochem. Biophys. Res. Comm.* **77**, 959-966.

McLendon, G. & Radany, E. (1978). Is protein turnover thermodynamically controlled? *J. Biol. Chem.* **253**, 6335-6337.

Merritt, E. A. & Murphy, M. E. P. (1994). Raster3D Version 2.0, a program for photorealistic molecular graphics. *Acta. Crystallogr., Sect. D* **50**, 869-873.

Messmore, J. M., Fuchs, D. N. & Raines, R. T. (1995). Ribonuclease A: Revealing structure – function relationships with semisynthesis. *J. Am. Chem. Soc.* **117**, 8057-8060.

Mihalyi, E. & Harrington, W. F. (1959). Studies on the tryptic digestion of myosin. *Biochim. Biophys. Acta* **36**, 447-466.

Mikulski, S. M., Chun, H. G., Mittleman, A., Panella, T., Puccio, C. A., Shogen, K. & Costanzi, J. J. (1995). Relationship between response and median survival in patients with advanced non-small cell lung cancer: Comparison of onconase with other anticancer agents. *Inter. J. Oncol.* **6**, 889-897.

Milburn, P. J. & Scheraga, H. A. (1988). Local interactions favor the native 8-residue disulfide loop in the oxidation of a fragment corresponding to the sequence Ser-50-Met79 derived from bovine pancreatic ribonuclease A. *J. Prot. Chem.* **7**, 377-398.

Moenner, M., Vosoghi, M., Ryazantsev, S. & Glitz, D. G. (1998). Ribonuclease inhibitor protein of human erthrocytes: Characterization, loss of activity in response to oxidative stress, and association with heinz bodies. *Blood Cells Molecules and Diseases* **24**, 149-164.

Ooi, T., Rupley, J. A. & Scheraga, H. A. (1963). Structural studies of ribonuclease. VIII. Tryptic hydrolysis of ribonuclease A at elevated temperatures. *Biochemistry* **2**, 432-437.

Pace, C. N. & Barrett, A. J. (1984). Kinetics of tryptic hydrolysis of the arginine-valine bond in folded and unfolded ribonuclease T1. *Biochem. J.* **219**, 411-417.

Pace, C. N., Grimsley, G. R., Thomas, S. T. & Makhatadze, G. I. (1999). Heat capacity change for ribonuclease A folding. *Protein Sci.* **8**, 1500-1504.

Pace, C. N., Grimsley, G. R., Thomson, J. A. & Barnett, B. J. (1988). Conformational stability and activity of ribonuclease T1 with zero, one, and two intact disulfide bonds. *J. Biol. Chem.* **263**, 11820-11825.

Pace, C. N., Shirley, B. A. & Thomson, J. A. (1989). Measuring the conformational stability of a protein. In *Protein Structure* (T. E. Creighton, Ed.), pp. 311-330, IRL Press, New York.

Pace, C. N., Vajdos, F., Fee, L., Grimsley, G. & Gray, T. (1995). How to measure and predict the molar absorption coefficient of a protein. *Protein Sci.* **4**, 2411-2423.

Parsell, D. A. & Sauer, R. T. (1989). The structural stability of a protein is an important determinant of its proteolytic susceptibility in *Escherichia coli*. *J. Biol. Chem.* **264**, 7590-7595.

Poland, D. C. & Scheraga, H. A. (1965). Statistical mechanics of noncovalent bonds in polyamino acids. VIII. Covalents loops in proteins. *Biopolymers* **3**, 379-399.

Privalov, P. L. & Potekhin, S. A. (1986). Scanning microcalorimetry in studying temperature-induced changes in proteins. *Advances Enzymol.* **131**, 4-51.

Privalov, P. L., Tiktopulo, E. I., Venyaminov, S. Y., Griko, Y. V., Makhatadze, G. I. & Khechinashvili, N. N. (1989). Heat capacity and conformation of proteins in the denatured state. *J. Mol. Biol.* **205**, 737-750.

Quirk, D. J., Park, C., Thompson, J. E. & Raines, R. T. (1998). His···Asp catalytic dyad of ribonuclease A: Conformational stability of the wild-type, D121N, D121A, and H119A enzymes. *Biochemistry* **37**, 17958-17964.

Radzicka, A. & Wolfenden, R. (1995). A proficient enzyme. *Science* **267**, 90-92.

Raines, R. T. (1998). Ribonuclease A. *Chem. Rev.* **98**, 1045-1065.

Raines, R. T. (1999). Ribonuclease A: from model system to cancer chemotherapeutic. In *Enzymatic Mechanisms* (P. A. Frey & D. B. Northrop, Ed.), pp. 235-249, IOS Press, Washington, DC.

Ramsay, G. & Freire, E. (1990). Linked thermal and solute perturbation analysis of cooperative domain interactions in proteins. Structural stability of diphtheria toxin. *Biochemistry* **29**, 8677-8683.

Rapoport, T. A., Jungnickel, B. & Kutay, U. (1996). Protein transport across the eukaryotic endoplasmic reticulum and bacterial inner membranes. *Annu. Rev. Biochem.* **65**, 271-303.

Rechsteiner, M., Rogers, S. & Rote, K. (1987). Protein structure and intracellular stability. *Trends Biochem. Sci.* **12**, 390-394.

Richards, F. M. (1997). Protein stability: still an unsolved problem. *Cell. Mol. Life Sci.* **53**, 790-802.

Richards, F. M. & Wyckoff, H. W. (1971). Bovine pancreatic ribonuclease. *The Enzymes* **IV**, 647-806.

Riordan, J. F. (1997). Structure and function of angiogenin. In *Ribonucleases: Structures and Functions* (G. D'Alessio & J. F. Riordan, Ed.), pp. 445-489, Academic Press, New York.

Robbins, J. C. & Nicolson, L. (1975). Surfaces of normal and tranformed cells. In *Cancer* (F. F. Becker, Ed.), pp. 31-32, Plenum Press, New York.

Rogers, S. W. & Rechsteiner, M. (1988). Degradation of structurally characterized proteins injected into HeLa cells. *J. Biol. Chem.* **263**, 19850-19862.

Rote, K., Rogers, S., Pratt, G. & Rechsteiner, M. (1989). Degradation of structurally characterized proteins injected into HeLa cells. *J. Biol. Chem.* **264**, 9772-9779.

Ruoppolo, M., Torella, C., Kanda, F., Panico, M., Pucci, P., Marino, G. & Morris, H. R. (1996). Identification of disulphide bonds in the refolding of bovine pancreatic RNase A. *Folding & Design* **1**, 381-390.

Rupley, J. A. & Scheraga, H. A. (1963). Structural studies of ribonuclease. VII. Chymotryptic hydrolysis of ribonuclease A at elevated temperatures. *Biochemistry* **2**, 421-431.

Russo, N., Shapiro, R. & Vallee, B. L. (1997). 5'-Diphosphoadenosine 3'-phosphate is a potent inhibitor of bovine pancreatic ribonuclease A. *Biochem. Biophys. Res. Commun.* **231**, 671-674.

Rybak, S. M. & Newton, D. L. (1999). *Exp. Cell Res.* **253**, 325-335.

Santoro, M. M., Liu, Y., Khan, S. M. A., Hou, L.-X. & Bolen, D. W. (1992). Increased thermal stability of proteins in the presence of naturally occurring osmolytes. *Biochemistry* **31**, 5278-5283.

Saunders, A. J., Young, G. B. & Pielak, G. J. (1993). Polarity of disulfide bonds. *Protein Sci* **2**, 1183-1184.

Saxena, S. K., Rybak, S. M., Winkler, G., Meade, H. M., McGray, P., Youle, R. J. & Ackerman, E. J. (1991). Comparison of RNases and toxins upon injection into *Xenopus* oocytes. *J. Biol. Chem.* **266**, 21208-21214.

Schein, C. H., Boix, E., Haugg, M., Holliger, P., Hemmi, S., Frank, G. & Shwalbe, H. (1992). Secretion of mammalian ribonucleases from *Escherichia coli* using the signal sequence of murine spleen ribonuclease. *Biochem. J.* **283**, 137-144.

Schultz, L. W., Quirk, D. J. & Raines, R. T. (1998). His···Asp catalytic dyad of ribonuclease A: Structure and function of the wild-type, D121N, and D121A enzymes. *Biochemistry* **37**, 8886-8898.

Sela, M., Anfinsen, C. B. & Harrington, W. F. (1957). The correlation of ribonuclease activity with specific aspects of tertiary structure. *Biochim. Biophys. Acta* **26**, 502-512.

Sela, M., White, F. H. J. & Anfinsen, C. B. (1957). Reductive cleavage of disulfide bridges in ribonuclease. *Science* **125**, 691-692.

Shimotakahara, S., Ríos, C. B., Laity, J. H., Zimmerman, D. E., Scheraga, H. A. & Montelione, G. T. (1997). NMR structural analysis of an analog of an intermediate formed in the rate-determining step of one pathway in the oxidative folding of bovine pancreatic ribonuclease A: Automated analysis of ^{1}H, ^{13}C, and ^{15}N resonance assignments for wild-type and [C65S, C72S] mutant forms. *Biochemistry* **36**, 6915-6929.

Spackman, D. H., Stein, W. H. & Moore, S. (1960). The disulfide bonds of ribonuclease. *J. Biol. Chem.* **235**, 648-659.

Staley, J. P. & Kim, P. S. (1992). Complete folding of bovine pancreatic trypsin inhibitor with only a single disulfide bond. *Proc. Natl. Acad. Sci. U.S.A.* **89**, 1519-1523.

Stowell, J. K., Widlanski, T. S., Kutateladze, T. G. & Raines, R. T. (1995). Mechanism-based inactivation of ribonuclease A. *J. Org. Chem.* **60**, 6930-6936.

Strydom, D. J., Fett, J. W., Lobb, R. R., Alderman, E. M., Bethune, J. L., Riordan, J. F. & Vallee, B. l. (1985). Amino acid sequence of human turmor derived angiogenin. *Biochemistry* **24**, 5486-5494.

Talluri, A., Falcomer, C. M. & Scheraga, H. A. (1993). Energetic and structural basis for the preferential formation of the native disulfide loop involving Cys65 and Cys72 in synthetic peptide fragments derived from the sequence of ribonuclease A. *J. Am. Chem. Soc.* **115**, 3041-3047.

Talluri, S., Rothwarf, D. M. & Scheraga, H. A. (1994). Structural characterization of a three-disulfide intermediate of ribonuclease A involved in both the folding and unfolding pathways. *Biochemistry* **33**, 10437-10449.

Tamburrini, M., Scala, G., Verde, C., Ruocco, M. R., Parente, A., Venuta, S. & D'Alessio, G. (1990). Immunosuppressive activity of bovine seminal RNase on T-cell proliferation. *Eur. J. Biochem.* **190**, 145-148.

Thompson, J. E., Kutateladze, T. G., Schuster, M. C., Venegas, F. D., Messmore, J. M. & Raines, R. T. (1995). Limits to catalysis by ribonuclease A. *Bioorg. Chem.* **23**, 471-481.

Thompson, J. E. & Raines, R. T. (1994). Value of general acid–base catalysis to ribonuclease A. *J. Am. Chem. Soc.* **116**, 5467-5468.

Thompson, J. E., Venegas, F. D. & Raines, R. T. (1994). Energetics of catalysis by ribonucleases: Fate of the 2',3'-cyclic intermediate. *Biochemistry* **33**, 7408-7414.

Thornton, J. M. (1981). Disulfide bridges in globular proteins. *J. Mol. Biol.* **151**, 261-287.

Tidor, B. & Karplus, M. (1993). The contribution of cross-links to protein stability: A normal mode analysis of the configurational entropy of the native state. *Proteins: Struct. Funct. Genet.* **15**, 71-79.

Trautwein, K., Holliger, P., Stackhouse, J. & Benner, S. A. (1991). Site-directed mutagenesis of bovine pancreatic ribonuclease: lysine-41 and aspartate-121. *FEBS Lett.* **281**, 275-277.

Ui, B. (1971). Isoelectric points and conformation of proteins: The effect of urea on the behavior of some proteins in isoelectric focusing. *Biochim. Biophys. Acta* **229**, 567-581.

van den Akker, F., Feil, I. K., Roach, C., Platas, A. A., Merritt, E. A. & Hol, W. G. J. (1997). Crystal structure of heat-labile enterotoxin from *Escherichia coli* with increased thermostability introduced by an engineered disulfide bond in the A subunit. *Protein Sci.* **6**, 2644-2649.

van den Burg, B., Vreind, G., Veltman, O. R., Venema, G. & Eijsink, V. G. H. (1998). Engineering an enzyme to resist boiling. *Proc. Natl. Acad. Sci. U.S.A.* **95**, 2056-2060.

Vicentini, A. M., Hemmings, B. A. & Hofsteenge, J. (1994). Residues 36-42 of liver RNase PL3 contribute to its uridine-preferring substrate specificity. Cloning of the cDNA and site-directed mutagenesis studies. *Protein Science* **3**, 459-466.

Vicentini, A. M., Kieffer, B., Matthies, R., Meyhack, B., Hemmings, B. A., Stone, S. R. & Hofsteenge, J. (1990). Protein chemical and kinetic characterization of recombinant procine ribonuclease inhibitor expressed in *Saccharomyces cerevisiae*. *Biochemistry* **29**, 8827-8834.

Villafranca, J. E., Howell, E. E., Oatley, S. J., Xuong, N.-h. & Kraut, J. (1987). An engineered disulfide bond in dihydrofolate reductase. *Biochemistry* **26**, 2182-2189.

Vindigni, A., De Fillipis, V., Zanotti, G., Visco, C., Orsini, G. & Fontana, A. (1994). Probing the structure of hirudin from *Hirudinaria manillensis* by limited proteolysis. *Eur. J. Biochem.* **226**, 323-333.

Vogl, T., Brengelmann, R., Hinz, H.-J., Scharf, M., Lotzbeyer, M. & Engels, J. W. (1995). Mechanism of protein stabilization by disulfide bridges: Calorimetric unfolding on disulfide-deficient mutants of the α–amylase inhibitor tendamistat. *J. Mol. Biol.* **254**, 481-496.

Wang, E. C. W., Hung, S.-H., Cahoon, M. & Hedstrom, L. (1997). The role of the Cys191-Cys220 disulfide bond in trypsin: New targets for engineering substrate specificity. *Protein Eng.* **10**, 405-411.

Wedemeyer, W. J., Welker, E., Narayan, M. & Scheraga, H. A. (2000). Disulfide bonds and protein folding. *Biochemistry* **39**, 4207-4216.

Weissman, J. S. & Kim, P. S. (1993). Efficient catalysis of disulphide bond rearrangements by protein disulphide isomerase. *Nature* **365**, 185-188.

Wells, J. A. & Powers, D. B. (1986). *In vivo* formation and stability of engineered disulfide bonds in subtilisin. *J. Biol. Chem.* **261**, 6564-6570.

White, F. H. J. (1961). Regeneration of native secondary and teriary structures by air oxidation of reduced ribonuclease. *J. Biol. Chem.* **236**, 1353-1360.

Wintrode, P. L., Makhatadze, G. I. & Privalov, P. L. (1994). Thermodynamics of ubiquitin unfolding. *Proteins: Struct. Funct. and Genet.* **18**, 246-253.

Wlodawer, A., Anders, L. A., Sjölin, L. & Gilliland, G. L. (1988). Structure of phosphate-free ribonuclease A refined at 1.26 Å. *Biochemistry* **27**, 2705-2717.

Wodak, S. Y., Liu, M. Y. & Wyckoff, H. W. (1977). The structure of cytidilyl(2',5') adenosine when bound to prancreatic ribonuclease S. *J. Mol. Biol.* **116**, 855-875.

Wolf, B., Lesnaw, J. A. & Reichmann, M. E. (1970). A mechanism of the irreversible inactivation of bovine pancreatic ribonuclease by diethylpyrocarbonate. A general reaction of diethylpyrocarbonate with proteins. *Eur. J. Biochem.* **13**, 519-525.

Wu, Y., Mikulski, S. M., Ardelt, W., Rybak, S. M. & Youle, R. J. (1993). A cytotoxic ribonuclease. *J. Biol. Chem.* **268**, 10686-10693.

Wu, Y.-N., Saxena, S.K., Wojciech, A., Gadina, M., Mikulski, S.M., De Lorenzo, C., D'Alesio, G., Youle, R.J. (1995). A study of the intracellular routing of cytotoxic ribonucleases. *J. Biol. Chem.* **270**, 17476-17481.

Wyckoff, H. W., Hardman, K. D., Allewell, N. M., Inagami, T., Johnson, L. N. & Richards, F. M. (1967). The structure of ribonuclease-S at 3.5 Å resolution. *J. Biol. Chem.* **242**, 3984-3988.

Wyckoff, H. W., Hardman, K. D., Allewell, N. M., Inagami, T., Tsernoglou, D., Johnson, L. N. & Richards, F. M. (1967). The structure of ribonuclease-S at 6 Å resolution. *J. Biol. Chem.* **242**, 3749-3753.

Xu, X., Rothwarf, D. M. & Scheraga, H. A. (1996). Nonrandom distribution of the one-disulfide intermediates in the regeneration of ribonuclease A. *Biochemistry* **35**, 6406-6417.

Xu, X. & Scheraga, H. A. (1998). Kinetic folding pathway of a three-disulfide mutant of bovine pancreatic ribonuclease A missing the [40-95] disulfide bond. *Biochemistry* **37**, 7561-7571.

Yamaguchi, S., Takeuchi, K., Mase, T., Oikawa, K., McMullen, T., Derewenda, U., McElhaney, R. N., Kay, C. M. & Derewenda, Z. S. (1996). The consequences of engineering an extra disulfide bond in the *Penicillium camembertii* mono- and diglyceride specific lipase. *Protein Eng.* **9**, 789-795.

Youle, R. J. & D'Alessio, G. (1997). Antitumor RNases. In *Ribonucleases: Structures and Functions* (G. D'Alessio & J. F. Riordan, Ed.), pp. 491-514, Academic Press, New York.

Youle, R. J., Newton, D., Wu, Y.-N., Gadina, M. & Rybak, S. M. (1993). Cytotoxic ribonucleases and chimeras in cancer therapy. *Crit. Rev. Therapeutic Drug Carrier Systems* **10**, 1-28.

Zhang, J. G., Matthews, J. M., Ward, L. D. & Simpson, R. J. (1997). Disruption of the disulfide bonds of recombinant murine interleukin-6 induces formation of a partially unfolded state. *Biochemistry* **36**, 2380-2389.

Zhao, W., Beintema, J. J. & Hofsteenge, J. (1994). The amino acid sequence of iguan (Iguana iguana) pancreatic ribonuclease. *Eur. J. Biochem.* **219**, 641-646.

Zhu, H., Dupureur, C. M., Zhang, X. & Tsai, M. D. (1995). Phospholipase A2 engineering. The roles of disulfide bonds in structure, conformational stability, and catalytic function. *Biochemistry* **34**, 15307-15314.